To the Graduate Council:

I am submitting herewith a thesis written by Michael Alan Lipkin entitled "Depth of Penetration of Honey Bee Venom Melittin in Lipid Bilayers." I have examined the final copy of this Thesis for form and content and recommend that it be accepted in partial fulfillment of the requirements for the degree of Master of Science, with a major in Physics.

Solon Georghiou, Major Professor

We have read this thesis
and recommend its acceptance:

Elizabeth E Howell

Ergin Sezpezm

Accepted for the Council:

Associate Vice Chancellor and
Dean of The Graduate School

# Depth of Penetration of Honey Bee Venom Melittin in Lipid Bilayers

A Thesis

Presented for the Degree of

Master of Science

The University of Tennessee, Knoxville

Michael Alan Lipkin

May 1997

# ACKNOWLEDGMENTS

I would like to gratefully acknowledge my research advisor, Dr. Solon Georghiou ("Σολων ο σοφος"). His support for me, both personally and professionally, has not only enabled me to do this project but has also guided me through some very trying times.

I would like to thank the other members of my committee, Dr. Elizabeth Howell, Dr. Engin Serpersu and Dr. Thomas D. Bradrick, for their time, patience, and keen insights which have shaped the present research.

I also am grateful to Dr. Thomas D. Bradrick for training me in the experimental techniques used in this work. I would also like to acknowledge Stacy Gerke, Angela K. Payongayong, and other members of the Molecular Biophysics Laboratory for their friendship.

I thank the Department of Physics, the University of Tennessee, Knoxville, through its former Head, Dr. William Bugg, for giving me the opportunity to be a Graduate Teaching Assistant while I pursued graduate studies in physics.

I would also like to thank the department of Biochemistry, the University of Tennessee, Knoxville for its very valuable help toward the completion of this project. Dr. Cynthia Peterson for allowing me to use her microcalorimeter and Dr. Ping Zhuang for her help with the microcalorimetric measurements. I would also like to thank Mr. Richard W. Williams for the electron microscopy measurements.

Lastly, I acknowledge the support that was given to me by my family and friends.

# ABSTRACT

Melittin is a naturally occurring protein in honey bee venom. The association of melittin with phospholipid vesicles is well documented. The present work uses its single tryptophan residue as an intrinsic fluorescent probe. Measurements were taken at the transition temperatures of the phospholipids used, 21° C and 37° C for DMPC and DPPC, respectively. In order to study the depth of penetration of melittin into the lipid bilayer, we have used the n-doxyl stearic acids, n-DS, as fluorescence quenchers (n defines the position along the acyl chain of the fatty acid). The greater the value for n the deeper into the bilayer the quencher moeity is located. Stopped-flow fluorometry has been used in the present work to study the quenching on the millisecond time scale before melittin-induced fusion takes place.

The relative quenching efficiencies for the differing depths of the n-DS quenchers are used to infer the accessibility of the tryptophan of melittin to different depths into the bilayer. It is found that the further down the acyl chains one puts the quencher the less efficient it is for both DMPC and DPPC. These findings imply that the tryptophan residue of melittin resides closer to the 5 position along the acyl chain than to either the 7 or 12 position.

Quenching efficiency is found to be dependent upon which lipid is used in conjunction with the n-DS. The n-DS are much more efficient when they are incorporated into DPPC vesicles rather than DMPC vesicles. This is thought to stem from a tighter binding of melittin which may reduce the distance between its tryptophan and the quenchers. The results of data analysis using the parallax method indicate that melittin inserts itself into approximately the first position along the acyl chains in DMPC vesicles.

However, the parallax method gives unrealistic results for DPPC, as it places the tryptophan at a distance of 30 Å away from the center of the bilayer. It should be added that for this lipid there is a significant contribution of instantaneous quenching of unknown origin. However, regardless of whether one takes into account the instantaneous quenching, a comparison of the quenching efficiencies of 5-DS and 12-DS suggests that the position of the tryptophan is closer to the bilayer surface and hence more external when binding to DPPC.

Interestingly the rate of quenching was also found to be dependent upon the location of the n-DS. It was found that the further down the acyl chain one puts the quencher the faster it quenches. This is attributed to the enhancement of segmental flexibility which the methylene groups closer to the center of the bilayer are known to possess. It should also be noted that the overall rate of quenching was found to be much higher for the n-DS in DPPC than in DMPC, which correlates with published results for the rate of melittin binding.

The relative orientation of the protein once bound to a vesicle is still unknown. However, the present experiments have provided information on the extent of penetration of the protein into the bilayer. The suggested deeper penetration in DMPC tends to favor the parallel-to-the-surface model rather than the other models, where the N-terminus would presumably limit the degree of freedom for the melittin to change its depth of insertion.

# TABLE OF CONTENTS

# LIST OF FIGURES

## FLUORESCENCE STUDIES



## DISCUSSION

# LIST OF TABLES

# LIST OF SYMBOLS USED

n = the position along the fatty acid at which the quencher moeity is attached

n-DS = refers to the n doxyl stearic acids that are being used as a quencher

DMPC = Dimyristoylphosphatidylcholine

DPPC = Dipalmitoylphosphatidylcholine

SUVs = Single Unilamellar Vesicles

EDTA = Ethylenediaminetetraacetic acid

$\varepsilon$ = molar extinction coefficient

[C] = the molar concentration of the quencher in methanol solution

d = the optical path length of the cuvette

$T_m$ = transition temperature

$\eta$ = the mean number of quencher molecules residing in a vesicle

[Ves] = the concentration of vesicles

[Lipid] = the concentration of lipid

$V_T$ = total volume of a lipid sample = $V_A + V_L$

$V_A$ = the volume of a lipid sample that is taken up by the aqueous phase

$V_L$ = the volume of a lipid sample that is taken up by the lipid phase

$V_{LSUV}$ = the volume of the lipid phase of a vesicle of radius $r_{suv}$

f = the volume fraction of water in a lipid sample

$K_{eq}$ = equilibrium constant for the quencher

$K_{P,ABS}$ = the absolute partitioning coefficient

I = the fluorescence intensity of bound melittin in the presence of quencher

$I_0$ = the fluorescence intensity of bound melittin in the absence of quencher

$\left[(I_o / I) - 1\right]$ = a quantitative description of quenching efficiency used to make a corrected Stern-Volmer plot

$R_c$ = the critical radius of quenching which is approximately 15 Å

C = [(mole fraction of quencher lipid in total lipid)/(area of lipid in $Å^2$)]

$z_{nF}$ = the distance between the depth of the quencher and the position of the fluorophore

$L_{21}$ = the difference in depth between the two quencher locations being compared

$F_n$ = the quantitative description of quenching used in the parallax method of analysis

$Z_{Cf}$ = the distance from the center of the bilayer to the tryptophan

$L_{CL}$ = the distance from the center of the bilayer to the lower quencher of the quenchers being compared

$\delta$ = the amount of fluorescence intensity change brought about by melittin binding to an unlabelled vesicles

k = the rate constant for melittin binding to an unlabelled DMPC vesicle

$k_2$ = the apparent rate of quenching in DMPC

A = the magnitude of the drop in fluorescence intensity upon melittin binding to a labelled DMPC vesicle

B = the final value the fluorescence intensity drops to at long times

$k_1$ = the true rate of quenching in DMPC

$A_1$ = the partial magnitude of the drop in fluorescence intensity upon melittin binding to a labelled DPPC vesicle

$A_2$ = the partial magnitude of the drop in fluorescence intensity upon melittin binding to a labelled DPPC vesicle

$k_f$ = the fast rate of quenching in DPPC

$k_S$ = the slow rate of quenching in DPPC

g = the amount of scattered light

t = time

$P_1$ = population of quenchers located within the critical radius of the binding site

$P_2$ = population of quenchers which are located outside the critical radius but can move close enough to quench

$P_0$ = population that is too far away to ever quench

# PART 1.
# INTRODUCTION

Melittin is a naturally occurring protein. It constitutes approximately 50% of the dry weight of honey bee venom (Haberman, 1980). The amino acid sequence of melittin was determined in 1967 (Haberman and Jentsch, 1967) and is shown in Figure 1. Melittin contains 26 amino acids. Amino acid residues 1-20 are hydrophobic, while residues 21-26 are mainly hydrophilic. Melittin has an amphipathic nature making it soluble in aqueous media, but it is also able to strongly associate with phospholipid bilayers (Schwarz, 1989). This association with bilayers is the crux of the present research, which is attempting to describe quantitatively the accessibility of the tryptophan residue of melittin to a quencher located in the lipid bilayer.

The properties of melittin that enable it to lyse cells, such as leukocytes, erythrocytes, lysosomes and mitochondria, include the ability to disrupt the lipid membranes (Haberman, 1972). Melittin is highly surface active. There is evidence that the surface and lytic activities arise from different structural features (Terwilliger et al., 1982). The initial interaction of melittin and bilayer is most probably electrostatic in nature, because melittin is positively charged. This electrostatic interaction serves to anchor the protein to the bilayer surface. Once melittin anchors itself to the phospholipid bilayer, it adopts an $\alpha$-helical conformation (Dawson, 1978).

At low concentrations and low salt content melittin exists in solution as a monomer. A single melittin polypeptide chain in lipid bilayers has been proposed to have the conformation of a bent alpha-helical rod according to the model of Terwilliger et al. (1982). Residues 1-10 form a straight $\alpha$-helix as do residues 13-26, but the axes of the two helices form an obtuse angle with each other of about 120 degrees. This model was based on x-ray crystalography results.

Physiologically, melittin has been found to enhance the activity of phospholipase $A_2$ . (Mollay and Kreill, 1974; Yunes et al., 1977). Once melittin is bound to a membrane, it

| 1 | 2 | 3 | 4 | 5 | 6 | 7 | 8 | 9 | 10 | 11 | 12 |
|---|---|---|---|---|---|---|---|---|---|---|---|
| GLY | ILE | GLY | ALA | VAL | LEU | LYS | VAL | LEU | THR | THR | GLY |
| 13 | 14 | 15 | 16 | 17 | 18 | 19 | 20 | 21 | 22 | 23 | 24 |
| LEU | PRO | ALA | LEU | ILE | SER | TRP | ILE | LYS | ARG | LYS | ARG |
| 25 | 26 | | | | | | | | | | |
| GLN | GLN | | | | | | | | | | |

**Figure 1.**

Amino acid composition of melittin. (From the Honey Bee: Apis Meliferra) (Dayhoff, 1968).

alters the structure of that membrane, thereby enhancing its permeability to ions and solutes (Sessa et al., 1969; Tosteson et al., 1990; Degrado et al., 1982). At high concentrations, melittin has shown the ability to lyse natural and model membranes (Sessa et al., 1969).

Earlier experiments performed by the Molecular Biophysics Group at the University of Tennessee, Knoxville have added to our understanding of the state of membrane-bound melittin. It has been shown that, if there are different 'species' of bound melittin they must have a similar fluorescence quantum yield (Bradrick Ph. D. Dissertation, 1995). These results were obtained using stopped-flow fluorometry to study the change in the fluorescence intensity of melittin during binding to phospholipid bilayers. Another study (Payongayong, 1995) followed the fluorescence anisotropy of melittin and concluded that any such species present do not have significantly different mobilities regarding their tryptophan residue. It was also shown that the quantum yield of melittin increases upon binding (Bradrick et al., 1995). This is thought to stem from the increased shielding of the trytophan moiety once it has left the aqueous environment and entered into the less polar environment of the lipid bilayer. These results were obtained using stopped-flow fluorometry to study the fluorescence intensity of melittin as it binds to phospholipid bilayers.

The last physiological phenomenon associated with melittin that is of interest in the current research is its ability to act as a fusogen. Melittin induces natural and artificial membranes to undergo fusion (Morgan et al., 1983; Eytan and Almary, 1983; and Bradrick and Georghiou, 1987). In the work presented here, all kinetic studies were on a time scale (milliseconds) considerably shorter than that required for fusion to take place (seconds to minutes).

In the experiments reported in the present work melittin exists as a monomer because of its low concentration and the fact that the ionic strength of the solution was low.

Melittin binds to lipid bilayers as a monomer when monomeric in solution (Bradrick, Friere and Georghiou, 1989). However, in solutions of melittin with a concentration above approximately 0.1 mM or in high salt solutions it has been shown that melittin exists as a tetramer in solution (Faucon, 1979). Melittin as a tetramer hides the hydrophobic residues from the aqueous solvent. Experiments by Lauterwein et al. (1980) and Brauner et al. (1980) indicate that the backbone conformations are similar in tetrameric melittin and melittin that is bound to a membrane. The melittin helix shows a distinctive orientational segregation of the hydrophilic and hydrophobic side chains. The hydrophobic side chains are oriented mainly towards the 'inside' of the bend of the helix, and the charged and polar side chains are oriented mainly towards the 'outside' of the bend (Terwilliger and Eisenberg, 1982) (see Figure 2).

The interaction of melittin with phospholipids depends on the relative and absolute concentrations of the two and also on the morphology and type of membrane being studied. Melittin perturbs membranes rapidly. These effects are long-range and in the case of DMPC and DPPC SUVs these effects are maximal at the transition temperature (Bradrick et al., 1995). This perturbation is modeled as a compressional wave. The effects are very weak for DPPC relative to those for DMPC. This is consistent with the finding that the melittin-vesicle molecular complex is much more stable for the case of DPPC (Bradrick et al., 1995).

Once binding has taken place, the lipid acyl chains may adopt a wider distribution of angles with respect to each other, which may account for the increase in permeability of the vesicles to ions prior to rupture (Dawson, 1978). Only a limited number of melittin molecules can be bound to a lipid membrane at once. In the case of DMPC vesicles fused by melittin, about 50-100 lipid molecules are required to host one bound melittin molecule

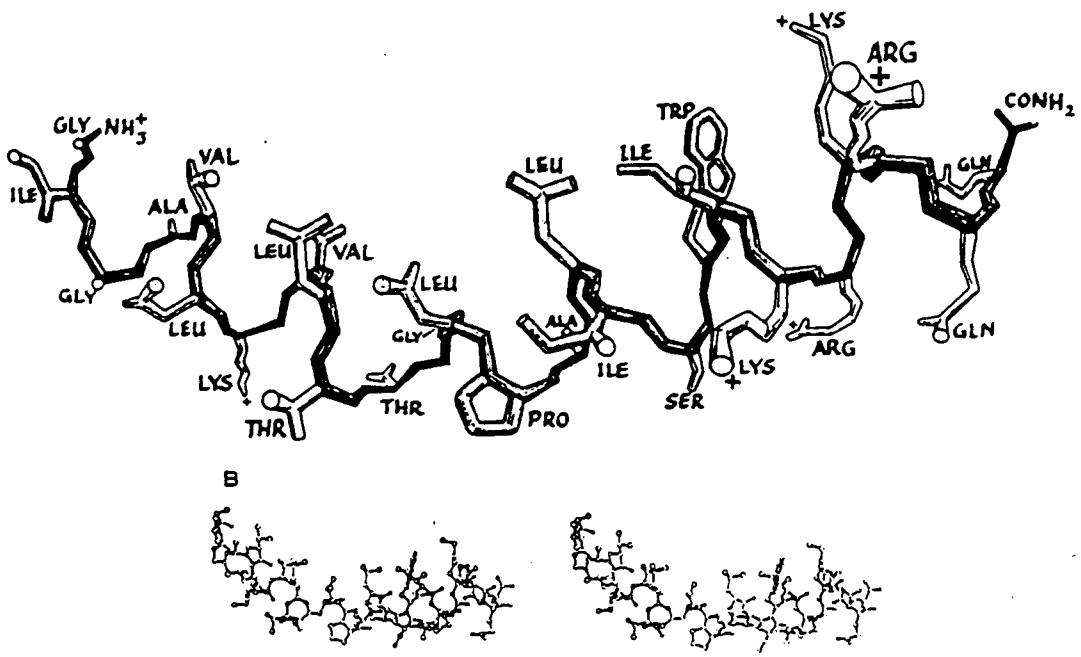


**Figure 2**

Hydrophilic and hydrophobic sidechains of melittin. Shown is the conformation of one melittin chain from the tetramer (Terwilliger and Eisenberg, 1982).

(Vogel et al., 1983). For a description of the number of lipid molecules required to 'host' a melittin molecule in the absence of vesicle fusion, see Bradrick et al. (1995).

The backbone conformation of melittin in lipid bilayers is considered to have some similarity to the bent rod conformation it has in crystals studied using x-ray crystallography by Terwilliger et al. (1982). This bent rod can lie in the plane of the bilayer or perpendicular to it. There is a debate over the conformation of melittin once it is bound to a membrane (see Figures 3 and 4). Vogel et al. (1983) support the trans-membranal model as illustrated in Figure 3A, while Terwilliger et al. (1982) support a model in which the helix axis of melittin is 'parallel-to-the-surface' of the bilayer as illustrated in Figure 3B, and Dawson (1978) support the 'wedge' model illustrated in Figure 3C. The structure in the crystal found by Terwilliger et al. is most compatible with the parallel-to-the-surface model (see also Figure 4). This is because of the orientational segregation of the side chains as described above, in which the hydrophilic side chains are directed mainly toward the outside of the bent rod and the hydrophobic side chains are directed predominantly toward the inside (Terwilliger et al., 1982). Terwilliger et al. also go on to say that since the rate of transport of charged species across the bilayer is slow, this suggests that the rate of crossing the bilayer by the N-terminus of melittin would be too slow for perpendicular insertion to be effective. Therefore, perpendicular insertion, as is the case in the trans-membranal model, is less likely than parallel insertion.

On the other hand, the data presented by Vogel et al. (1983) show an order parameter that is much more consistent with the perpendicular insertion model. Vogel goes on to make the statement that hydrogen bonding could greatly reduce the energetic cost of having the hydrophilic side chains of melittin inserted into the nonpolar interior of the bilayer. The energy gained from incorporating the whole of the hydrophobic helical regions of the melittin into the apolar membrane is considered to compensate for the few

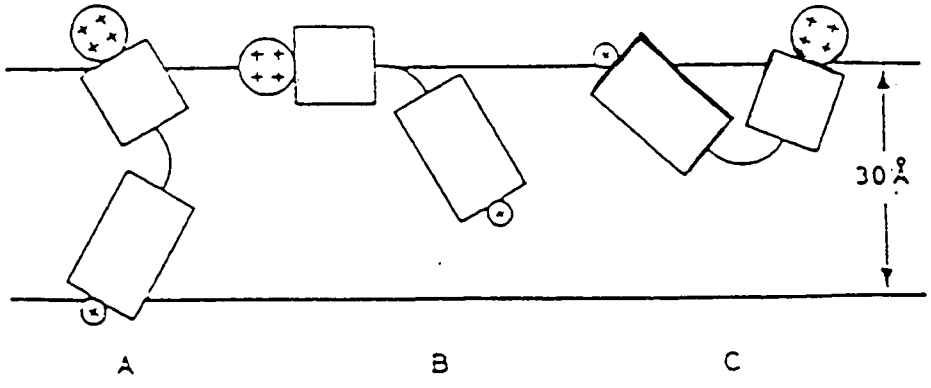


**Figure 3**

Models for the structure of a membrane-bound α-helical melittin monomer. Melitin consists of two helical segments (represented by the two rectangles) with a diameter of 10 Å (Terwilliger and Eisenberg, 1982) and an overall length (30 Å) that just spans the bilayer (Vogel and Jahnig, 1986). Helix 1 extends from residues 1 to 11 and helix 2 extends from 14 to 20. The bend occurs near the proline residue at position 14. The single positive charge on the N-terminus and the four positive charges at the hydrophilic amino terminal end (residues 21-26) are shown. The angle between the helix axes is about 120°. (A) Trans-membrane bent α-helix (Vogel et al.,1983). (B) Parallel-to-the-surface model (Terwilliger et al., 1982). (C) "Wedge" model (Dawson, 1978).

**Figure 4**

Longitudinal (upper) and axial (lower) views of the proposed space-filling model of a membrane-bound melittin monomer with its helix axis parallel to the bilayer surface and its nonpolar amino acid residues embedded into the membrane. The possible conformation of adjacent lipid molecules is shown in the lower figure to illustrate the effect that binding of such a melittin species might have on the lipid bilayer (Terwilliger et al., 1982).

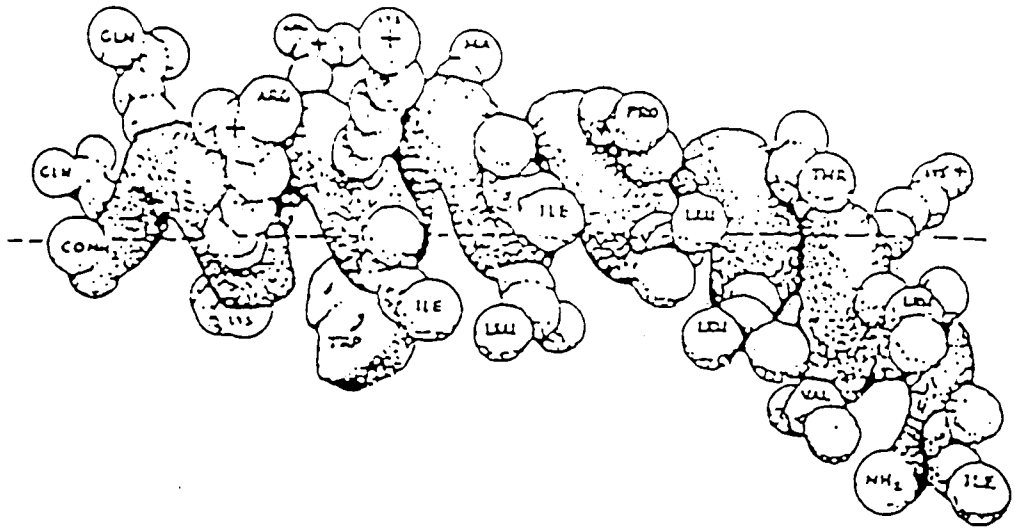
GLN
ARG
GLN
ILE
LEU
THR
ILE
LEU
ILE
LEU
LEU
LEU
LEU
NH2
ILE

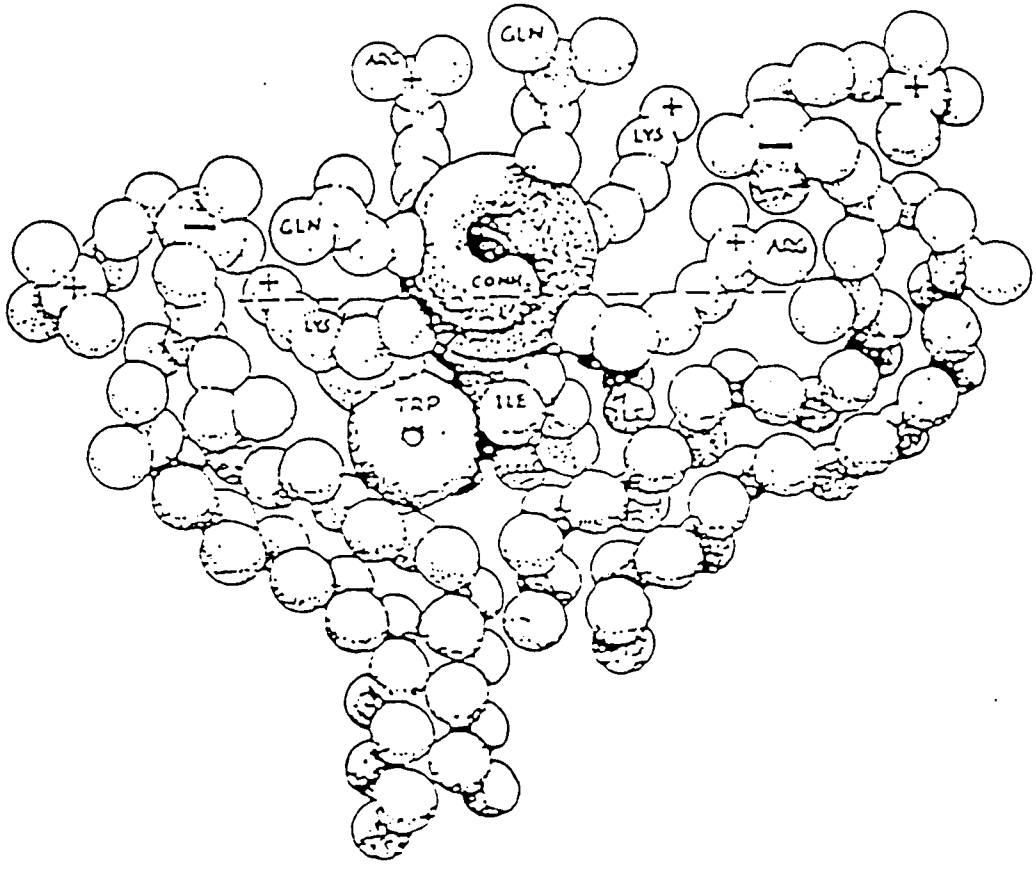
ARG
GLN
LYS
GLN
ARG
LEU
TRP
ILE

kilocalories per mol necessary for insertion of the polar residues into the membranes (Vogel et al., 1983). It is important to point out that Vogel's data were taken for oriented membranes with a relatively low water content, which may not be an ideal environment for the lipids. In the Discussion, an attempt is made to determine which model is consistent with the findings of the present study.

# PART 2.
# MATERIALS
# AND
# METHODS

# MATERIALS

LIST OF CHEMICALS USED

HCl.....Fisher
NaOH.....Fisher
Ethylenediaminetetraacetic acid (EDTA).....Sigma
Triply Distilled Water.....Carolina Biological Supply Co.
Tris (Hydroxymethyl) Aminomethane.....Fisher
5-Doxyl Stearic Acid (5-DS).....Molecular Probes
7-Doxyl Stearic Acid (7-DS).....Molecular Probes
12-Doxyl Stearic Acid (12-DS).....Molecular Probes
Dimyristoylphosphatidylcholine (DMPC).....Avanti
Dipalmitoylphosphatidylcholine (DPPC) .....Avanti
Melittin.....Sigma
Methanol (spectrophotometric grade).....Mallinckrodt
Chloroform.....Mallinckrodt
Nitrogen Gas (Ultra Pure).....National Welders

All inorganic materials were of analytical grade. The n-doxyl stearic acids (n-DS) and melittin were used with no further purification. DMPC and DPPC were used in an aqueous buffer. The buffer used was 50 mM Tris, 1 mM EDTA, pH 7.6 prepared in triply distilled water. EDTA was added to restrict the activity of phospholipase $A_2$ which is a contaminant in melittin. Methanol was used as a solvent to determine the concentrations of the n-DS (see Preparation of Vesicles). The pure nitrogen gas was used to remove the organic solvent.

# PREPARATION OF VESICLES

This section will go through the details of the vesicle preparative process. First, unlabelled vesicles will be discussed and then the process for labeling them will follow. It is important to note that all vesicles were prepared the day of each experiment, and kept at a temperature which was higher than their respective transition temperatures; under these conditions the vesicles did not fuse (Bradrick et al., 1995).

DMPC and DPPC vesicles were prepared in a similar manner. Once the amount of lipid was weighed out using a Mettler Balance (±0.1 mg), the dry lipid was hydrated using buffer. Typically, the amount of dry lipid used was 25 mg dissolved in 6.3 ml of buffer. The lipids were hydrated and kept at 10 C above their respective phase transition temperatures of 21 C and 37 C for DMPC and DPPC for the remainder of the preparative process. The lipids were given 15 minutes to fully hydrate during which time they were vortexed routinely. The vesicles were then sonicated for 20 minute intervals with 5 minute waiting time in between sonication periods until the vesicles were clear. (Generally, this takes approximately 40 minutes.) This insured that we obtained unilamellar bilayers. The vesicles were then given 30 minutes to anneal at their transition temperature before they were ultracentrifuged at 65,000 g for 30 minutes to remove any large multilamellar vesicles that were present. The supernatant was then extracted, which consisted of only single unilamellar vesicles, SUVs, and used in the experiments.

It was somewhat more technically difficult to prepare labelled vesicles. The first difficulty was associated with the accurate determination of the concentration of the quencher. This was overcome by taking the absorption spectra for each of the n-DS. Once it was proven that the absorption data were reproducible, it was a simple calculation to establish a molar extinction coefficient, ε, at 300 nm.

$$\text{ABSORBANCE} = [C]\,\varepsilon\, d \qquad (1)$$

Here, [C] is the molar concentration of the quencher in methanol solution, and d is the optical path length of the cuvette being used (in this case 1 cm.) The values of ε obtained at 300 nm are listed below, since they do not seem to be available in the literature.

| n-Doxyl Stearic Acid | $\varepsilon \left(\frac{1}{\text{mole} \cdot \text{cm}}\right)$ |
|---|---|
| 5-DS | 64.7 ± 1.3 |
| 7-DS | 65.4 ± 1.3 |
| 12-DS | 68.5 ± 1.3 |

As can be seen, ε becomes larger the further down the acyl chain one goes.

For technical reasons, it was easiest to determine the concentration of the stock quencher solution and then determine the concentration of lipid desired for a certain aliquot of the stock quencher. The lipid was then dissolved in chloroform, and an aliquot of quencher was added to the lipid. It is possible at that stage that methanol could disturb the bilayer, but it was added in such a small aliquot (≈50 μl) that this is unlikely.

The absolute molar concentrations of the lipid and quencher were then fixed, for example at a 90 to 1 ratio. (The concentration of the quencher in the lipid bilayer will be discussed later.) The organic solvent was removed under a stream of pure nitrogen gas. The labelled vesicles were then placed in a vacuum desiccator overnight to remove all traces of organic solvent. The preparative process is identical to that stated for the unlabelled case, from this point on. By simply adding a certain amount of buffer to the dry lipid/quencher it was possible to make a consistent concentration of vesicles.

# STOPPED-FLOW FLUOROMETRY

The stopped-flow apparatus is capable of mixing two liquids very quickly, following which fluorescence intensity measurements are made. For a detailed description of the apparatus, consult Figure 5. First , one fills the two reservoirs; one with a melittin solution, the other with a labelled or unlàbelled lipid solution. As the plunger pushes these two reservoirs down, it forces the two solutions to mix in the observation cell. It is in this

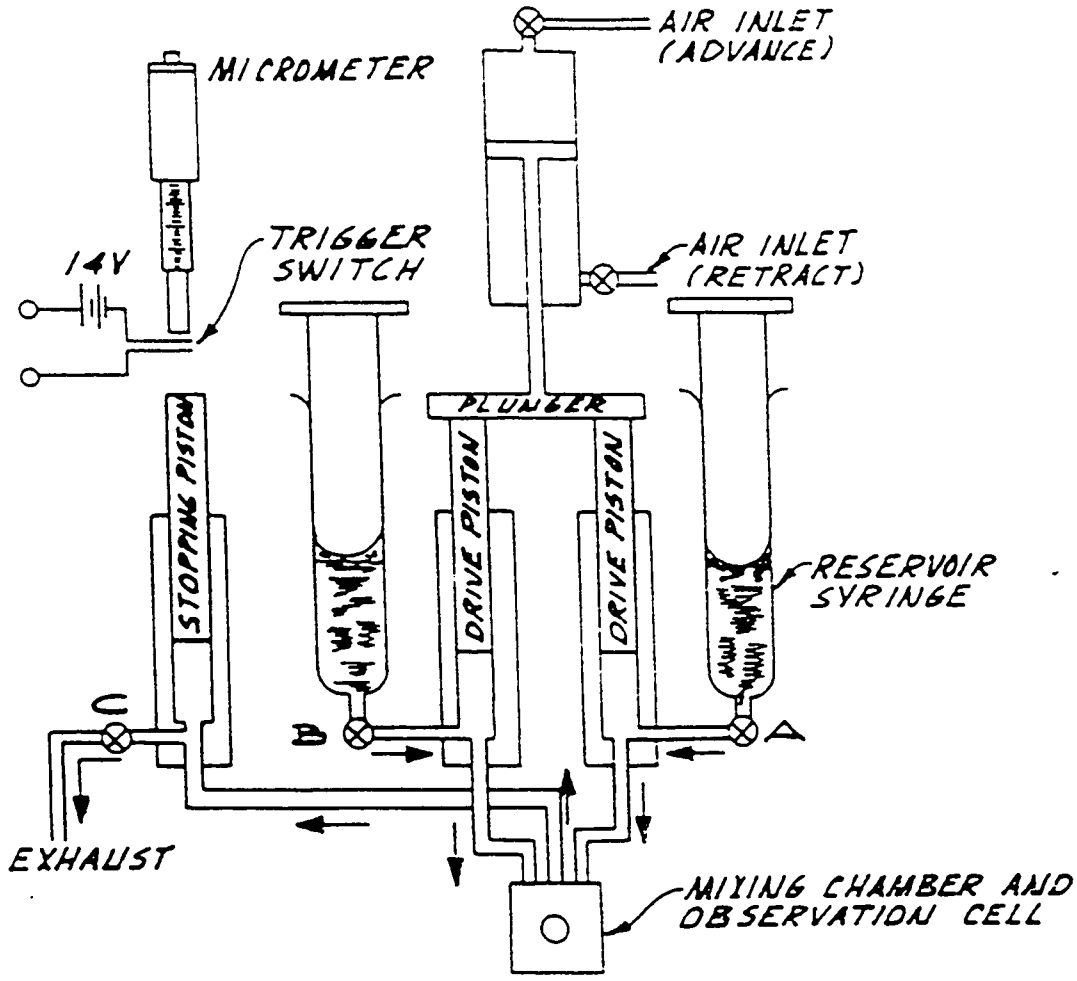


**Figure 5**

Schematic diagram of the stopped-flow apparatus. The two cylinders containing the seperate aqueous solutions of melittin and lipid were used to push the solutions into the mixing chamber very quickly. (Our stopped-flow apparatus has a 'dead' time of only 3.5 ms.) The mixing chamber is where the fluorescence intensity is measured.

mixing chamber that the sample is excited at 300 nm and fluorescence is collected at a right angle relative to the excitation beam.

The light source for the stopped-flow apparatus used in the present study is a 600 W Mercury-Xenon arc lamp (see Figure 6). The light is then passed through a condensing lens which allows the user to select how intensely the light illuminates the sample. Next, the beam is passed through a triply distilled water-containing filter to absorb infrared photons. The light beam then goes through a lens, a depolarizer, and another lens. At this point, the light goes through quartz neutral density filters which are selected by the user. The present study used a 20% neutral density filter combined with a 10% neutral density filter. (This was done in order to cut the intensity of the light down to such a low level that the interference filter and the photomultiplier are not damaged by the exciting light.) The excitation wavelength is then selected using an interference filter; the present study used a Corion 300 nm interference filter. The light beam then gets refocused using another lens that is placed so that its focal point is the observation cell. Some of the exciting light is then absorbed by the sample and fluorescence is emitted. To eliminate exciting light as much as possible, fluorescence is collected at a right angle relative to the excitation beam. The fluorescence is then passed through a lens placed so that its focal point is the photomultiplier. The fluorescence then goes through a depolarizer and on to the emission filter. The emission filter used was a Corning 4-71. This particular emission filter was selected because it reduces the magnitude of the change in the fluorescence intensity in the control experiment (see Data Analysis). The photomultiplier was set to 1300 V and data were collected on an IBM PC that had an analog-to-digital converter connected to it. Sample temperature was kept constant by a circulating water bath. At lower temperatures, it is necessary to blow a stream of pure nitrogen on the observation cell to eliminate water condensation.

**Figure 6.**

Schematic diagram of the lens sytem used to filter light during measurement. (From the Ms. Thesis of Angela Payongayong, 1995.)

# STOPPED-FLOW FLUOROMETER


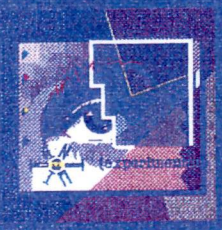

It is the nature of the experiment that melittin will go from being in a free state in the aqueous phase to binding to the lipid bilayer, which we consider to be the lipid phase. In the case considered here, once melittin is bound to the bilayer it becomes accessible to the quencher which is located there. Fluorescence, therefore, changes as a function of time for two reasons. The first reason is that the environment of the tryptophan of melittin is changing as it goes from the polar aqueous solution into the nonpolar lipid bilayer (see Introduction). The emission filter was picked for its ability to keep to a minimum the change in the fluorescence of melittin as it binds to an unlabelled bilayer. This was done so that we could measure the magnitude of quenching more effectively. The second reason is that once melittin is bound, its fluorescence has a much higher probability of being quenched. (Since the quenching of N-doxyl stearic acids is thought to be collisional, the probability of quenching in the aqueous phase can be assumed to be negligible.)

Stopped-flow fluorometry is a very useful technique for studying melittin binding to lipid bilayers. The measurements can be carried out before melittin-induced fusion of the vesicles takes place (Bradrick and Georghiou, 1987). Even though the rate constants reported here are a convolution of the rate constant of binding and the rate constant of quenching, qualitatively they reflect the actual rate at which the protein is capable of becoming accessible to a quencher located in the membrane. The study also presents information on the overall fluidity of the acyl chains of the bilayer.

# CALORIMETRIC STUDY

There is a possibility that the presence of the quencher causes a change in the structure of the vesicles. Microcalorimetric experiments were carried out to test this possibility. Any significant effect on the vesicles due to the label would result in a change

in the transition temperature, $T_m$, and the transition enthalpy. Thus, we used microcalorimetry to examine the effects of the quencher on the vesicles. In order to avoid temperature-induced vesicle fusion we performed cooling scans.

The preparative process for both lipids is discussed in the Preparation of Vesicles section. There is no difference in the preparation of the vesicles for the stopped-flow experiments and the calorimetry experiment. However, we only investigated one concentration of vesicle (2.25 mM) for both DMPC and DPPC. The quencher concentration used in the labelled case is the highest used in the stopped-flow experiments and corresponds to $\eta = 72$ (see section on mean occupation number, $\eta$). We used DMPC large multilamellar vesicles for calibration purposes.

The transition temperature, $T_m$ , was compared for the labelled and unlabelled case. In SUVs there is a higher degree of disorganization than in large multilamellar vesicles. This results in a lower $T_m$ in the former vesicles. Also, there is a broader transition region in SUVs than in large multilamellar vesicles which tends to raise the amount of error associated with the microcalorimetric data, especially in the case of DMPC .

DMPC has been found to have a very broad transition region with a low transition enthalpy. We found that, to within the uncertainty of a couple of degrees, the quencher had no drastic effect on the $T_m$ (see Figures 7 and 8).

DPPC has a sharper transition than DMPC. In this case it was found that the $T_m$ for the labelled and unlabelled case agreed to within a half of a degree, which was only slightly outside the experimental error found in the literature (Marsh, 1990) for large multilamellar vesicles. Qualitatively the transition enthalpies were also quite similar (see Figures 9 and 10). We feel that any perturbation introduced in the bilayer by the presence of the quencher appears to be small.

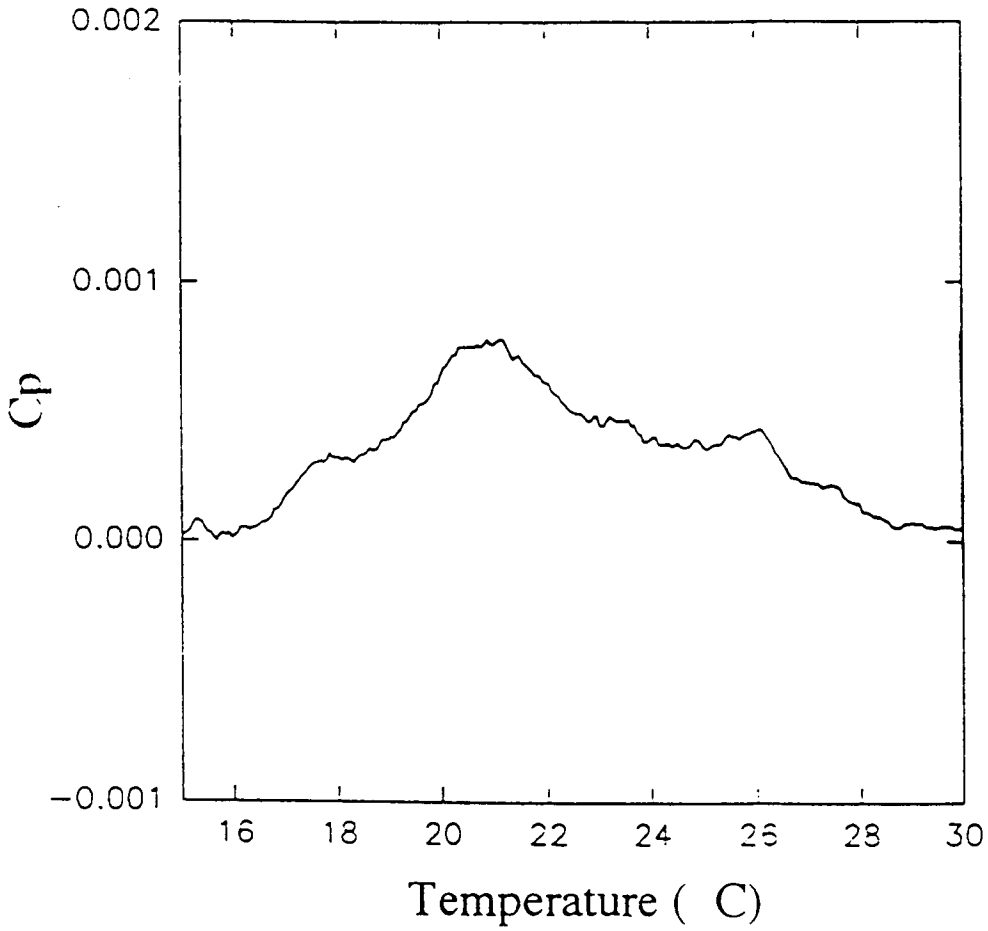


**Figure 7**

CALORIMETRIC STUDY

Plot of specific heat capacity, $C_p$, as a function of temperature for DMPC. The lipid concentration was 2.25 mM. To avoid aggregation of the vesicles, a cooling scan was performed.

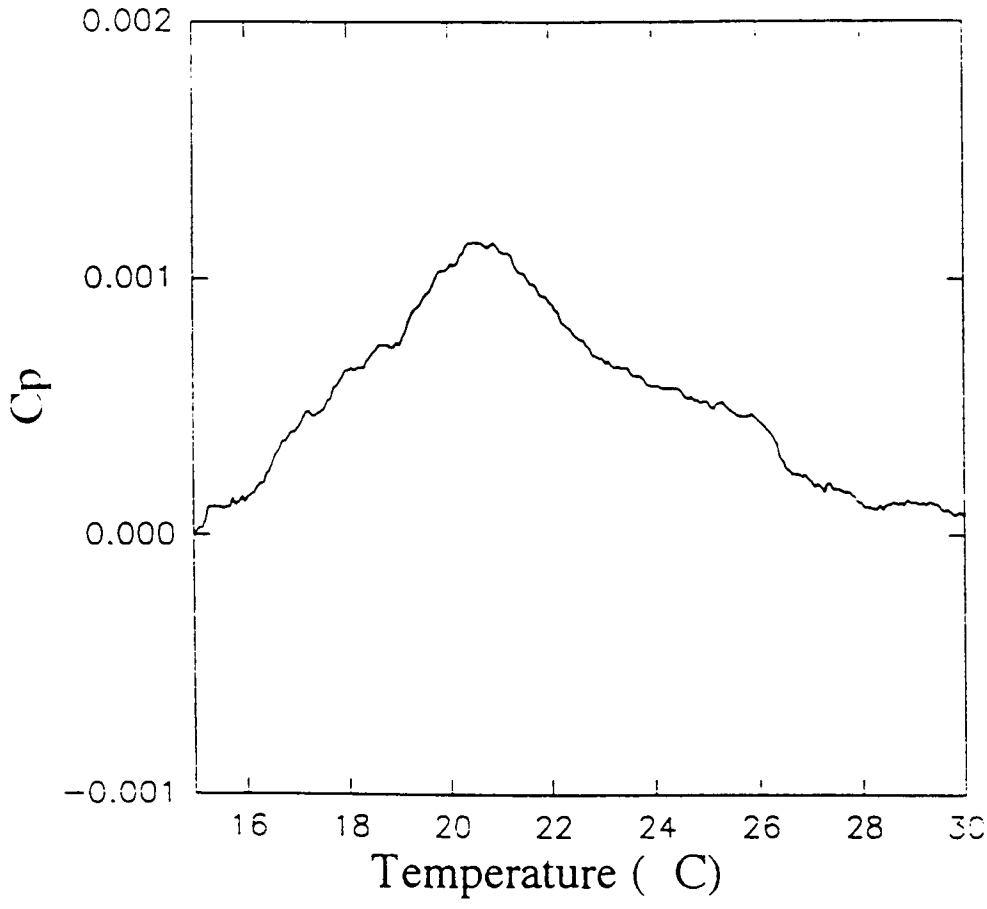


**Figure 8**

CALORIMETRIC STUDY

Plot of specific heat capacity, $C_p$, as a function of temperature for DMPC labelled with 5-DS. The lipid concentration was 2.25 mM and the mean occupation number of the quencher was $\eta = 74$. To avoid aggregation of the vesicles, a cooling scan was performed.

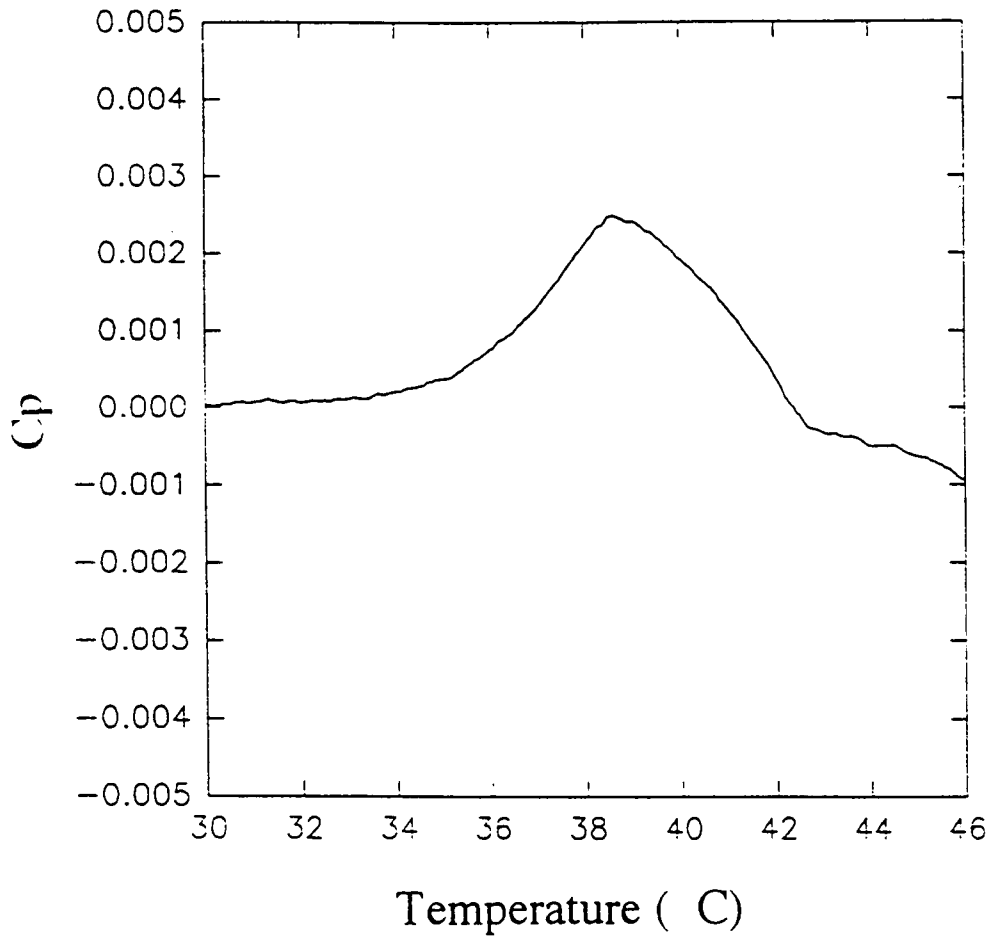


**Figure 9**

CALORIMETRIC STUDY

Plot of specific heat capacity, $C_p$, as a function of temperature for DPPC. The lipid concentration was 2.25 mM. To avoid aggregation of the vesicles, a cooling scan was performed.

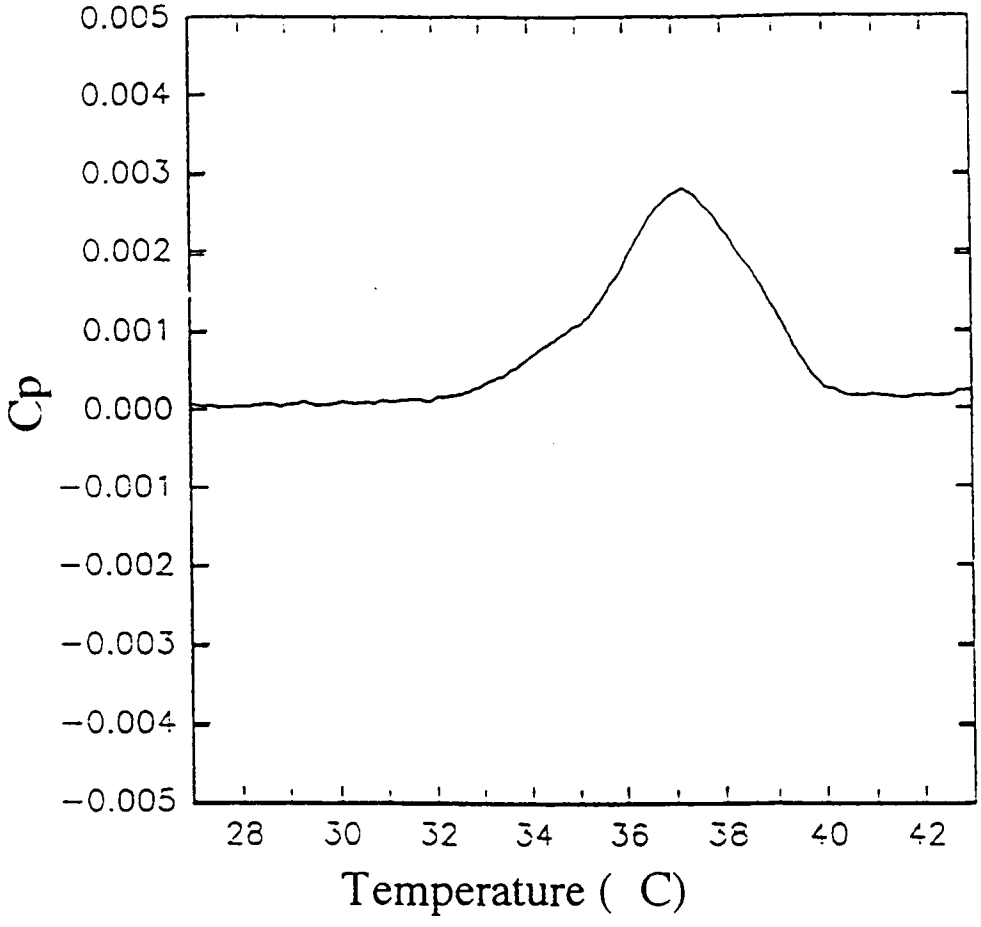


**Figure 10**

CALORIMETRIC STUDY

Plot of specific heat capacity, $C_p$, as a function of temperature for DPPC labelled with 5-DS. The lipid concentration was 2.25 mM and the mean occupation number of the quencher was $\eta = 74$. To avoid aggregation of the vesicles, a cooling scan was performed.

# ELECTRON MICROSCOPY

We have employed the technique of electron microscopy in order to investigate the possibility that the quenchers altered the morphology or size of the vesicles. The samples were prepared in the same manner as was previously discussed in the section on the Preparation of Vesicles. Dilute solutions were needed for electron microscopy, and so we used the lowest vesicle concentration in the fluorescence study or [Ves] = 0.55 μmol (see section on Mean Occupation Number,η). The sample was placed on a 400 mesh copper grid that was coated with 0.5% Formvar and a thin carbon layer. The sample was then stained with 1% aqueous Uranyl Acetate. The stained samples were examined in a H-600 Hitachi electron microscope at 100 KV.

We have found that there was no detectable effect on the appeaerance or the size of the vesicles by the quenchers. Figures 11 and 12 show DMPC in the absence and presence of 5-DS, respectively. Figures 13 and 14 show DPPC in the absence and presence of 5-DS, resectively. We have found that the average diameter of the SUVs was 275 Å ± 59 Å. This is in agreement with the results reported by Huang (1968) in the absence of quenchers. Regarding the micrographs for DMPC (Figures 11 and 12) some structures appear which are elongated. Here, the question is raised as to the stability of the samples used in this microscopy study in view of the fact that the DMPC vesicles are much less stable than the DPPC vesicles.

**Figure 11**

Electron micrograph of unlabelled DMPC. Samples were stained using 1% aqueous uranyl acetate. Photograph is at x100,000.

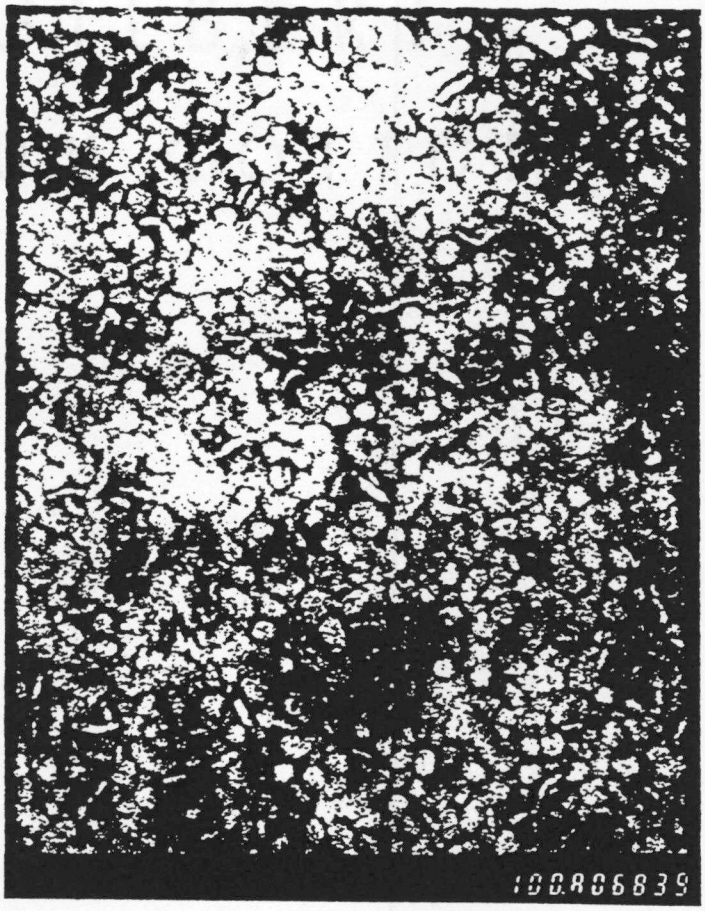


**Figure 12**

Electron micrograph of DMPC labelled with 5-DS. Samples were stained using 1% aqueous uranyl acetate. Photograph is at x100,000.

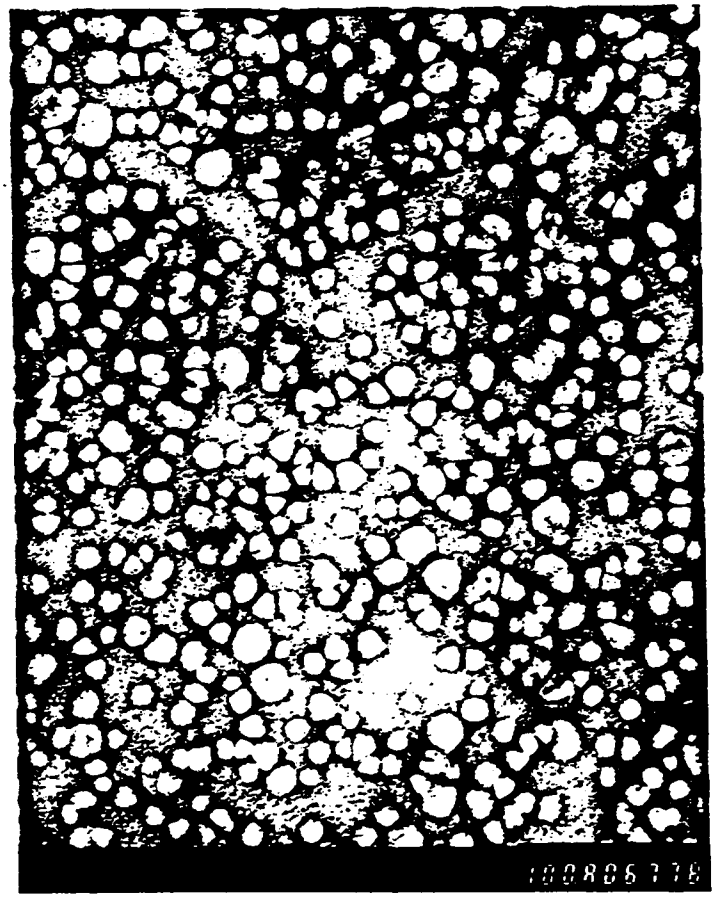

**Figure 13**

Electron micrograph of unlabelled DPPC. Samples were stained using 1% aqueous uranyl acetate. Photograph is at x100,000.

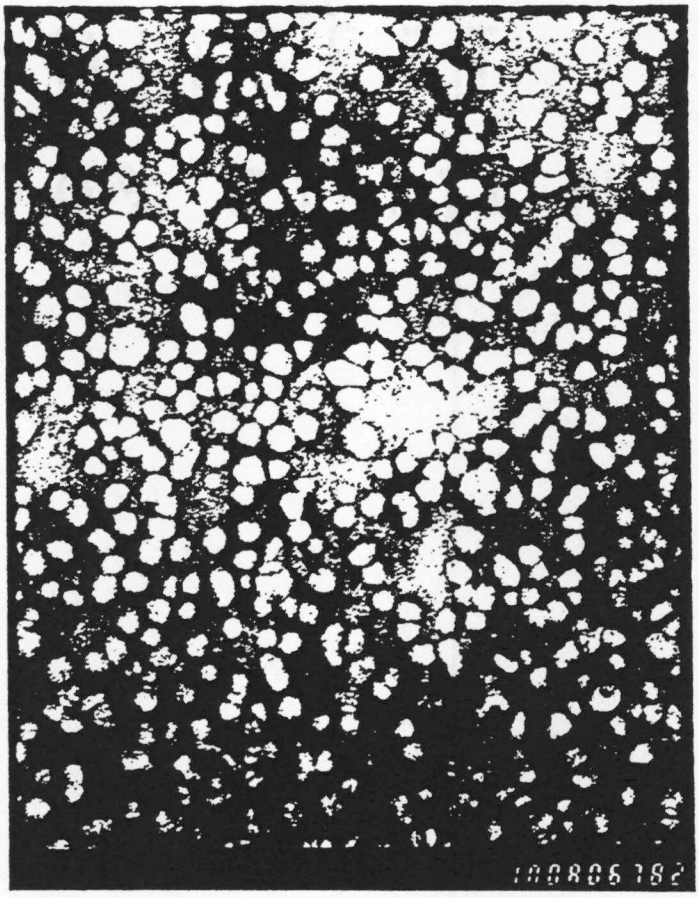

**Figure 14**

Electron micrograph of DPPC labelled with 5-DS. Samples were stained using 1% aqueous uranyl acetate. Photograph is at x100,000.

# PART 3.
# ANALYSIS

# REVIEWS OF LITERATURE USED IN THE ANALYSIS OF DATA.

## CALCULATION OF THE MEAN OCCUPATION NUMBER, $\eta$.

Proper analysis of quenching data requires a knowledge of exactly how many quenchers are in the lipid phase. Since the n-DS quenchers used in this study have an affinity for the vesicle bilayer which varies with the position of the quencher, n, it becomes necessary to determine the mean occupation number, $\eta$, in order to calculate the amount of quencher located in the lipid phase. The different affinities between the quenchers for association with the bilayer are thought to be due to steric hindrance, which increases as the doxyl group is placed further down the acyl chain. This method of analysis was first performed by Encinas and Lissi in 1982, and has shown itself to be very useful. (This is by no means a complete list of references where the method was used, but it gives the reader an idea of where to find some references on the subject: Encinas and Lissi, 1982; Sikaris, 1982; Chatelier, 1984; Blatt et al., 1984).

It will be assumed that the average vesicle in solution has a diameter of 250 Å. This is the value reported by Huang (1969), which is very similar to that of 275 Å we obtained (see section on Electron Microscopy) The number of lipid molecules in a typical SUV has been reported to be approximately equal to 2700 (Huang, 1969). The uncertainty in the number used for the total number of lipid molecules in an SUV was shown not to be affected by the labelling of the vesicles (see section on Electron Microscopy). Therefore, the concentration of vesicles, $[Ves]$, would be given by

$$[Ves] = \frac{[Lipid]}{2700} \tag{2}$$

The quantities in brackets are given in units of molar concentration. The average cross sectional area of a DMPC molecule is 65.7 $Å^2$ (Lewis, 1983). For reasons that will become apparent later, it is also necessary to know the volume of the lipid phase ($V_L$) and the volume of the aqueous phase ($V_A$). Obviously the total volume $V_T$ is equal to

$$V_T = V_A + V_L \tag{3}$$

The volume taken up by the lipid phase of a single, spherical vesicle, $V_{LSUV}$ , of radius $r_{SUV}$ = 125 Å is given by

$$V_{LSUV} = \frac{4}{3}\pi\left(r_{SUV}^3 - r_{Aq.C}^3\right) \tag{4}$$

where $r_{Aq.C}$ = 85 Å is the radius of the aqueous compartment (Huang, 1969). Now it is possible to derive $V_L$ in 1 ml of total volume aqueous solution, ($V_T$ = 1 ml).

$$V_L = \frac{V_{LSUV}[Ves]N}{1000} \tag{5}$$

Here, N is Avogadro's number. f is defined as the volume fraction,

$$f = \frac{V_A}{(V_A + V_L)} \tag{7}$$

Since $V_L << V_A$ , f≈1 (Encinas, 1982). It is now possible to write the following equation concerning the quencher concentrations [$Q_L$] and [$Q_A$] in the lipid and aqueous phase, respectively.

$$[Q_T] = [Q_L] + f[Q_A] \tag{6}$$

Note that at this point the concentration of the quencher is defined with respect to $V_T$. We now find it possible to evaluate the equilibrium constant, $K_{eq}$, in terms of the quencher concentrations in their various compartments (Blatt, 1984).

$$K_{eq} = \frac{[Q_L]}{[Q_A][Ves]} \tag{8}$$

The mean occupation number, $\eta$, is defined as the average number of quenchers in an SUV, so that

$$[Q_L] = \eta\,[Ves] \tag{9}$$

It has been shown by Encinas that

$$[Q_T] = \frac{\eta}{K_{eq}} + \eta[Ves] \tag{10}$$

A plot of $[Q_T]$ versus [Ves] allows the evaluation of $\eta$ from the slope and $K_{eq}$ from the y intercept. Any error in the [Ves] term because of an uncertainty in the number of lipid molecules per vesicle would have the tendency to change the magnitude of $\eta$ but would not significantly alter the trends observed in the data.

The n-DS quenchers have a variable affinity for association with the lipid bilayer. Therefore, they would all have different concentrations in the aqueous and bilayer environment, even when the concentration in the total volume is the same. Since the quenching of melittin in the aqueous environment can be considered as insignificant, we are concerned with the quenching in the lipid environment. Thus quenching would be dependent on the quencher concentration in the lipid phase. If corrections for differences in $\eta$ are not applied, the order of quenching efficiency thus determined may be incorrect.

If the fluorescence intensity of bound melittin in the presence of the quencher is defined as I, and that in the absence of quencher as $I_0$, then when one plots $\left[(I_o / I) - 1\right]$

versus $\eta$, the differences in $\eta$ for the different quenchers are taken into account. Thus, it is possible to establish the corrected Stern-Volmer plot of quenching efficiency for the different localizations of the doxyl group. When one is trying to locate a fluorophore's depth of insertion into the membrane, this is a key consideration since the concentration of quencher located in the vesicles is dependent on which position of n-DS is used. This is thought to be due to the 12-DS having more steric hindrance than the 5-DS (Blatt et al., 1984). Therefore, one must compare the quenching efficiencies for the different localizations of the doxyl stearic group at the same $\eta$ to determine precisely which position is more efficient. It is only in this way that one can start to make comments about the local environment of the tryptophan moeity, such as fluidity and segmental flexibility.

The procedure outlined above was used for the analysis of the data. This requires that a collection of data for $\left[(I_o / I) - 1\right]$ be made at different quencher and lipid concentrations. During any series of measurements, the concentration of the lipid is kept constant while the concentration of the quencher is varied. For the next series of measurements a different lipid concentration is needed. Once several different concentrations have yielded an $\left[(I_o / I) - 1\right]$ which is constant, it is possible to graph these results as indicated above for $\eta$. This was done for several different values of $\left[(I_o / I) - 1\right]$, which allowed the determination of $\eta$. It is in this way that the corrections were made to the Stern-Volmer plots and the order of the quenching efficiency of the n-DS probes in phospholipid vesicles was determined (this aspect becomes clear upon inspecting Figures 22 and 23, see below under Data Analysis). From the corrected order of quenching efficiency it should be a straightforward argument to place the tryptophan residue at a certain depth in the bilayer.

# THE PARALLAX METHOD

The relative quenching efficiencies of the different n-DS quenchers can be used to solve for the average distance of the fluorophore from the center of the bilayer. This method was introduced by London (1981). $R_c$ is defined as the critical radius of quenching for a fluorophore. Quenching is described in terms of a step function when a quencher is located within $R_c$

$$\frac{I}{I_0} = e^{-\pi R_c^2 C} \tag{11}$$

Here, I and $I_0$ are the intensities of fluorescence in the presence and absence of an n-DS quencher, respectively, and C is calculated by [(mole fraction of quencher lipid in total lipid)/(area of lipid in $Å^2$)] (see Abrams and London, 1992). The term $\pi R_c^2$ represents the area of a circle around the quencher in which fluorescence is completely extinguished. Since C is a function of the mole fraction of quencher lipid in the total lipid it should be independent of the size of the vesicle. Therefore, there is no uncertainty in the C term due to differing vesicle sizes.

It is possible to derive an expression to solve for the distance between the presumed quencher depth and the position of the fluorophore, $z_{nF}$, where n designates either 5,7, or 12-DS. C is used as a subscript, to designate the center of the bilayer . This method is described in London (1981) and Chattopadhay and London (1987). $L_{XY}$ is defined as the difference in depth between the two quencher locations being studied. If one is comparing 5-DS and 12-DS then one would use $L_{5\text{-}12}$ in the place of $L_{XY}$ below. The parameters $F_n$ are defined as follows

$$F_5 = I_5 / I_0 \qquad (12a,b,c)$$

$$F_7 = I_7 / I_0$$

$$F_{12} = I_{12} / I_0$$

The subscript, n, stands for the quencher position which is being used. The $F_n$ can be calculated from Tables 1 and 2 in the Data Analysis section by $\{1/([(I_o / I) - 1] + 1)\}$. The equation for the determination of $Z_{nf}$ is only dependent on C, $F_5$, $F_7$, $F_{12}$ and $L_{XY}$.

$$Z_{nf} = -\frac{\left(\frac{1}{\pi C}\ln\frac{F_L}{F_H} - L_{XY}^2\right)}{2L_{XY}} \qquad (13)$$

In equation (13) the subscripts of L and H on the F term stand for lower and higher depth, respectively. Thus, when comparing 5-DS and 12-DS we have to take the natural logarithm of $(F_5 / F_{12})$.

If $Z_{nf}$ is the difference between the depth of an n-DS and the tryptophan residue in melittin (see equation 13), then the distance from the center of the bilayer to the tryptophan, $Z_{Cf}$, is calculated from

$$Z_{cf} = Z_{nf} + L_{CL} \qquad (14)$$

Here, $L_{CL}$ is the distance from the center of the bilayer to the lower quencher. If one wants to compare 5-DS and 12-DS then one would use the $L_{C5}$, which is listed below, in the place of $L_{CL}$.

We will carry out this type of analysis for both DMPC and DPPC. In DMPC we also studied 7-DS but felt that the distance along the acyl chain between 5-DS and 7-DS was not sufficient to compare these two directly. This is why 7-DS was omitted in the DPPC experiments.

The x-ray crystallographic results of Chattopadhay and London provide strong support for the assumption that the depth of the doxyl stearic group is the same as the depth

of the carbon to which it is attached on the fatty acid (Chattopadhay and London, 1987). Therefore, we will use the depth of the n carbon along the fatty acid as analogous to the depth of the fluorophore. The parallax method has been applied to the data obtained in the present study and has allowed the determination of the mean depth of penetration of the tryptophan residue of melittin into the bilayer. We make the comparison at the highest concentration of quencher or $\eta = 74$.

What follows is a compilation of some of the constant values that are associated with the Parallax Method:

Thickness of the bilayer starting from the 1 position (Huang, 1969).

DMPC = 23 Å
DPPC = 26 Å

Average bond length

DMPC = 23 Å / 26 bonds
DPPC = 26 Å / 30 bonds

Let the mean number of quenchers located in a vesicle be
$\eta = 74$

Mole fraction of quenchers in the vesicle phase
M.F. = $\eta$ /(total number of lipids in a vesicle = 2700)

Surface area of a lipid

S.A. = 66 $Å^2$

C= M.F./ S.A. = $\eta$ /(2700 x 66 $Å^2$)
= 0.000417 $Å^{-2}$

Distances used in Parallax

DMPC-
$L_{C5}$ = 8.0 Å
$L_{C7}$ = 6.2 Å
$L_{5\text{-}12}$ = 6.1 Å
$L_{7\text{-}12}$ = 4.4 Å

DPPC-
$L_{C5}$ = 9.5 Å = length of 11 bonds (26 Å/30)
$L_{5\text{-}12}$ = 6.1 Å

# ANALYSIS OF DATA

The data for the quenching of melittin fluorescence by the n-DS located in both DMPC and DPPC lipid environments is provided in this section. All the measurements were made at 21° C and 37° C, which are the respective transition temperatures of DMPC and DPPC. Conclusive remarks will be postponed until the Discussion after the raw data are presented.

The intensity of scattered light is at a constant level. This level will be called g and must be subtracted from the total fluorescence signal. This quantity is equal to about 500 and 600 for DMPC and DPPC, respectively. The addition of the quencher does not in either case add significantly to the amount of scattered light.

When melittin binds to the lipid bilayer, there is a blue shift of the tryptophan fluorescence (Georghiou et al., 1982). This shift is a result of the protein leaving the polar environment of the aqueous solution when it binds to the lipid bilayer. As was discussed in the Introduction, the protein is thought to insert its tryptophan residue into the nonpolar environment of the bilayer. The 4-71 emission filter was chosen in an attempt to minimize the change in the fluorescence of tryptophan when melittin binds to the bilayer. Nevertheless, there was some change as a function of time and this is seen in Figures 15-18 for DMPC and DPPC. All fluorescence intensity graphs are then fitted to an exponential plus a constant equation. The intensity of fluorescence, $I_o$, in the case of melittin binding to an unlabelled vesicle is given by equation 15

$$I_o = \delta e^{-kt} + \text{constant} \qquad (15)$$

Thus, $\delta$ is the amount of fluorescence intensity change brought about by melittin binding. k is the apparent rate constant for melittin binding to an unlabelled vesicle.

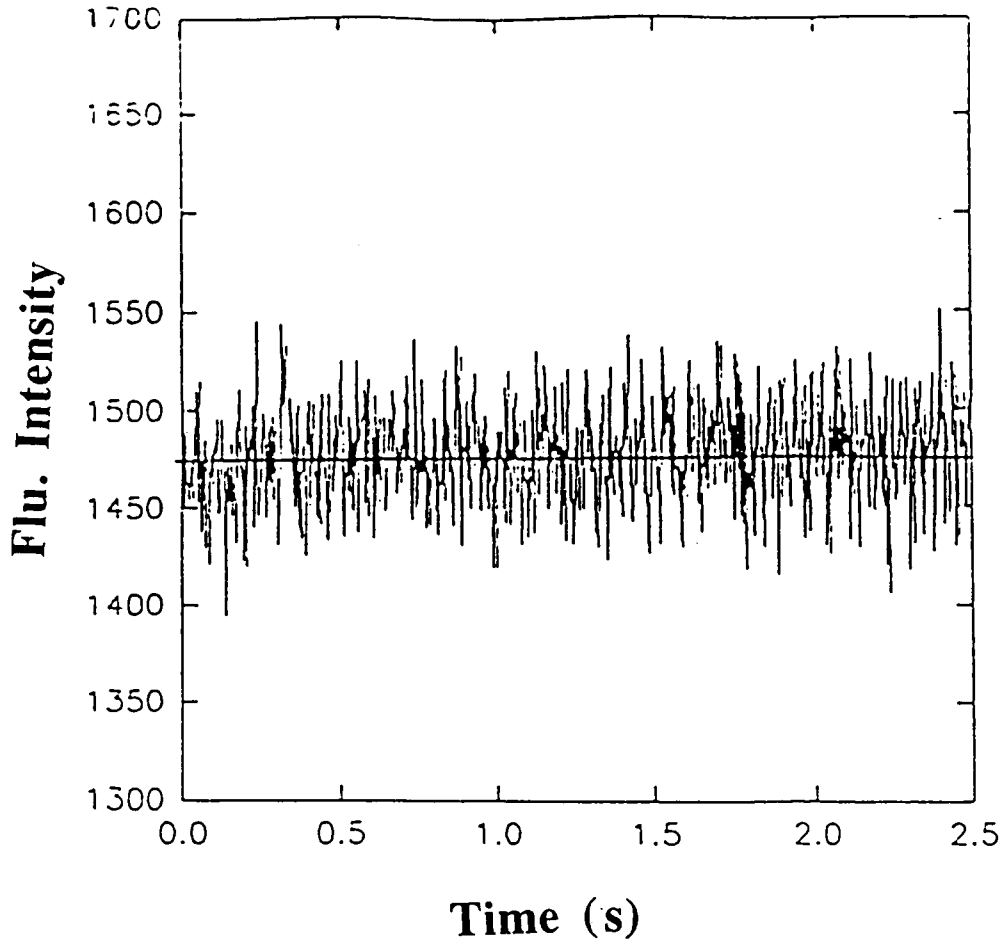


**Figure 15**

The fluorescence intensity of melittin plotted as a function of time when binding to DPPC,

[Ves] = 0.55 μmol.

$\partial = 0 \pm 25$

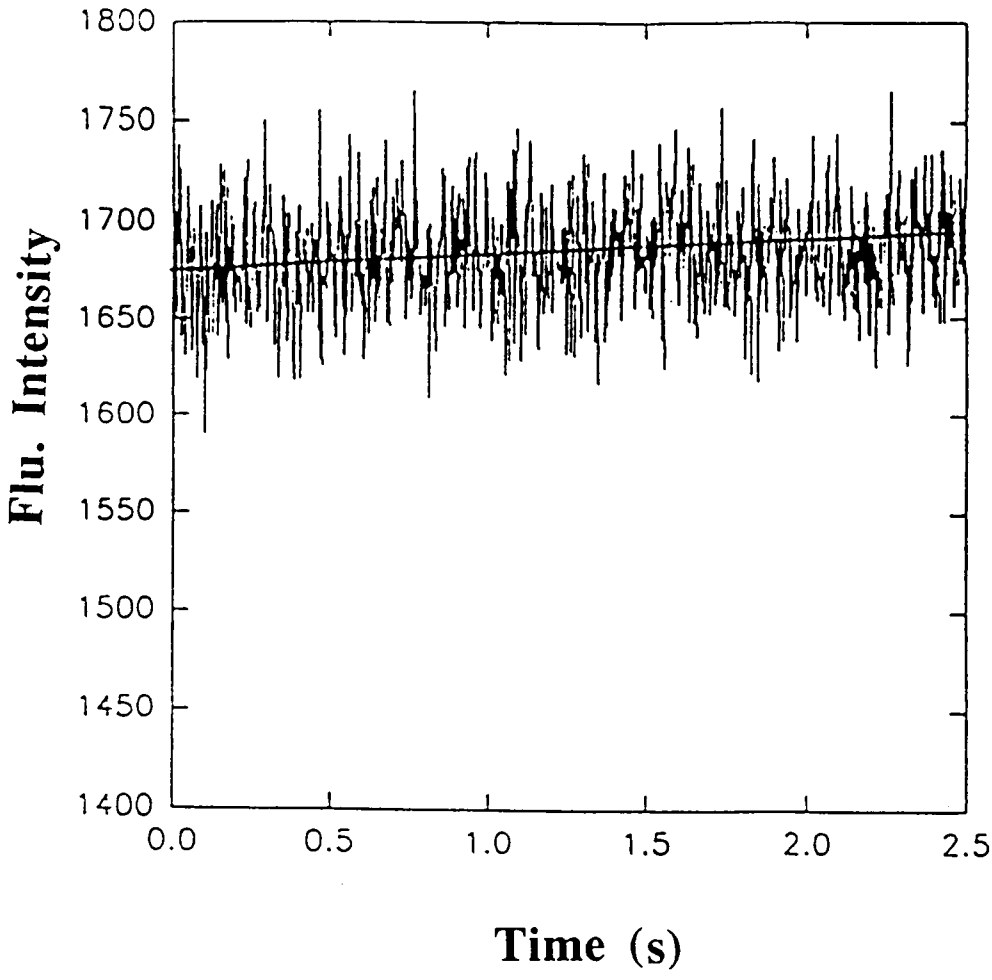


**Figure 16**

The fluorescence intensity of melittin plotted as a function of time when binding to DPPC,

[Ves] = 0.83 μmol.

$\partial = 25 \pm 25$

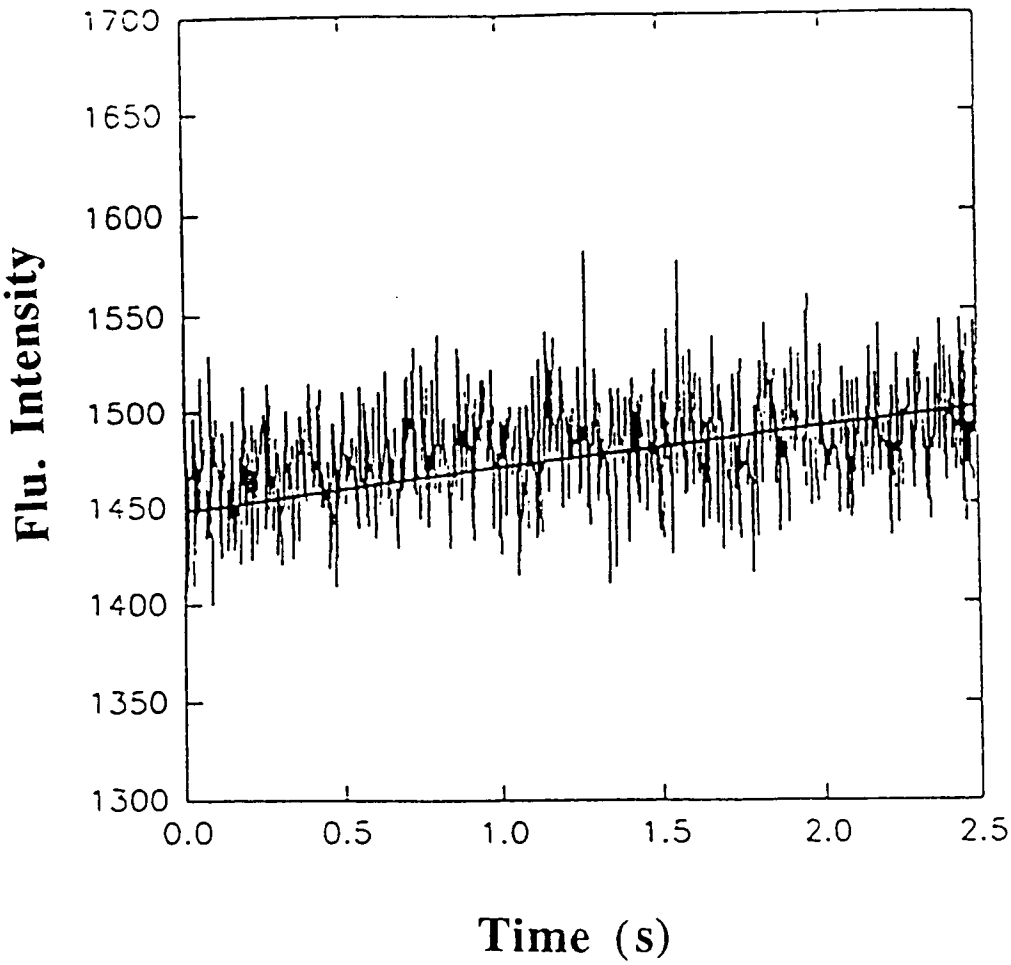


**Figure 17**

The fluorescence intensity of melittin plotted as a function of time when binding to DPPC,

[Ves] = 1.10 μmol.

$\partial = 50 \pm 25$

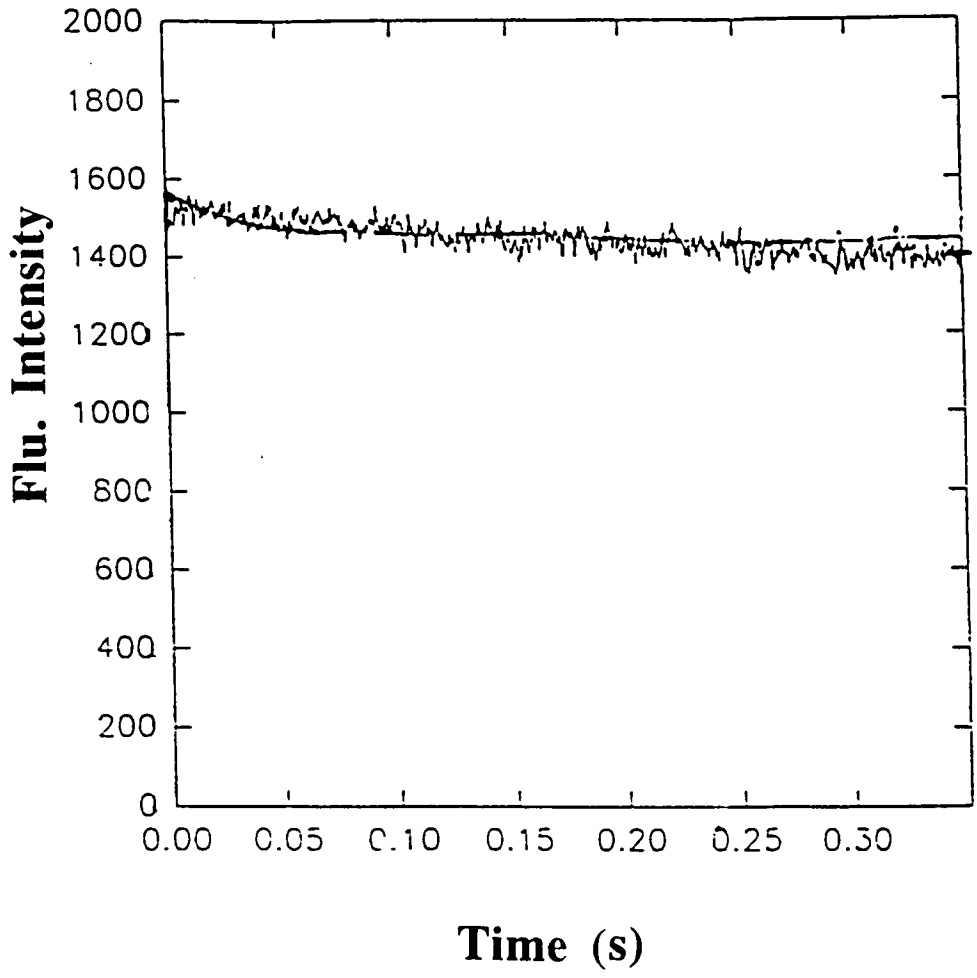


**Figure 18**

The fluorescence intensity of melittin plotted as a function of time when binding to DPPC,

[Ves] = any concentration.

$\partial = 175 \pm 25$

$k = 3.5 \pm 0.5\ s^{-1}$

In the case of melittin binding to unlabelled DPPC, $\delta$ has been found to be very small and to vary from virtually 0 to about 25 and 50 for the vesicle concentrations of 1.1 μmol, 0.83 μmol and 0.55 μmol, respectively (see Figures 15-17). Thus, in DPPC it was found that the amount of change in the unlabelled curve was dependent on the concentration of the lipid. Since $\delta$ was very small for DPPC, it was not practical to determine values for k (see Figures 15-17). In the case of melittin binding to unlabelled DMPC, the fluorescence intensity was found to drop as a function of time. For this case the values of $\delta$ and k are 175 and 3.5 $s^{-1}$, respectively (see Figure 18). These values were found to be independent of vesicle concentration and were used for the analysis of the data.

The quenching curves of melittin fluorescence by the n-DS incorporated into DMPC vesicles are shown in Figures 19. By using a nonlinear least-squares minimization technique, the Marquardt method, the following single exponential plus a constant equation

$$I = A\, e^{-k_2 t} + B \tag{16}$$

was fitted to the plots of fluorescence intensity as a function of time. A is the magnitude of the drop in fluorescence intensity and B can be considered the final value that the fluorescence intensity drops to at long times. The apparent rate for quenching, $k_2$, can be considered to approximately be the sum of the rate of binding, k, and the true rate of quenching, $k_1$

$$k_2 = k + k_1 \tag{17}$$

A complete list of the values of $k_2$ as a function of $\eta$ is shown in Table 1. As was stated above k was very small, equal to about 3.5 $s^{-1}$. Consequently, the trend shown in Table 1 for the values of $k_2$is not significantly altered.

A comparison of the values for the rate $k_2$ for 5-DS and 12-DS shows that 12-DS actually quenches the fluorophore faster (see Table 1). This is consistent with the fact that

**Table 1 -** Values for the parameters for quenching of the fluorescence of the tryptophan of melittin incorporated into DMPC SUVs for the three n-doxyl stearic acid quenchers.

DMPC

5-DS

| η | A | B | $k_2$ ($s^{-1}$) | $[(I_o / I) - 1]$ |
|---|---|---|---|---|
| 29 | 473 ± 30 | 1208 ± 22 | 13 ± 1 | 0.34 ± 0.02 |
| 35 | 652 ± 25 | 1045 ± 10 | 23 ± 1 | 0.66 ± 0.03 |
| 66 | 791 ± 26 | 918 ± 18 | 39 ± 3 | 1.04 ± 0.04 |
| 74 | 814 ± 26 | 865 ± 16 | 55 ± 3 | 1.19 ± 0.03 |

7-DS

| η | A | B | $k_2$ ($s^{-1}$) | $[(I_o / I) - 1]$ |
|---|---|---|---|---|
| 29 | 506 ± 25 | 1212 ± 13 | 14 ± 1 | 0.35 ± 0.03 |
| 37 | 559 ± 15 | 1088 ± 14 | 21 ± 2 | 0.50 ± 0.03 |
| 63 | 696 ± 21 | 1020 ± 32 | 40 ± 4 | 0.75 ± 0.04 |
| 74 | 760 ± 42 | 957 ± 42 | 56 ± 4 | 0.93 ± 0.03 |

12-DS

| η | A | B | $k_2$ ($s^{-1}$) | $[(I_o / I) - 1]$ |
|---|---|---|---|---|
| 29 | 477 ± 11 | 1076 ± 11 | 22 ± 2 | 0.37 ± 0.03 |
| 43 | 593 ± 29 | 1238 ± 35 | 35 ± 3 | 0.46 ± 0.03 |
| 62 | 690 ± 23 | 1061 ± 24 | 47 ± 4 | 0.70 ± 0.03 |
| 71 | 824 ± 46 | 1080 ± 39 | 69 ± 5 | 0.84 ± 0.04 |

**Figure 19**

The fluorescence intensity is plotted as a function of time for DMPC which is labelled with an n-DS quencher. (The particular n-DS which is being used, the mean occupation number for the quencher in the vesicle phase, the concentration of the lipid, the quenching efficiency, $\left[(I_o / I) - 1\right]$, and the apparent rate of quenching, $k_2$, are indicated on each figure.) The lipid-protein ratio was 90 and the sample temperature was 21 C. The best fit to equation (16) is shown as a smooth line in the plot. The residuals of the fit for all the figures are shown in the Appendix for Figures. The constants A and B obtained from these fits are listed in Table 1.

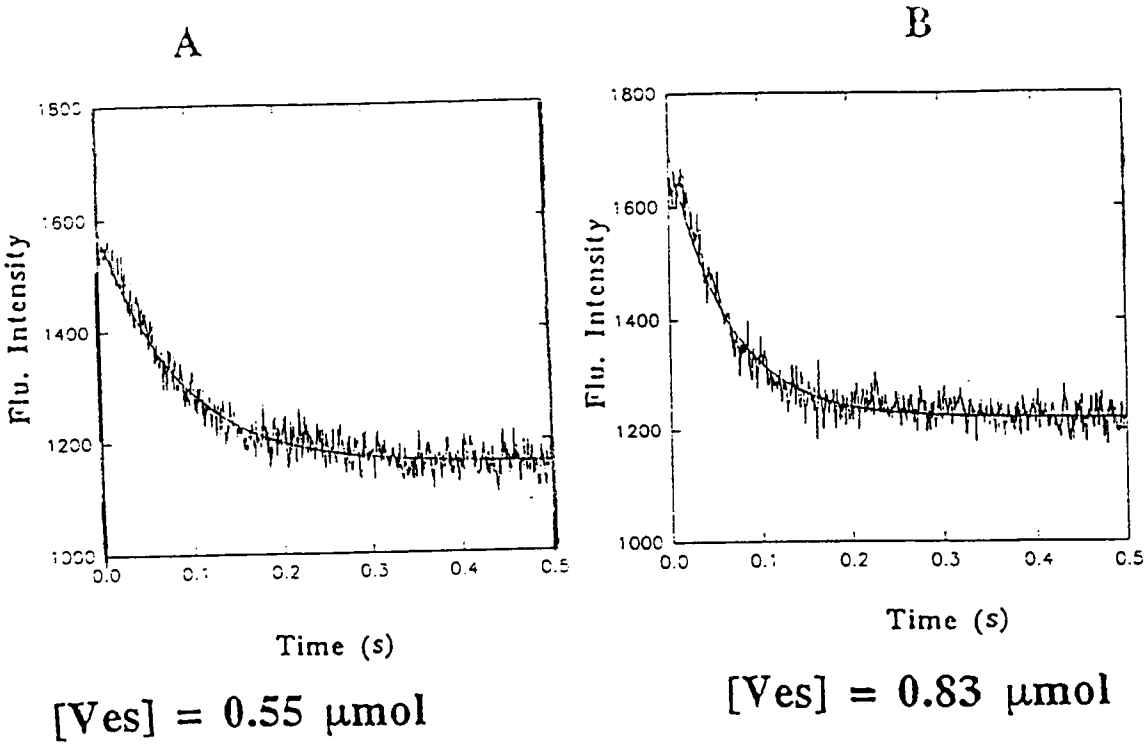


**Figure 19.1**
DMPC labelled with 5-DS.

$\eta = 29$

$k_2 = 13 \pm 1\ s^{-1}$

$[(I_o / I) - 1] = 0.34 \pm 0.02$

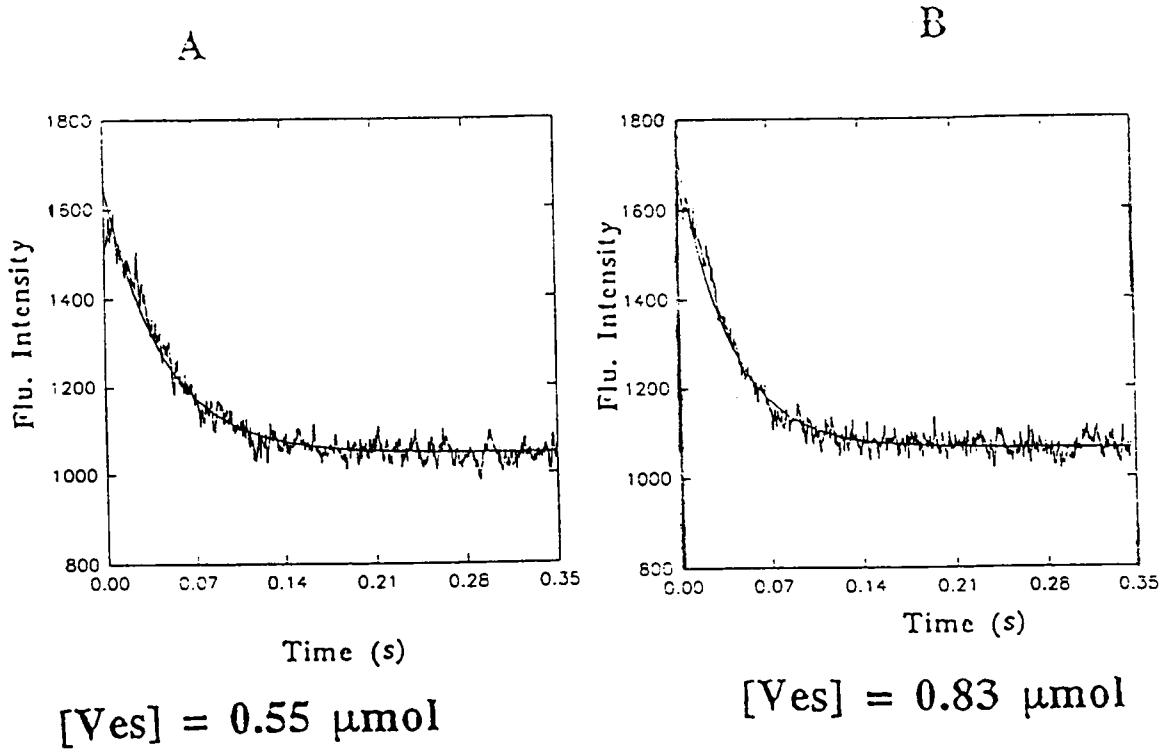


**Figure 19.2**

DMPC labelled with 5-DS.

$\eta = 35$

$k_2 = 23 \pm 2\ s^{-1}$

$[(I_o / I) - 1] = 0.66 \pm 0.03$

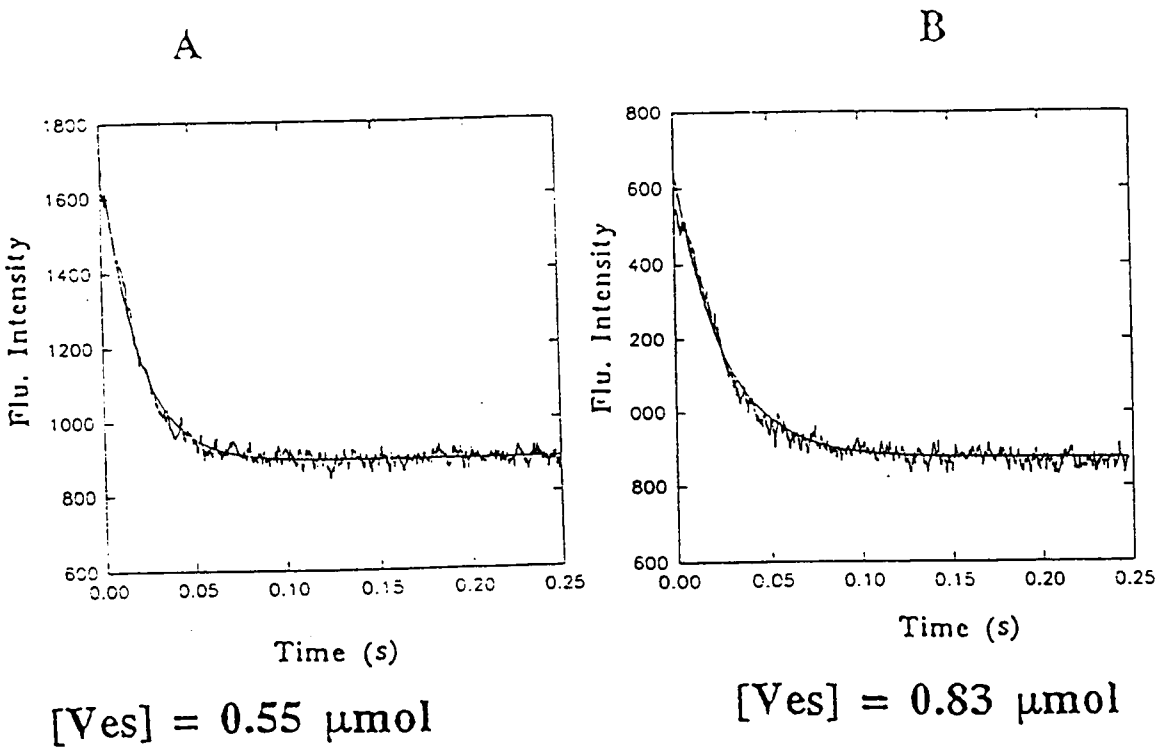


**Figure 19.3**

DMPC labelled with 5-DS.

$\eta = 66$

$k_2 = 39 \pm 3\ s^{-1}$

$\left[(I_o / I) - 1\right] = 1.04 \pm 0.04$

A

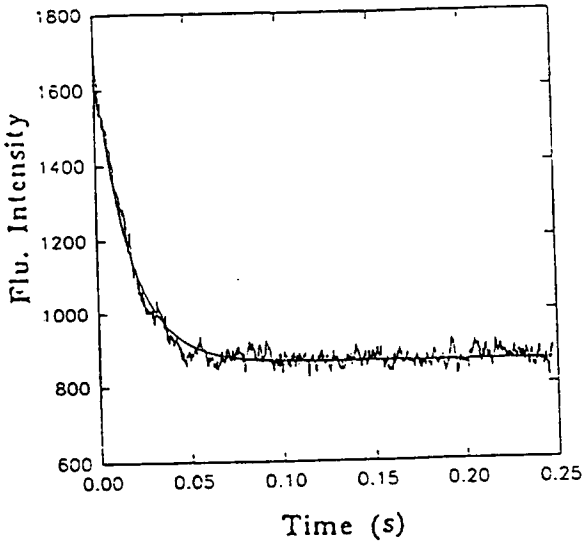


[Ves] = 0.55 μmol

B

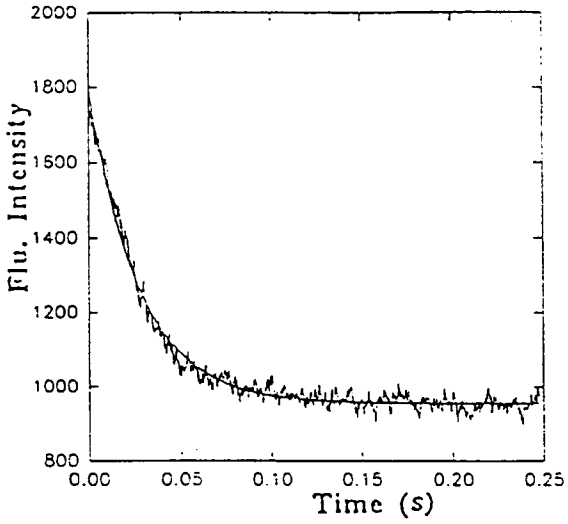


[Ves] = 0.83 μmol

C

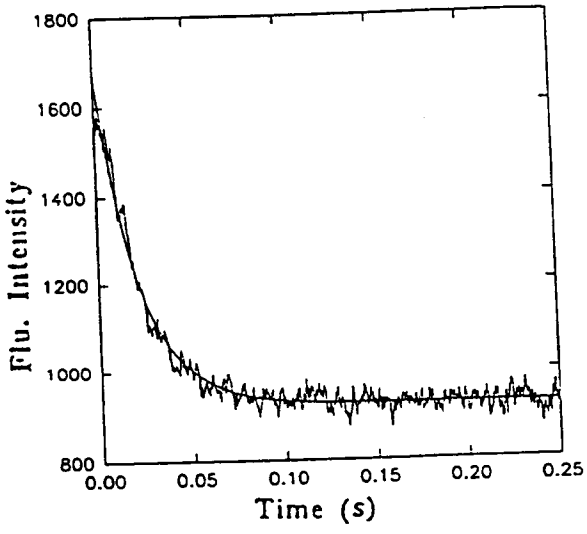


[Ves] = 1.10 μmol

**Figure 19.4**

DMPC labelled with 5-DS.

$\eta = 74$

$k_2 = 55 \pm 3\ s^{-1}$

$[(I_o / I) - 1] = 1.19 \pm 0.03$

A

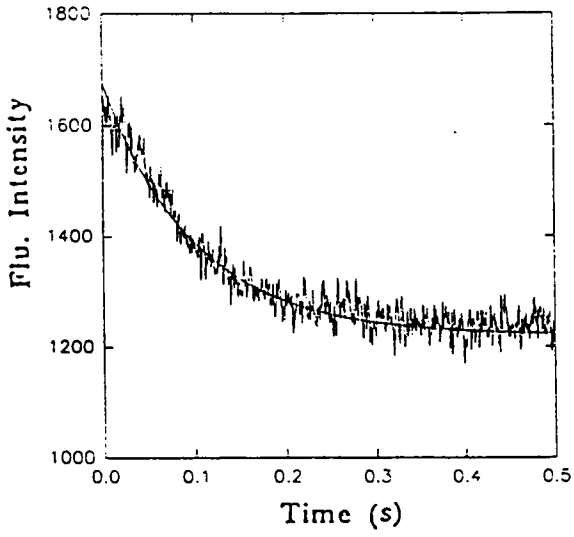


[Ves] = 0.55 μmol

B

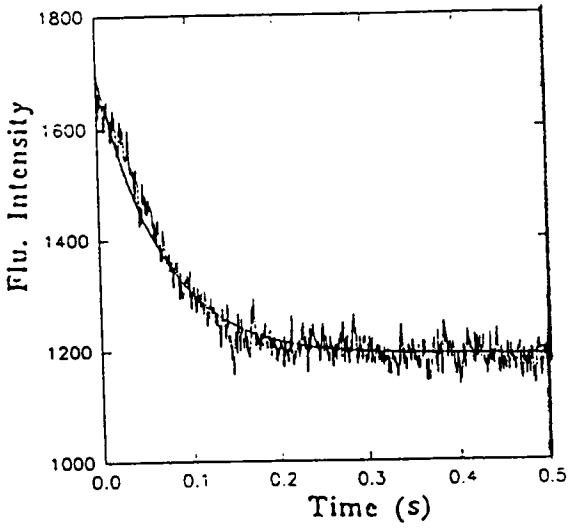


[Ves] = 0.83 μmol

C

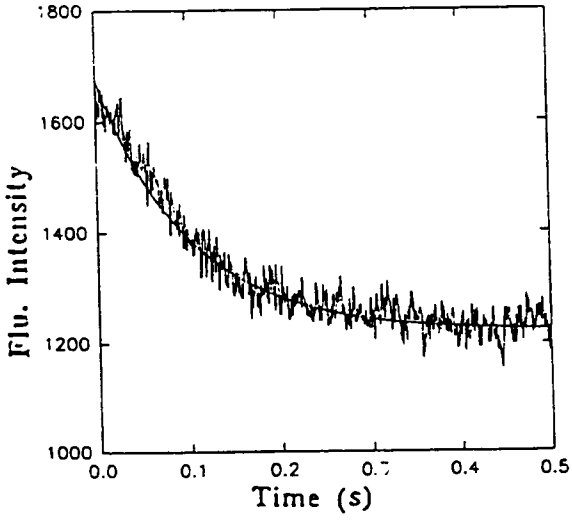


[Ves] = 1.10 μmol

**Figure 19.5**

DMPC labelled with 7-DS.

$\eta = 29$

$k_2 = 14 \pm 1\ s^{-1}$

$[(I_o / I) - 1] = 0.35 \pm 0.02$

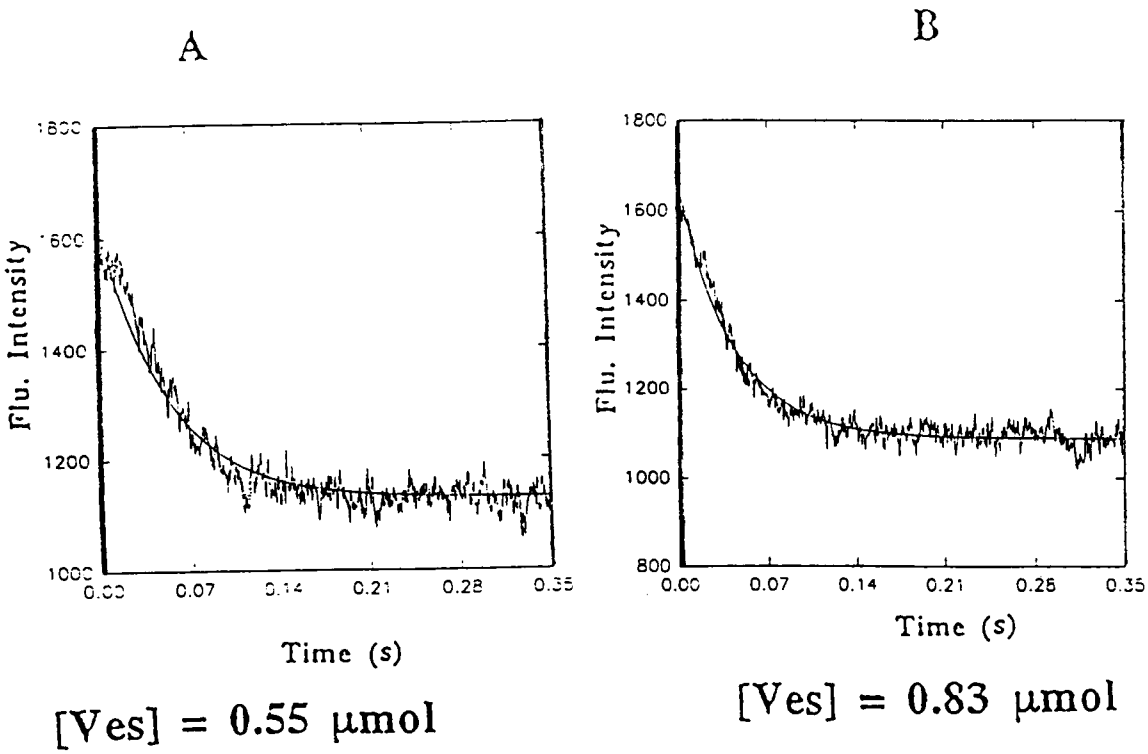


**Figure 19.6**

DMPC labelled with 7-DS.

$\eta = 35$

$k_2 = 21 \pm 2\ s^{-1}$

$\left[(I_o / I) - 1\right] = 0.50 \pm 0.03$

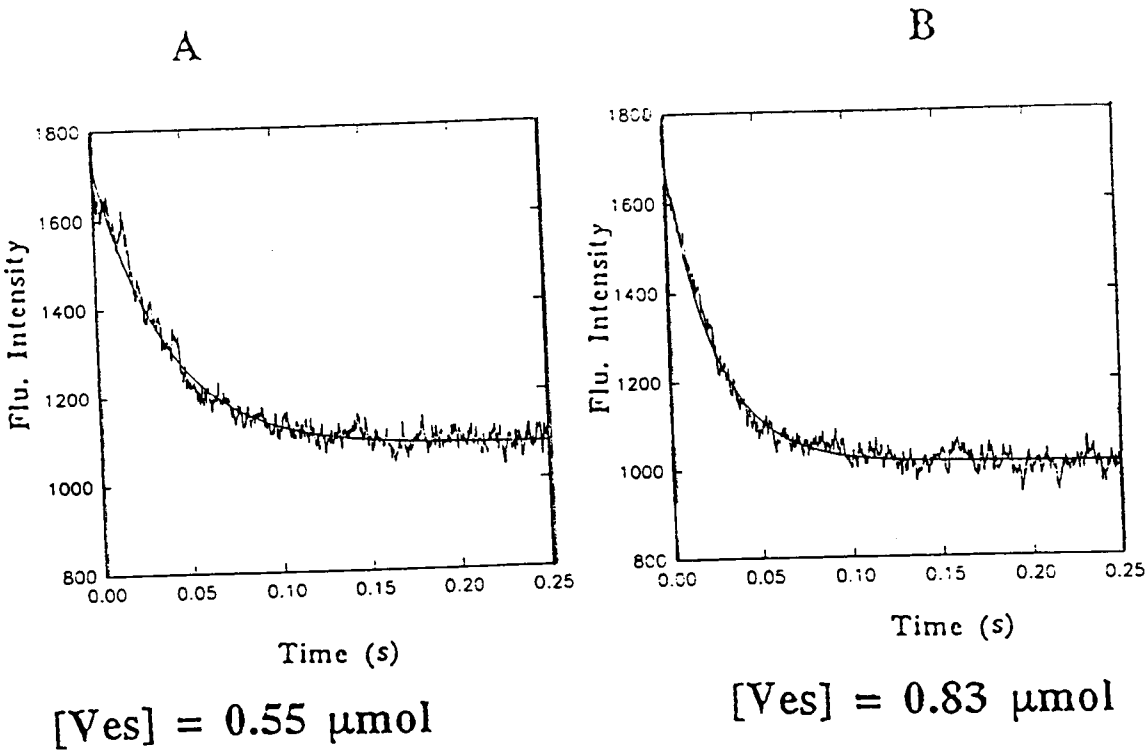


**Figure 19.7**

DMPC labelled with 7-DS.

$\eta = 63$

$k_2 = 40 \pm 4\ s^{-1}$

$[(I_o / I) - 1] = 0.75 \pm 0.04$

A

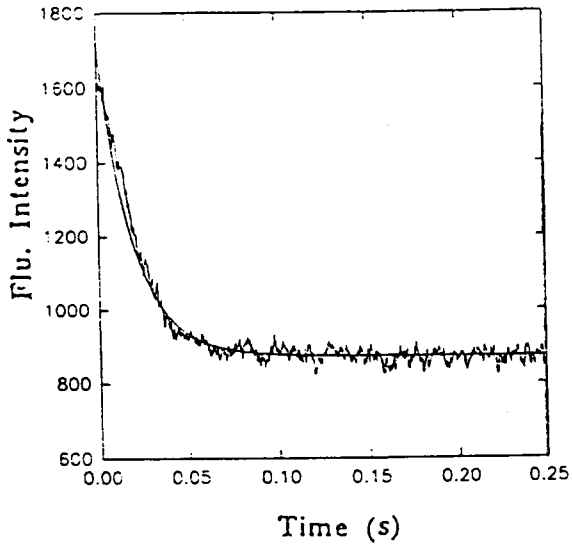


[Ves] = 0.55 μmol

B

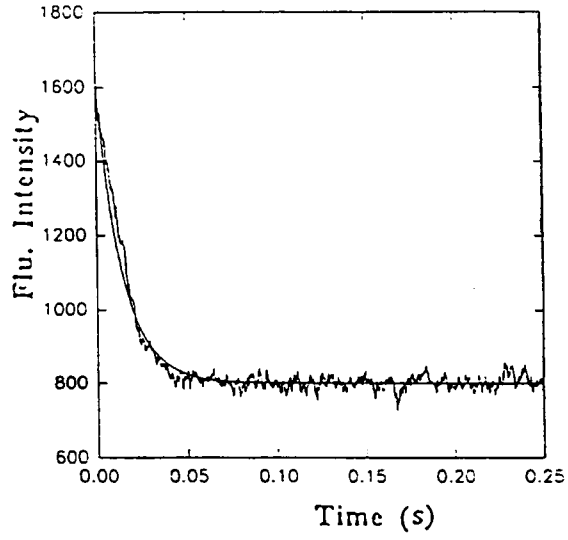


[Ves] = 0.83 μmol

C

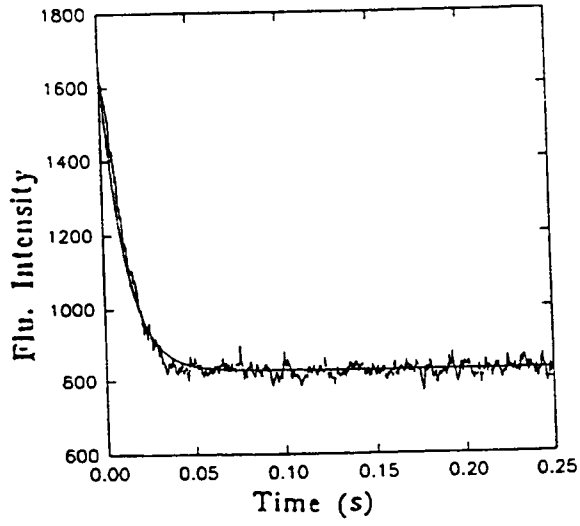


[Ves] = 1.10 μmol

**Figure 19.8**

DMPC labelled with 7-DS.

$\eta = 74$

$k_2 = 56 \pm 6\ s^{-1}$

$[(I_o / I) - 1] = \quad 0.93 \pm 0.03$

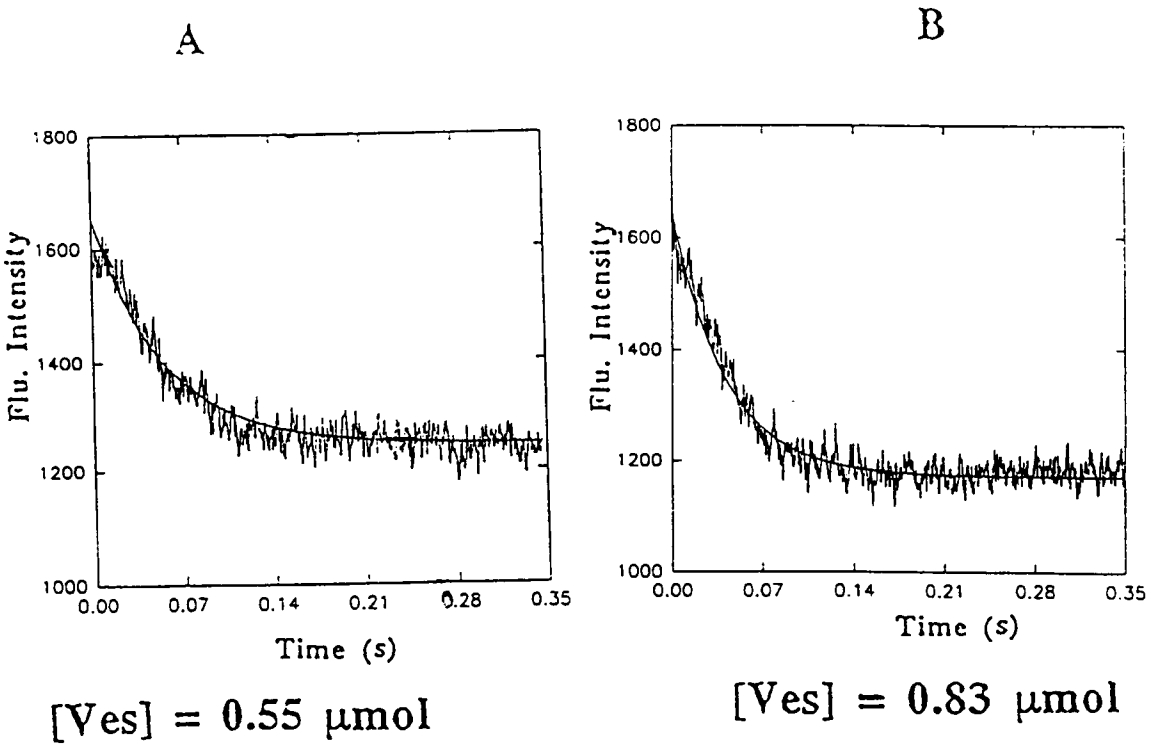


**Figure 19.9**

DMPC labelled with 12-DS.

$\eta = 29$

$k_2 = 22 \pm 1\ s^{-1}$

$[(I_o / I) - 1] = 0.37 \pm 0.03$

A

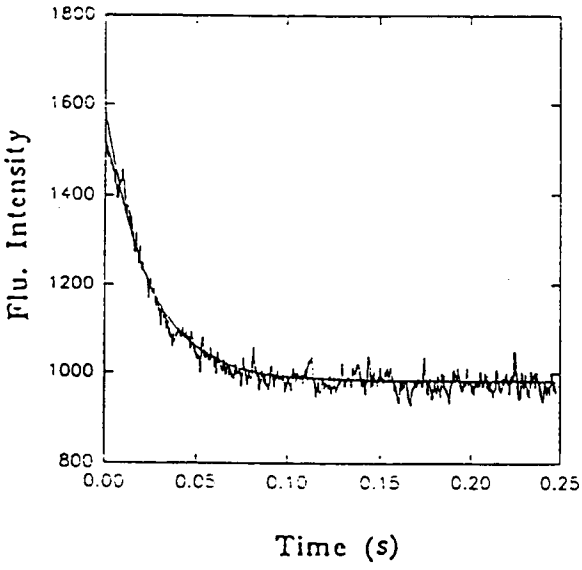


[Ves] = 0.55 μmol

B

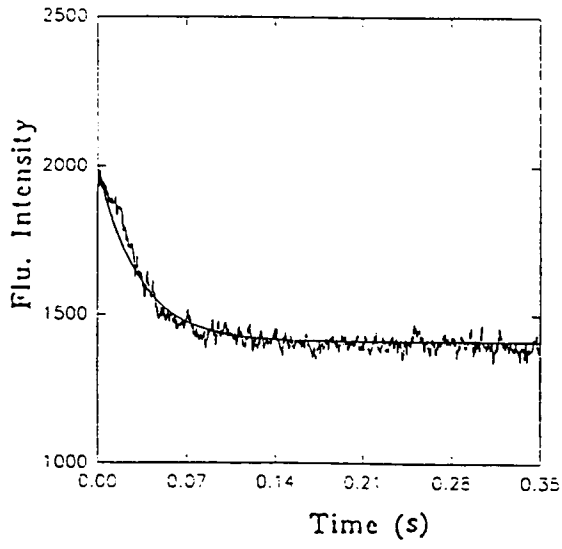


[Ves] = 0.83 μmol

C

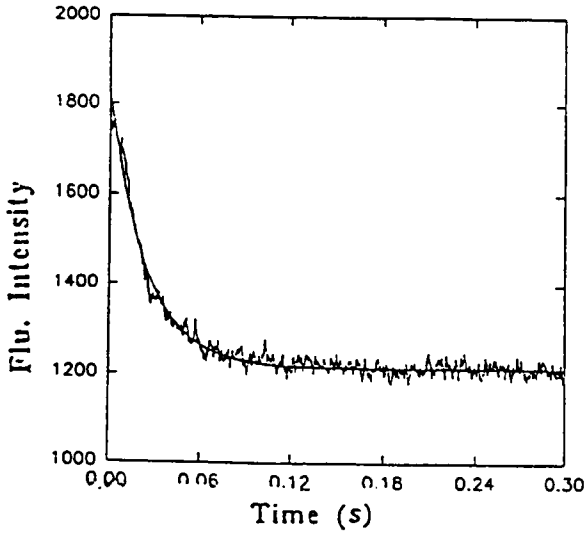


[Ves] = 1.10 μmol

**Figure 19.10**

DMPC labelled with 12-DS.

$\eta = 35$

$k_2 = 35 \pm 3\ s^{-1}$

$[(I_o / I) - 1] = 0.46 \pm 0.03$

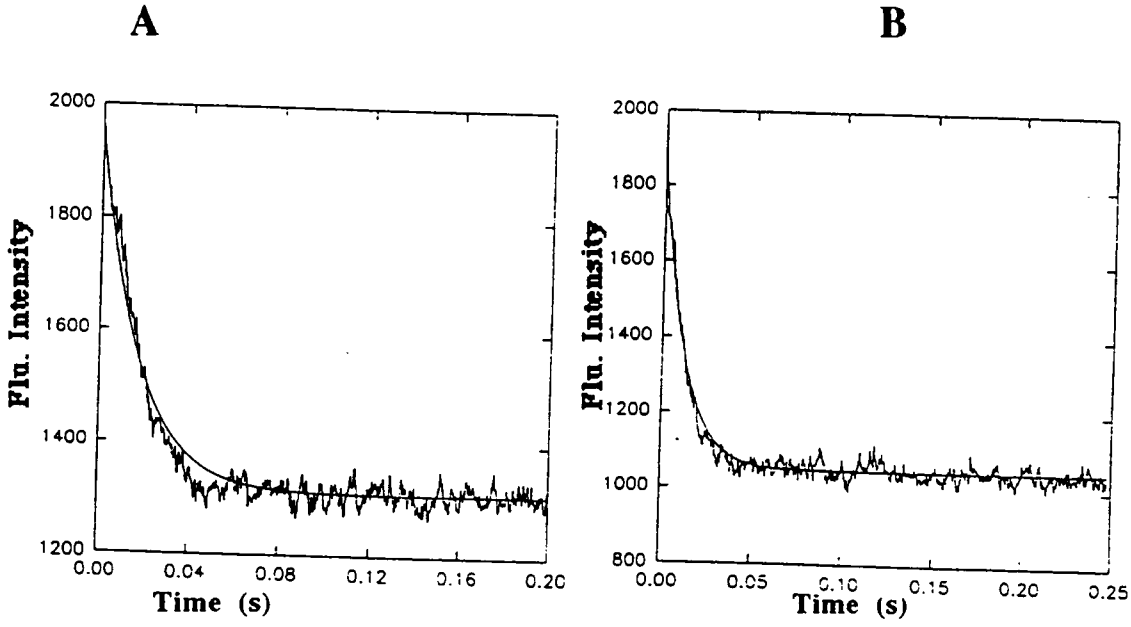


[VES] = 0.55 μmol

[VES] = 0.83 μmol

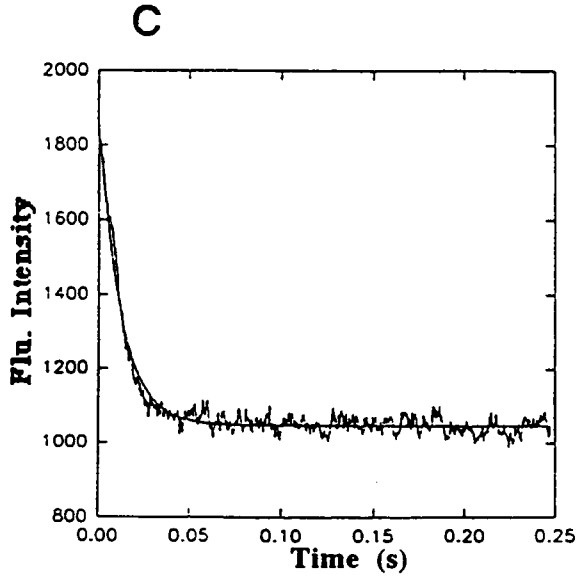


**[Ves] = 1.10 μmol**

**Figure 19.11**

DMPC labelled with 12-DS.

$\eta = 62$

$k_2 = 47 \pm 4\ s^{-1}$

$\left[(I_o / I) - 1\right] = 0.70 \pm 0.03$

A

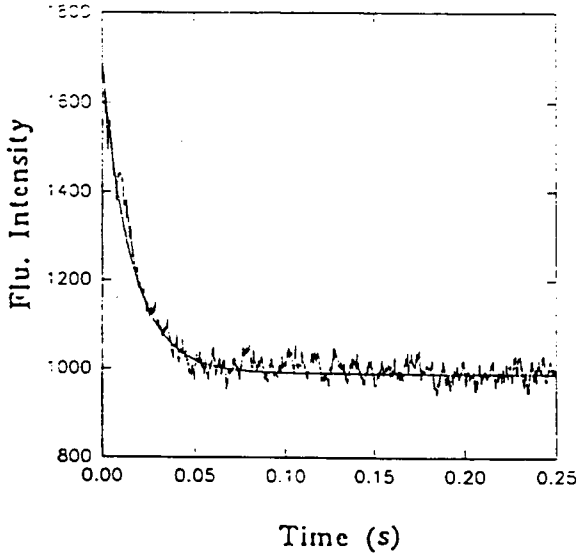


[Ves] = 0.55 μmol

B

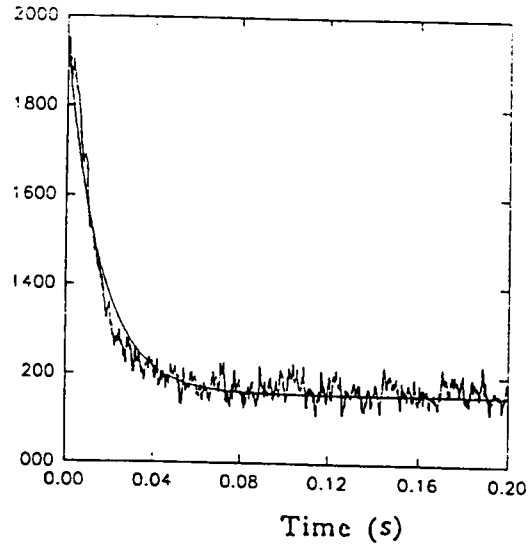


[Ves] = 0.83 μmol

C

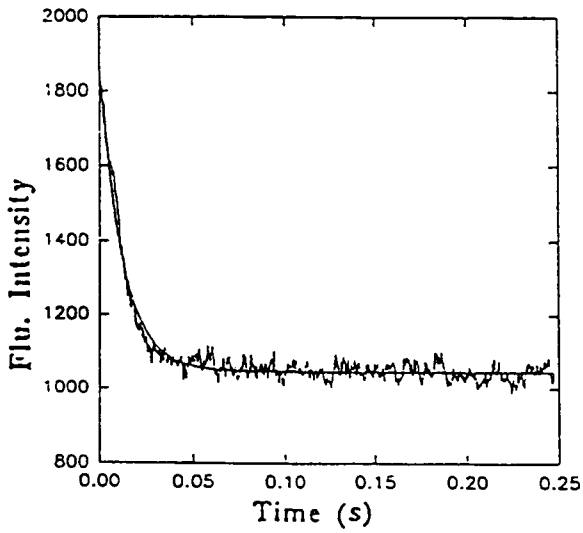


[Ves] = 1.10 μmol

**Figure 19.12**

DMPC labelled with 12-DS.

$\eta = 71$

$k_2 = 69 \pm 7\ s^{-1}$

$\left[(I_o / I) - 1\right] = 0.84 \pm 0.04$

12-DS has a much larger area of interaction because of increased segmental flexibility as one proceeds from the glycerol region toward the methyl groups of the acyl chains (Marsh, 1990) (see Discussion).

In the case of DPPC it is more difficult to find an equation that is suitable to describe the fluorescence quenching. A sample graph of quenching over a 1s time scale (see below for example such as Figure 20.4) shows why this is the case. First, there is an extremely fast drop that is too fast for the fluorometer to resolve. On the millisecond time scale there is a smooth drop which stems from slower quenching. There is then a slower drop that occurs on the time scale of seconds. Consequently, we have employed a double exponential function to model the quenching decay curve using the Scientist computer program for an IBM PC. In this model,

$$I = A_1 e^{-k_F t} + A_2 e^{-k_S t} + B \tag{18}$$

where I is fluorescence intensity as a function of time, B is the level to which the fluorescence intensity drops at long times, and $k_f$ and $k_S$ are the fast and slow rate constants, respectively. The total amplitude, A, in the drop of the fluorescence intensity observed is merely the sum of $A_1$ and $A_2$

$$A = A_1 + A_2 \tag{19}$$

Because of the occurrence of a very fast drop in the fluorescence intensity within the dead time of the fluorometer for DPPC, we have

for DPPC $\quad I_o \neq A + B$ , whereas (20a)

for DMPC $\quad I_0 = A + B$ (20b)

We have found it necessary to use the level of the unlabelled DPPC curve to establish $I_o$. See Table 2 for the results of the DPPC experiment. The graphs of the quenching of melittin fluorescence by n-DS incorporated in DPPC vesicles are shown in Figure 20.

**Table 2** - Values for the parameters for quenching of the fluorescence of the tryptophan of melittin incorporated into DPPC SUVs for the two n-doxyl stearic acid quenchers.

DPPC
5-DS

| $\eta$ | $A_1$ | $A_2$ | B | $k_F$ ($s^{-1}$) | $k_S$ ($s^{-1}$) | $[(I_o / I) - 1]$ |
|---|---|---|---|---|---|---|
| 29 | 107 ± 14 | 42 ± 16 | 1328 ± 24 | 37 ± 2 | 2 ± 0.5 | 0.33 ± 0.04 |
| 35 | 138 ± 17 | 37 ± 15 | 1301 ± 18 | 39 ± 3 | 2 ± 0.5 | 0.38 ± 0.03 |
| 68 | 275 ± 23 | 125 ± 13 | 881 ± 35 | 41 ± 4 | 2 ± 0.5 | 1.89 ± 0.17 |
| 74 | 284 ± 27 | 118 ± 42 | 834 ± 51 | 63 ± 12 | 7 ± 0.5 | 2.29 ± 0.23 |

12-DS

| $\eta$ | $A_1$ | $A_2$ | B | $k_F$ ($s^{-1}$) | $k_S$ ($s^{-1}$) | $[(I_o / I) - 1]$ |
|---|---|---|---|---|---|---|
| 29 | 142 ± 34 | 52 ± 28 | 1384 ± 41 | 37 ± 2 | 2 ± 0.5 | 0.24 ± 0.05 |
| 34 | 181 ± 15 | 61 ± 33 | 1245 ± 35 | 38 ± 2 | 2 ± 0.5 | 0.48 ± 0.07 |
| 63 | 185 ± 35 | 125 ± 15 | 1063 ± 49 | 61 ± 6 | 2.5 ± 0.5 | 0.95 ± 0.15 |
| 71 | 213 ± 56 | 130 ± 23 | 993 ± 28 | 98 ± 8 | 3.5 ± 1 | 1.23 ± 0.12 |

**Figure 20**

The fluorescence intensity is plotted as a function of time for DPPC which is labelled with an n-DS quencher. (The particular n-DS which is being used, the mean occupation number for the quencher in the vesicle phase, the concentration of the lipid, the quenching efficiency, $\left[(I_o / I) - 1\right]$, and the rates of quenching, $k_F$ and $k_S$, are indicated on each figure.) The lipid-protein ratio was 90 and the sample temperature was $37^{o}$ C. The best fit to the double exponential equation (18) is shown as a smooth line in the plot. The residuals of the fit for all the figures are shown in the Appendix for Figures. The constants $A_1$, $A_2$ and B obtained from these fits are listed in Table 2.

A

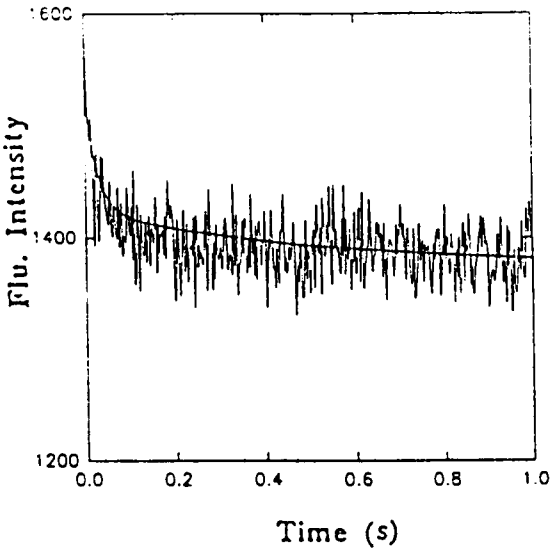


[Ves] = 0.55 μmol

B

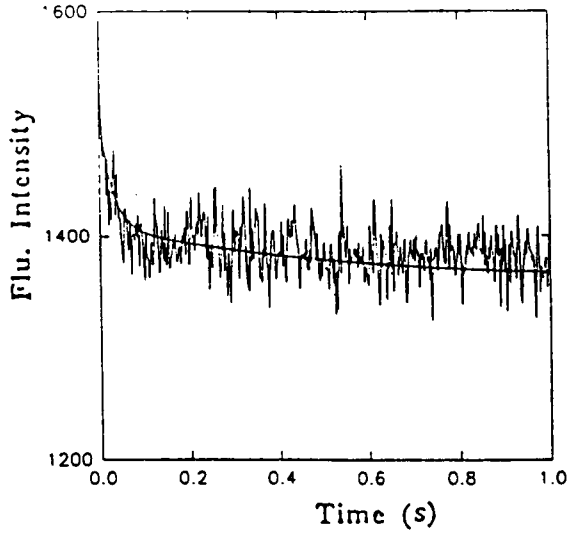


[Ves] = 0.83 μmol

C

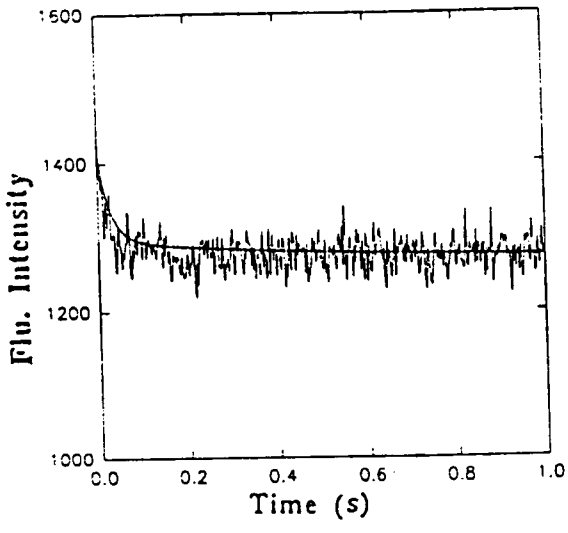


[Ves] = 1.10 μmol

**Figure 20.1**

DPPC labelled with 5-DS.

$\eta = 29$

$k_F = 37 \pm 2\ s^{-1}$

$k_S = 2 \pm 0.5\ s^{-1}$

$\left[(I_o / I) - 1\right] = 0.33 \pm 0.04$

A

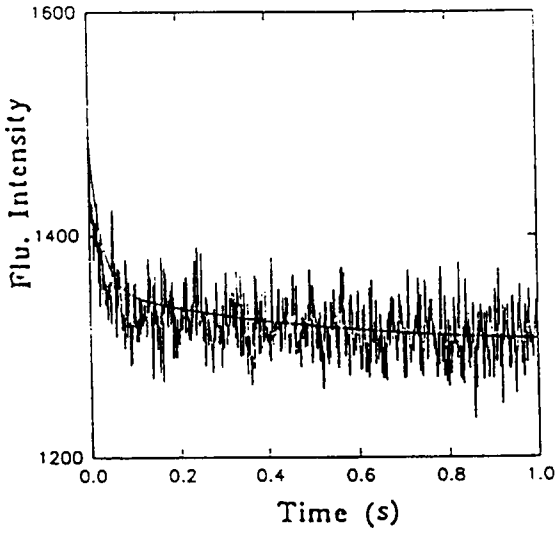


[Ves] = 0.55 μmol

B

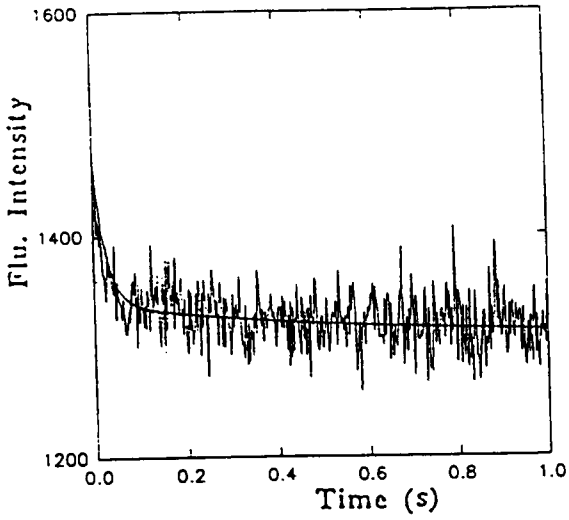


[Ves] = 0.83 μmol

C

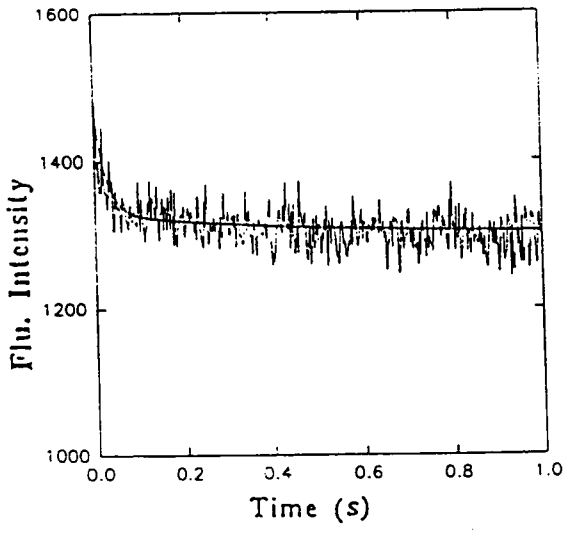


[Ves] = 1.10 μmol

**Figure 20.2**

DPPC labelled with 5-DS.

$\eta = 35$

$k_F = 39 \pm 3\ s^{-1}$

$k_S = 2 \pm 0.5\ s^{-1}$

$\left[(I_o / I) - 1\right] = 0.38 \pm 0.04$

A

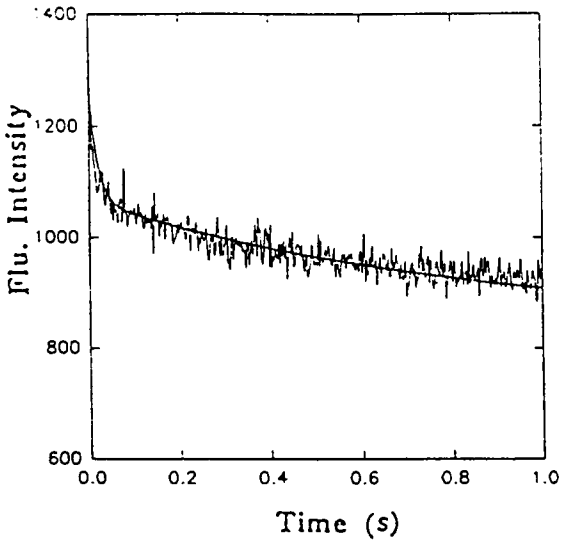


[Ves] = 0.55 μmol

B

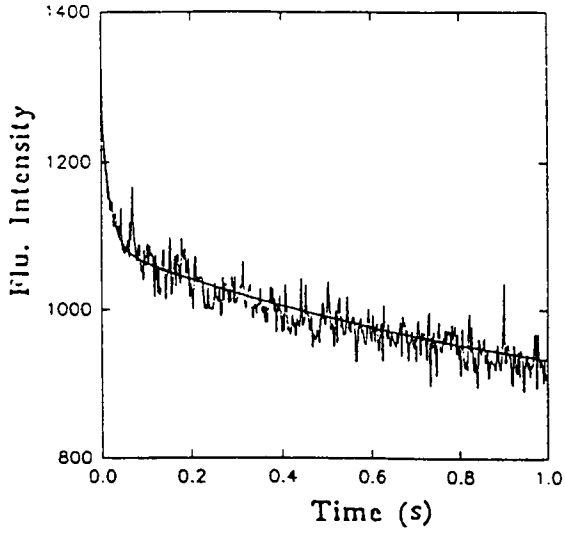


[Ves] = 0.83 μmol

C

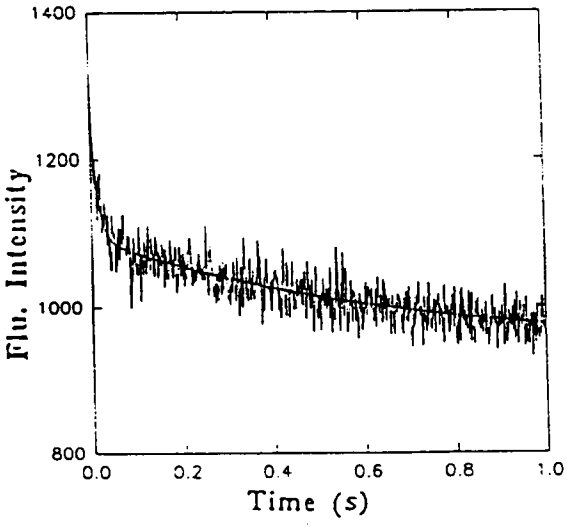


[Ves] = 1.10 μmol

**Figure 20.3**

DPPC labelled with 5-DS.

$\eta = 68$

$k_F = 41 \pm 4\ s^{-1}$

$k_S = 2 \pm 0.5\ s^{-1}$

$\left[(I_o / I) - 1\right] = 1.89 \pm 0.17$

A

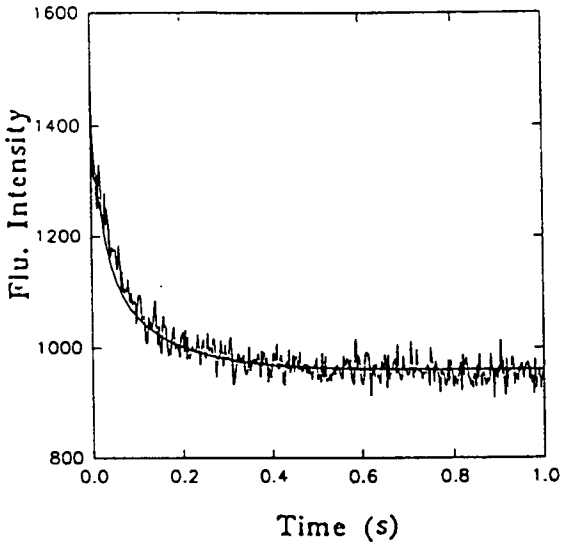


[Ves] = 0.55 μmol

B

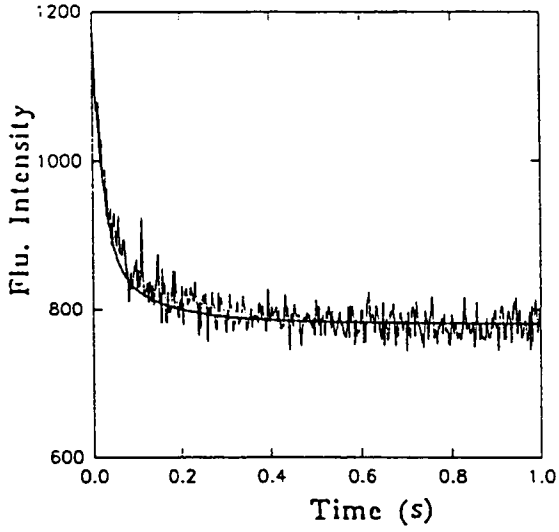


[Ves] = 0.83 μmol

C

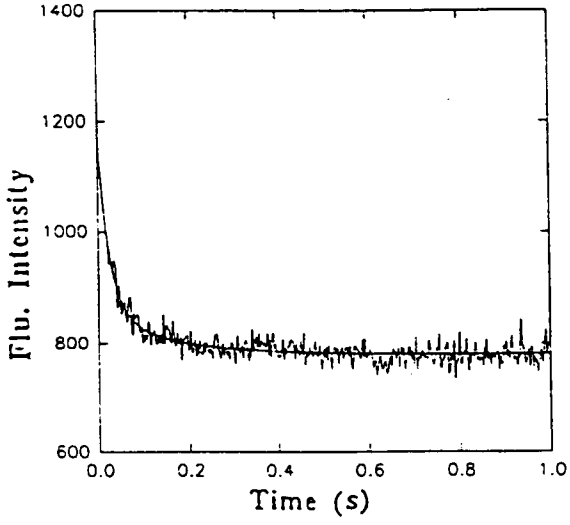


[Ves] = 1.10 μmol

**Figure 20.4**

DPPC labelled with 5-DS.

$\eta = 74$

$k_F = 63 \pm 12\ s^{-1}$

$k_S = 7 \pm 1\ s^{-1}$

$\left[(I_o / I) - 1\right] = 2.29 \pm 0.23$

A

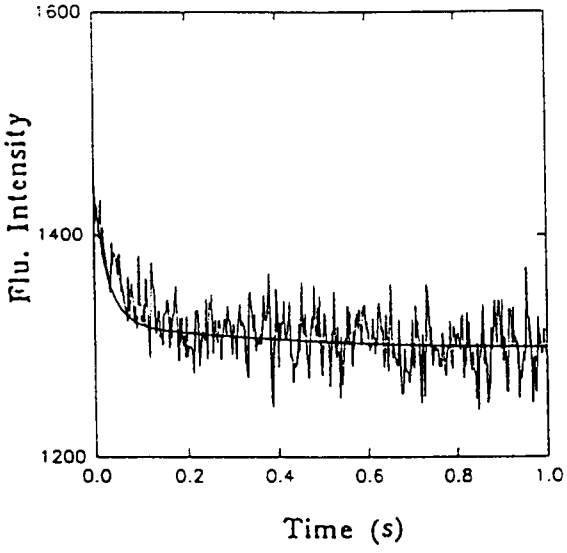


[Ves] = 0.55 μmol

B

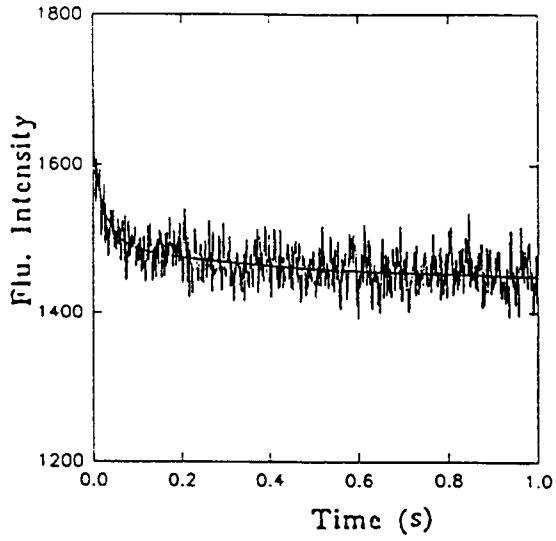


[Ves] = 0.83 μmol

C

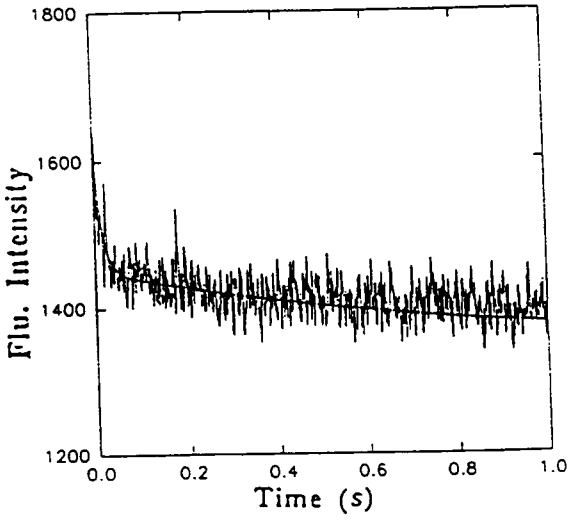


[Ves] = 1.10 μmol

**Figure 20.5**

DPPC labelled with 12-DS.

$\eta = 29$

$k_F = 37 \pm 2\ s^{-1}$

$k_S = 2 \pm 0.5\ s^{-1}$

$\left[(I_o / I) - 1\right] = 0.24 \pm 0.05$

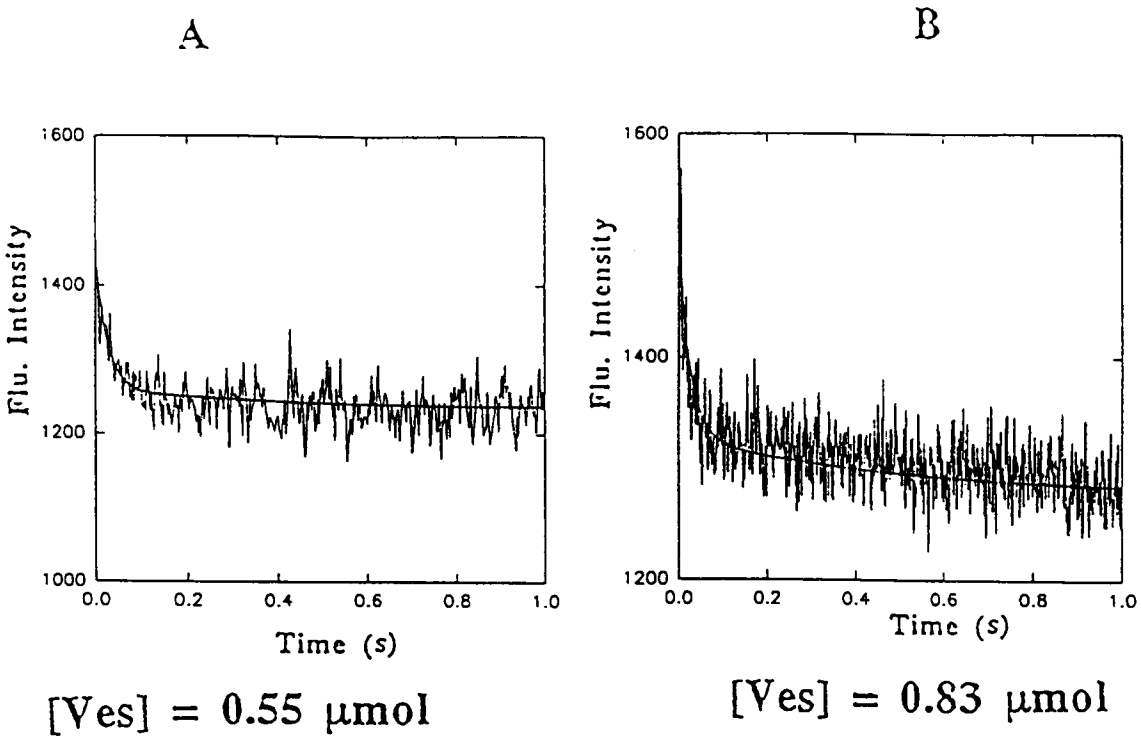


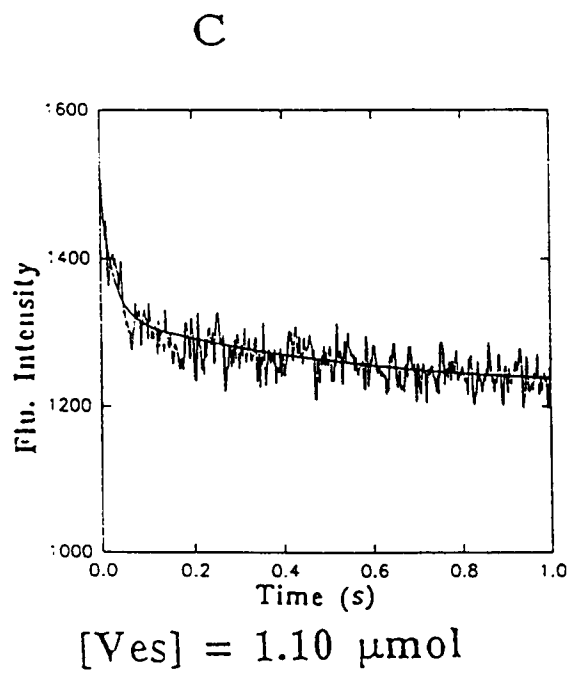


**Figure 20.6**

DPPC labelled with 12-DS.

$\eta = 34$

$k_F = 38 \pm 2\ s^{-1}$

$k_S = 2 \pm 0.5\ s^{-1}$

$\left[(I_o / I) - 1\right] = 0.48 \pm 0.07$

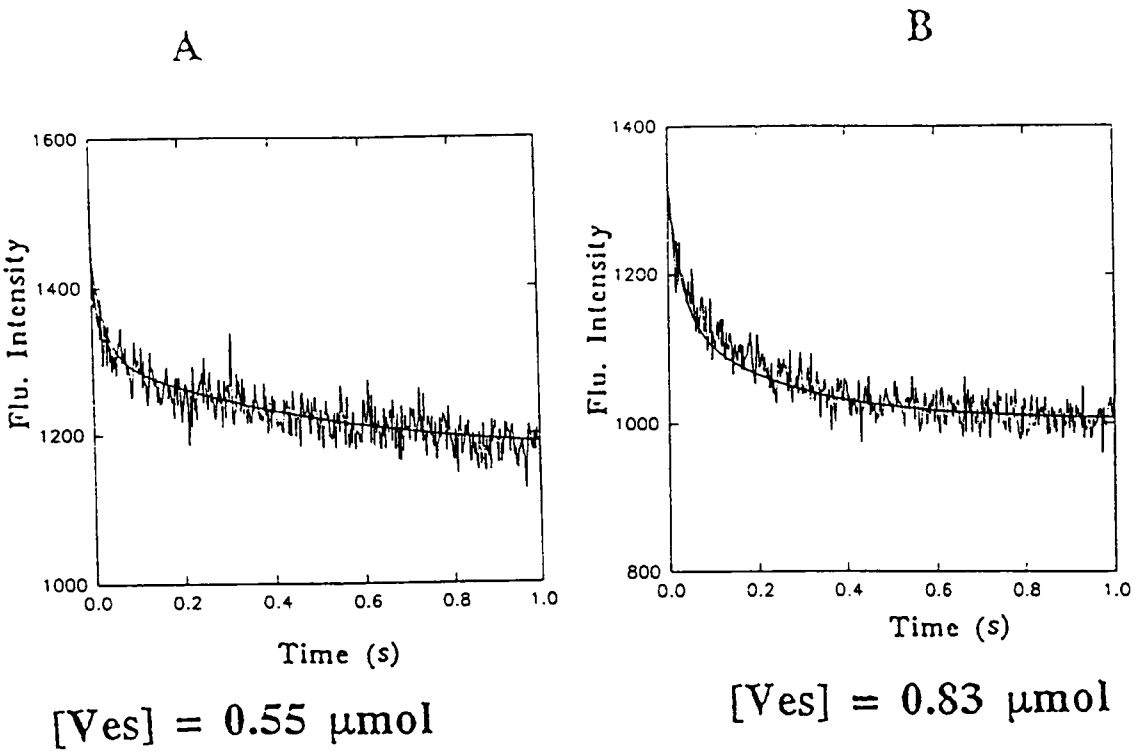


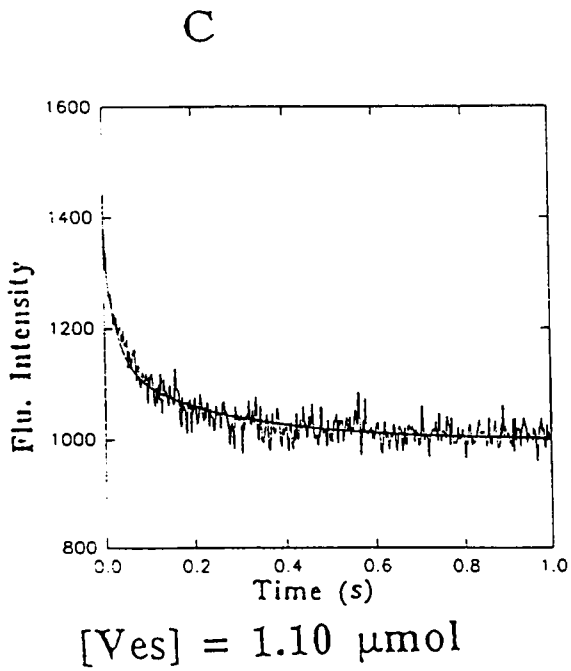


**Figure 20.7**

DPPC labelled with 12-DS.

$\eta = 63$

$k_F = 61 \pm 6\ s^{-1}$

$k_S = 2.5 \pm 0.5\ s^{-1}$

$\left[(I_o / I) - 1\right] = 0.95 \pm 0.11$

A

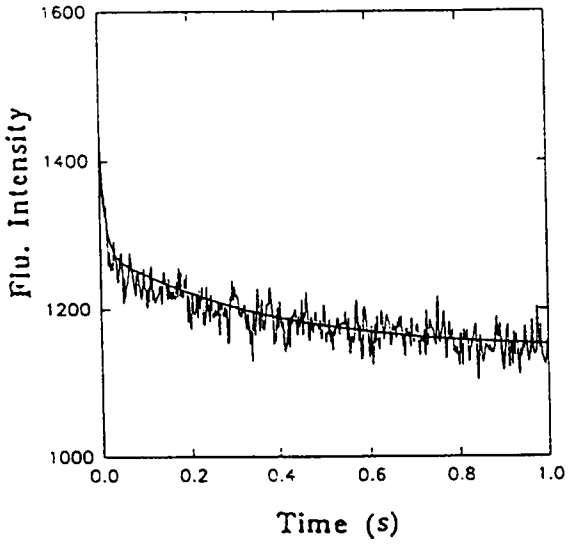


[Ves] = 0.55 μmol

B

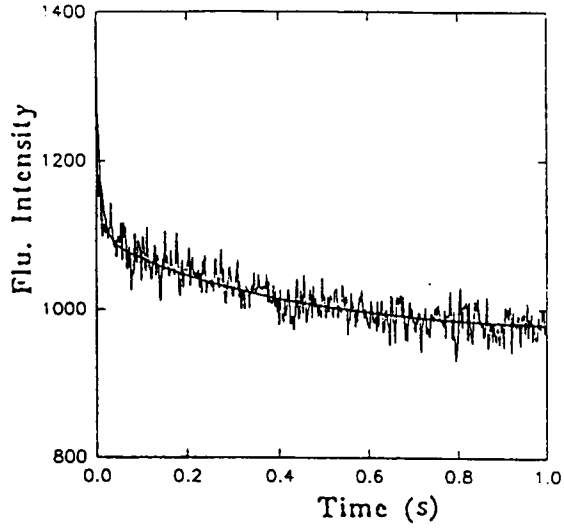


[Ves] = 0.83 μmol

C

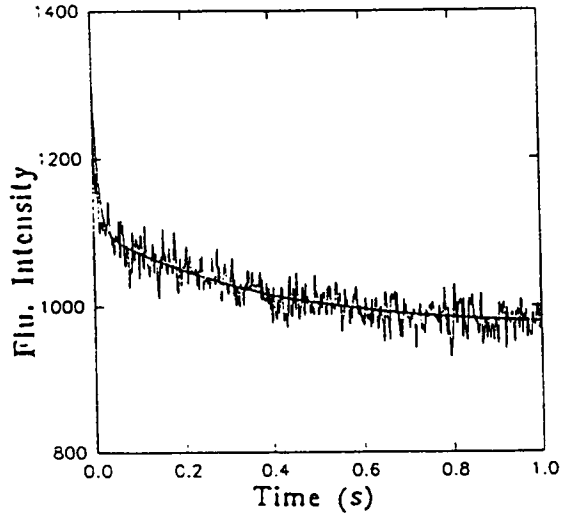


[Ves] = 1.10 μmol

**Figure 20.8**

DPPC labelled with 12-DS.

$\eta = 71$

$k_F = 98 \pm 10\ s^{-1}$

$k_S = 3.5 \pm 1\ s^{-1}$

$[(I_o / I) - 1] = 1.23 \pm 0.12$

The quantitative value of quenching, as detailed in the section on the calculation of the absolute partition coefficient, is $\left[(I_o / I) - 1\right]$. $I_0$ is the intensity of fluorescence in the absence of quencher and I is the intensity level in the presence of quencher. The preexponential term, A, in equations 16, 18, and 19 is a combination of the intensity drop from melittin binding, $\delta$, and the amount of quenching. Thus, when one wishes to describe quantitatively the amount of quenching, it is important to subtract out $\delta$. The equation used to solve for this is the following

$$\left[(I_o / I) - 1\right] = \frac{I_0 - g}{B + \delta - g} - 1 \tag{21}$$

When $\left[(I_o / I) - 1\right]$ is the same at different concentrations, then the mean occupation number, $\eta$, is also constant at these concentrations. The total quencher concentration, $[Q_T]$, is then plotted against [Ves] for points that have the same $\left[(I_o / I) - 1\right]$ to obtain $\eta$ and $K_{eq}$. (Figure 21 is shown as an example.) The values of $K_{eq}$ are listed in Table 3. A more useful parameter is the absolute partitioning coefficient, $K_{P,ABS}$, which is equal to the ratio of the molar concentration of the quencher in the lipid phase to that in the aqueous phase (Blatt, 1984). This parameter can be calculated from

$$K_{P,ABS} = \frac{K_{eq} V_A [Ves]}{V_L} \tag{22}$$

(Blatt, 1984). We have calculated the values of $K_{P,ABS}$ for a [Ves] = 1.1μmol and listed them in Table 3. The calculation of $V_L$ and $V_A$ was done as described under the section on the Mean Occupation Number, $\eta$ (see equations 4 and 5). It is seen from this Table that for values of $\eta$ greater than about 60 $K_{P,ABS}$ is on the order of $10^3$. This implies that the quencher concentration in the lipid phase is about a thousand times larger than the concentration of the quencher in the aqueous phase. For values of $\eta$ less than 60, the value

**Table 2** - Values for the parameters for quenching of the fluorescence of the tryptophan of melittin incorporated into DPPC SUVs for the two n-doxyl stearic acid quenchers.

| DPPC 5-DS | | | | | | |
|---|---|---|---|---|---|---|
| $\eta$ | $A_1$ | $A_2$ | B | $k_F\ (s^{-1})$ | $k_S\ (s^{-1})$ | $[(I_o / I) - 1]$ |
| 29 | 107 ± 14 | 42 ± 16 | 1328 ± 24 | 37 ± 2 | 2 ± 0.5 | 0.33 ± 0.04 |
| 35 | 138 ± 17 | 37 ± 15 | 1301 ± 18 | 39 ± 3 | 2 ± 0.5 | 0.38 ± 0.03 |
| 68 | 275 ± 23 | 125 ± 13 | 881 ± 35 | 41 ± 4 | 2 ± 0.5 | 1.89 ± 0.17 |
| 74 | 284 ± 27 | 118 ± 42 | 834 ± 51 | 63 ± 12 | 7 ± 0.5 | 2.29 ± 0.23 |
| **12-DS** | | | | | | |
| $\eta$ | $A_1$ | $A_2$ | B | $k_F\ (s^{-1})$ | $k_S\ (s^{-1})$ | $[(I_o / I) - 1]$ |
| 29 | 142 ± 34 | 52 ± 28 | 1384 ± 41 | 37 ± 2 | 2 ± 0.5 | 0.24 ± 0.05 |
| 34 | 181 ± 15 | 61 ± 33 | 1245 ± 35 | 38 ± 2 | 2 ± 0.5 | 0.48 ± 0.07 |
| 63 | 185 ± 35 | 125 ± 15 | 1063 ± 49 | 61 ± 6 | 2.5 ± 0.5 | 0.95 ± 0.15 |
| 71 | 213 ± 56 | 130 ± 23 | 993 ± 28 | 98 ± 8 | 3.5 ± 1 | 1.23 ± 0.12 |

**Table 3.** The equilibrium constant, $K_{eq}$, and the absolute partitioning coefficient, $K_{P,ABS}$, for the association of the n-DS quenchers with phosphotidylcholine vesicles are listed as a function of $\eta$ for [Ves] = 1.1 μmol.

| | $\eta$ | $K_{eq}$ ($mol^{-1}$) | $K_{P,ABS}$ |
|---|---|---|---|
| **DMPC** | | | |
| 5-DS | 29 | $3.5 \times 10^{20} \pm 2 \times 10^{20}$ | $9.6 \times 10^{16} \pm 5 \times 10^{16}$ |
| | 35 | $3.9 \times 10^{6} \pm 2 \times 10^{6}$ | $1.1 \times 10^{3} \pm 5 \times 10^{2}$ |
| | 66 | $4.9 \times 10^{6} \pm 2 \times 10^{6}$ | $1.3 \times 10^{3} \pm 5 \times 10^{2}$ |
| | 74 | $6.3 \times 10^{6} \pm 2 \times 10^{6}$ | $1.7 \times 10^{3} \pm 5 \times 10^{2}$ |
| 7-DS | 29 | $3.5 \times 10^{20} \pm 2 \times 10^{20}$ | $9.6 \times 10^{16} \pm 5 \times 10^{16}$ |
| | 37 | $3.9 \times 10^{6} \pm 2 \times 10^{6}$ | $1.1 \times 10^{3} \pm 5 \times 10^{2}$ |
| | 64 | $4.9 \times 10^{6} \pm 2 \times 10^{6}$ | $1.3 \times 10^{3} \pm 5 \times 10^{2}$ |
| | 74 | $6.3 \times 10^{6} \pm 2 \times 10^{6}$ | $1.7 \times 10^{3} \pm 5 \times 10^{2}$ |
| 12-DS | 29 | $3.5 \times 10^{20} \pm 2 \times 10^{20}$ | $9.6 \times 10^{16} \pm 5 \times 10^{16}$ |
| | 43 | $3.9 \times 10^{20} \pm 2 \times 10^{20}$ | $1.1 \times 10^{17} \pm 5 \times 10^{16}$ |
| | 62 | $3.9 \times 10^{6} \pm 2 \times 10^{6}$ | $1.1 \times 10^{3} \pm 5 \times 10^{2}$ |
| | 71 | $3.1 \times 10^{6} \pm 2 \times 10^{6}$ | $8.5 \times 10^{2} \pm 5 \times 10^{2}$ |
| **DPPC** | | | |
| | $\eta$ | $K_{eq}$ ($mol^{-1}$) | $K_{P,ABS}$ |
| 5-DS | 29 | $3.5 \times 10^{20} \pm 2 \times 10^{20}$ | $9.6 \times 10^{16} \pm 5 \times 10^{16}$ |
| | 43 | $3.9 \times 10^{20} \pm 2 \times 10^{20}$ | $1.1 \times 10^{17} \pm 5 \times 10^{16}$ |
| | 68 | $4.9 \times 10^{6} \pm 2 \times 10^{6}$ | $1.3 \times 10^{3} \pm 5 \times 10^{2}$ |
| | 74 | $6.3 \times 10^{6} \pm 2 \times 10^{6}$ | $1.7 \times 10^{3} \pm 5 \times 10^{2}$ |
| 12-DS | 29 | $3.5 \times 10^{20} \pm 2 \times 10^{20}$ | $9.6 \times 10^{16} \pm 5 \times 10^{16}$ |
| | 34 | $3.9 \times 10^{20} \pm 2 \times 10^{20}$ | $1.1 \times 10^{17} \pm 5 \times 10^{16}$ |
| | 63 | $3.9 \times 10^{6} \pm 2 \times 10^{6}$ | $1.1 \times 10^{3} \pm 5 \times 10^{2}$ |
| | 71 | $3.1 \times 10^{6} \pm 2 \times 10^{6}$ | $8.5 \times 10^{2} \pm 5 \times 10^{2}$ |

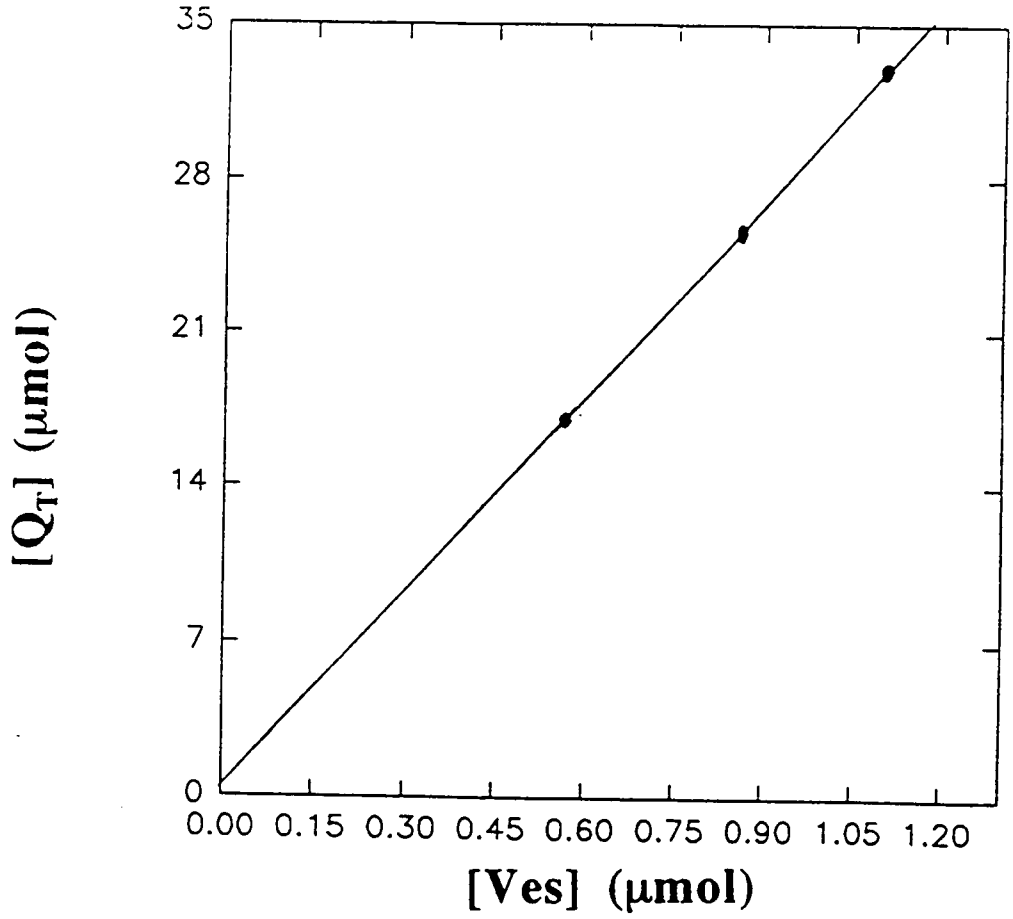


**Figure 21**

Plot of $[Q_T]$ as a function of [Ves] for samples where $\left[(I_o / I) - 1\right]$ was constant. A linear regression fit was performed to calculate $\eta$ and $K_{eq}$. The variable affinity of the n-DS for the lipid phase is described by $\eta$.

of $K_{P,ABS}$ is very sensitive to the value of $\eta$. Finally, for $\eta = 29$ (the lowest value used in these experiments), $K_{P,ABS}$ becomes $\approx 10^{17}$, which implies that the concentration of the quencher in the aqueous phase is negligibly small.

Tables 1 and 2 give the values for $\left[(I_o / I) - 1\right]$ and $\eta$ for the quenchers when located in the two lipids. From Tables 1 and 2 it is possible to make a corrected Stern-Volmer plot of $\left[(I_o / I) - 1\right]$ vs. $\eta$ as discussed in the section on the Mean Occupation Number, $\eta$. This is shown in Figure 22 and Figure 23 for DMPC and DPPC, respectively. Therefore, it can be seen that 5-DS in DMPC bilayers is a more efficient fluorescence quencher of the tryptophan residue than 12-DS.

There is a debate over how to treat the data in the DPPC case. Quenching will be quantified at 1 s which is presumably before fusion occurs. This is illustrated by looking at any of the graphs used for analysis, which would be an example with a time scale of 1 second. As it was stated above, unlike the case of DMPC, for which $I_0 = A + B$, where A and B are well defined, for DPPC because of the very fast initial drop, it is debatable what the value of $I_0$ is. Here, we consider the initial fast drop to be part of the quenching process and we identify $I_0$ with the value of the fluorescence intensity in the absence of quencher at t = 0 s. B is the value that the fluorescence falls to in the presence of quencher in 1 s. Of course, g must be accounted for in equation 21 for $\left[(I_o / I) - 1\right]$.

It is readily seen from Figures 22 and 23 that for both DMPC and DPPC 5-DS is a more efficient quencher than 12-DS. Thus, in both lipid bilayers the fluorophore is located closer to position 5 of the acyl chains, rather than to position 12. It is also seen that the quenching efficiencies for both 5-DS and 12-DS are higher when they are located in DPPC rather than in DMPC. The ramifications of this finding will be examined in more detail in the Discussion.

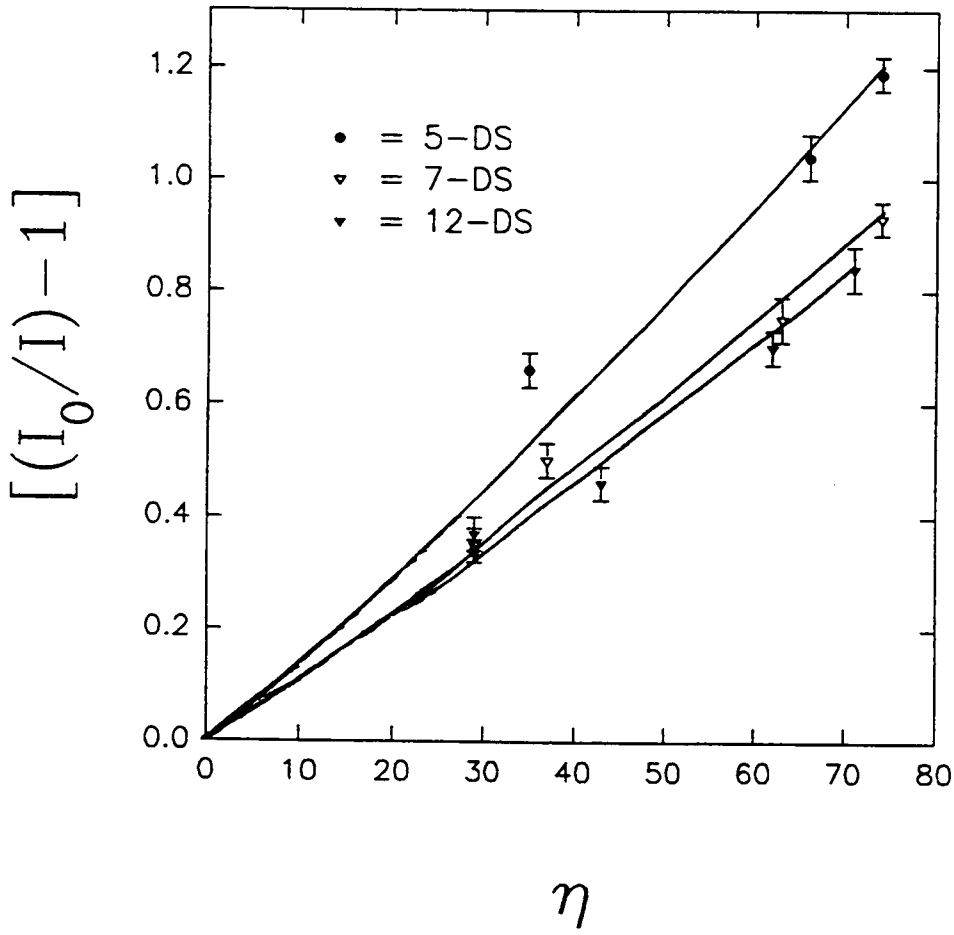


**Figure 22**

Corrected Stern-Volmer plot for DMPC of $\left[(I_o / I) - 1\right]$ as a function of the mean occupation number of the quencher, $\eta$, in the vesicle phase. Here, "corrected" means that $\eta$ is used instead of the total molar concentration of the quencher in solution.

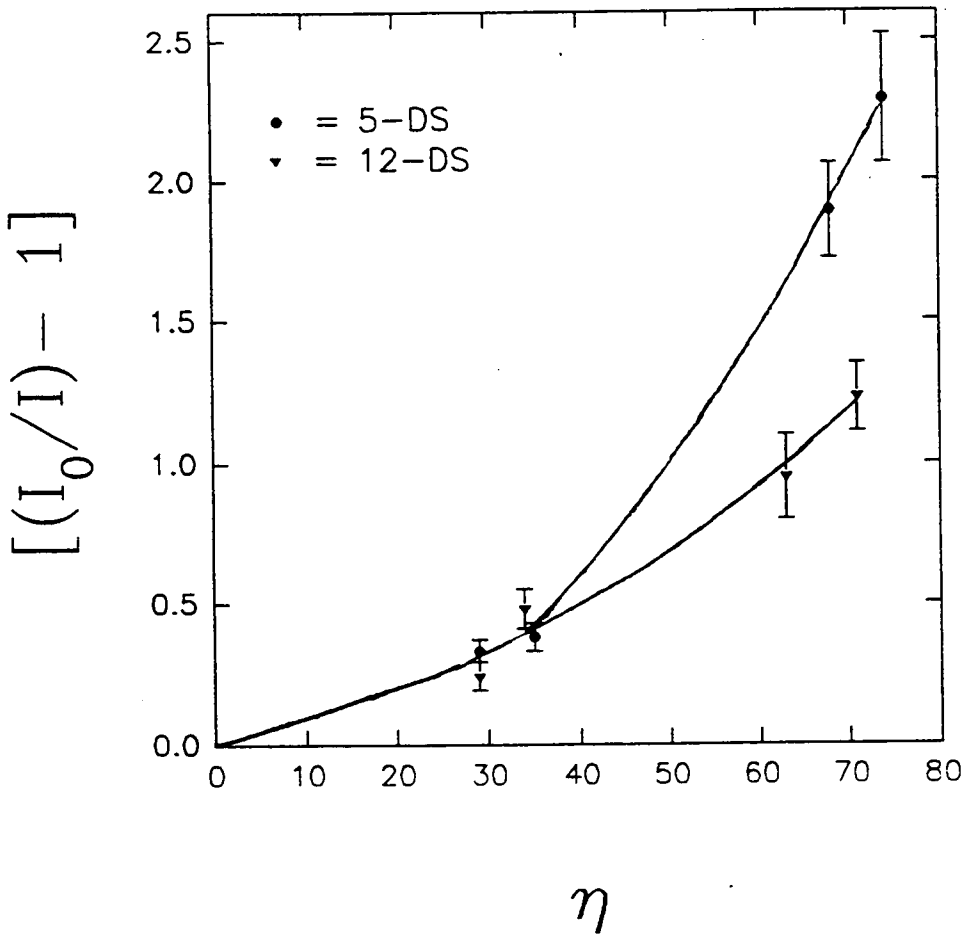


**Figure 23**

Corrected Stern-Volmer plot for DPPC of $\left[(I_o / I) - 1\right]$ as a function of the mean occupation number of the quencher, η, in the vesicle phase. Here, "corrected" means that η is used instead of the total molar concentration of the quencher in solution.

Once the values for $\left[(I_o / I) - 1\right]$ are known for a certain $\eta$, it is possible to apply the parallax method for the quenchers. We felt that it was most appropriate to use the highest $\eta$, $\eta$=74, to make this comparison. What follows is the direct calculation of the position of the fluorophore in the bilayer (see section on the Parallax Method).

Thickness of the bilayer starting from position 1
DMPC = 23 Å
DPPC = 26 Å

Average bond length
DMPC = 23 Å / 26 bonds
DPPC = 26 Å / 30 bonds

Let the mean number of quenchers located in a vesicle be
$\eta = 74$

Surface area of a lipid
S.A. = 66 $Å^2$

C= M.F./ S.A. = $\eta$ /(2700 x 66 $Å^2$)
= 0.000417 $Å^{-2}$

Mole fraction of quenchers in the lipid phase
M.F. = $\eta$ /(total number of lipids in a vesicle = 2700)

Distances used in Parallax
DMPC-
$L_{C5}$ = 8.0 Å
$L_{C7}$ = 6.2 Å
$L_{5\text{-}12}$ = 6.2 Å
$L_{7\text{-}12}$ = 4.4 Å

DPPC-
$L_{C5}$ = 9.5 Å = length of 11 bonds(26 Å/30)
$L_{5\text{-}12}$ = 6.1 Å

$L_{XY}$ is defined as the difference in depth between the two quencher locations being studied. When comparing 5-DS and 12-DS then we would use $L_{5\text{-}12}$ in the place of $L_{XY}$ below. $L_{CL}$ is the distance from the center of the bilayer to the lower quencher. When comparing 5-DS and 12-DS we use the $L_{C5}$,which is listed above, in the place of $L_{CL}$. Combining the following equations

$$Z_{nf} = [((-1/\pi C) \ln F_L/F_H - L_{XY}^2)/ 2 L_{XY}] \quad (13)$$

$$Z_{Cf} = Z_{nf} + L_{CL} \quad (14)$$

we can derive

$$Z_{Cf} = [((-1/\pi C) \ln F_L/F_H - L_{XY}^2)/ 2 L_{XY}] + L_{CL}$$

Here, the distance from the center of the bilayer to the fluorophore is $Z_{Cf}$ . $Z_{nf}$ is the difference between the depth of an n-DS and the tryptophan residue. $F_L$ and $F_H$ stand for the $F_n$ of the lower and higher quencher respectively.

# DMPC

$F_n = \{1/([(I_O/I) - 1] + 1)\}$

| | $[(I_O/I) - 1]$ |
|---|---|
| $F_5 = 0.457 \pm 0.007$ | 5-DS $1.19 \pm 0.03$ |
| $F_7 = 0.518 \pm 0.008$ | 7-DS $0.93 \pm 0.03$ |
| $F_{12} = 0.543 \pm 0.011$ | 12-DS $0.84 \pm 0.04$ |

$$Z_{Cf} = [((-1/\pi C) \ln F_L/F_H - L_{XY}^2)/ 2 L_{XY}] + L_{CL}$$

Compare 5-12

$Z_{Cf} = [((-1/\pi C) \ln F_L/F_H - L_{XY}^2)/ 2 L_{XY}] + L_{CL}$

$= [((-1/\pi C) \ln(0.457/0.543) - (6.1)^2)/ 2 (6.1)] + 8.0$

$= 8 + 7.5 = 15.5$ Å $\pm$ 2.7 Å or 3 Å in the glycerol backbone

Compare 7-12

$Z_{Cf} = [((-1/\pi C) \ln F_L/F_H - L_{XY}^2)/ 2 L_{XY}] + L_{CL}$

$= [((-1/\pi C) \ln (0.518/0.543) - (4.4)^2)/ 2 (4.4)] + 6.1$

$= 6.2 + 1.9 = 8.1$ Å $\pm$ 3.1 Å or position 5 along the acyl chain

# DPPC

$F_n = \{1/([(I_O/I) - 1] + 1)\}$ $\quad [(I_O/I) - 1]$

$F_5 = 0.304 \pm 0.020$ $\quad$ 5-DS $\quad 2.29 \pm 0.23$

$F_{12} = 0.448 \pm 0.022$ $\quad$ 12-DS $\quad 1.23 \pm 0.12$

$Z_{cf} = [((-1/\pi C) \ln F_L/F_H - L_{XY}^2)/ 2 L_{XY}] + L_{CL}$

$= [((-1/\pi C) \ln (0.304/0.448) - (6.1)^2)/ 2 (6.1)] + 9.5$

$= 9.5 + 20.8 = 30.3$ Å $\pm$ 7.1 Å which is outside the bilayer

If one excludes the fast drop, the expression for $[(I_O/I) - 1]$ becomes identical to that for DMPC or

$$[(I_O/I) - 1] = [(A_1 + A_2 + B - \gamma)/ (B - \gamma + \delta) - 1]$$

$F_n = \{1/([(I_O/I)-1]+1)\}$ $\quad [(I_O/I) - 1]$

$F_5 = 0.368 \pm 0.023$ $\quad$ 5-DS $\quad 1.718 \pm 0.18$

$F_{12} = 0.534 \pm 0.022$ $\quad$ 12-DS $\quad 0.873 \pm 0.08$

$Z_{cf} = [((-1/\pi C) \ln F_L/F_H - L_{XY}^2)/ 2 L_{XY}] + L_{cL}$

$= [((-1/\pi C) \ln(0.368/0.534) - (6.2)^2)/ 2 (6.2)] + 9.5$

$= 9.5 + 19.8 = 29.3$ Å $\pm$ 6.3 Å which is still outside the bilayer.

Taking the average value of $Z_{Cf}$ in DMPC we obtain a presumed depth of the fluorophore to be about 12 Å or the first position along the acyl chain. This is consistent with the fact that 5-DS is the more efficient quencher in DMPC.

# PART 4.
# DISCUSSION

In the Discussion section we will try to interpret the results of the quenching study. To facilitate this discussion, the results which are common for both lipids will be considered first, and then those separately for DMPC and DPPC. Lastly, the implications of these experiments regarding the models for melittin binding to lipid bilayers will be discussed. All fluoresence intensity measurements were made at the transition temperatures of the lipids, 21°C and 37°C for DMPC and DPPC, respectively.

The final plots of the Data Analysis section (Figures 22 and 23) show the corrected order of quenching efficiency for the n-DS. These plots show that 5-DS is a more efficient quencher of the tryptophan fluorescence of melittin than 12-DS no matter which lipid the n-DS are residing in. This result implies that upon binding the tryptophan residue is located in the upper portion of the bilayers. This is consistent with a mode of binding according to which melittin attaches the C-terminus to the head groups of the phospholipids. According to the x-ray crystallographic study of Terwilliger et al. (1982), the indole ring of the tryptophan residue is within 4-6 Å of the 4 positively charged groups of melittin that are acting as an anchor to the membrane. Since the tryptophan is located very close to the C-terminus of the protein which carries four positive charges, it seems that the tryptophan residue should be located in the vicinity of the glycerol backbone. However, the fact that 12-DS does quench fairly effectively implies that melittin may be inserting itself into the bilayer to some extent.

It is important to note that one must think in terms of populations to understand this system. There are three different populations of a quencher in the lipid phase. The first ($P_1$) comprises quenchers located within the critical radius of the binding site; these are instantaneous quenchers. $P_1$ would presumably be responsible for the instantaneous drop in the fluorescence intensity for DPPC. The second population comprises quenchers which are out of range but can move close enough to quench ($P_2$). Since the lifetime of the excited

state of the fluorophore is very short, the probability that a quencher would move within its critical radius toward a fluorophore during the excited state is small. However, at any instant there would be a population of quenchers, which at other times would be too far away. It is in this population that the distance between the position of the quencher makes the largest difference in population size. Lastly, there is a population that is too far away to ever quench ($P_0$). The quencher has a large critical radius $R_C$,which is equal to 15 Å (Vogel, 1981), and thus any quencher located within about 15 Å of a binding site of a melittin molecule has a very high quenching efficiency. This is an example of $P_1$ quenching. The vertical displacement of the doxyl stearic group accounts for the differences in the size of the total population of quenchers, $P_T = P_1 + P_2$, for the various n-DS. $P_T$ must be different for the differing quencher positions, otherwise the fluorescence intensity would be the same for any n-DS. $P_T$ is larger for 5-DS than for any other position. Therefore, 5-DS has a higher probability of being closer to the tryptophan than does either 7-DS or 12-DS.

Since the doxyl stearic group is thought to be a collisional quencher (see Vogel, 1981) with a critical radius, $R_C = 15$ Å, it may be assumed that any 5-DS quencher located in the inner half of the bilayer will not be able to quench since it would be too far away and thus will be considered $P_o$. This seems to be a reasonable assumption based on Figure 24. If inner leaflet quenching were important, it would make the observed quenching for 12-DS artificially high because any contribution made by a quencher from the inner leaflet would tend to enhance its quenching efficiency relative to that of 5-DS. The position of the fluorophore obtained by the parallax method for DMPC indicates that quenching by the inner leaflet should be rather inefficient no matter which position the quencher is located at. In DPPC the bilayer is actually larger because of the extra two carbons on the acyl chain. Therefore an inner leaflet 12-DS would be more efficient in DMPC than in DPPC.

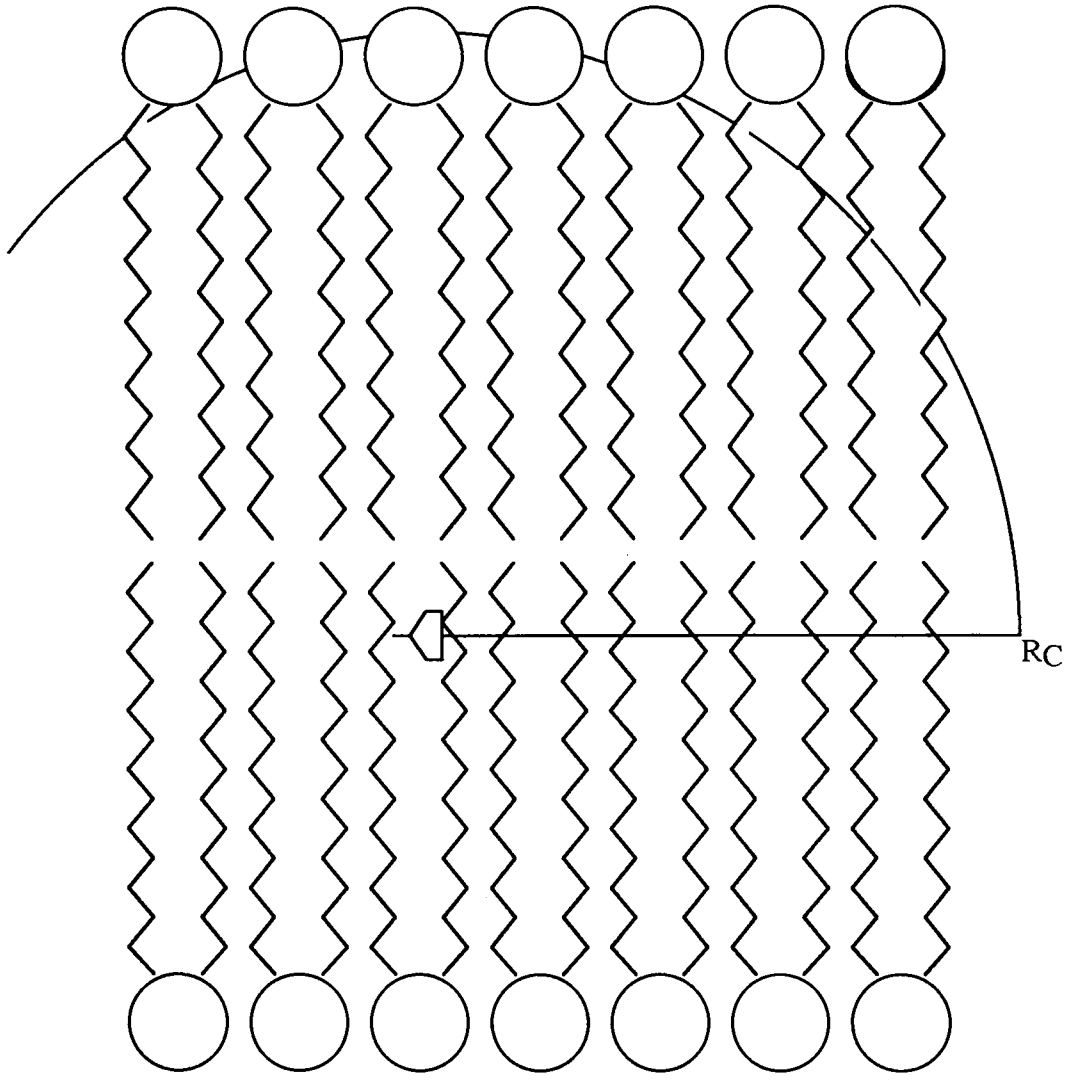


**Figure 24 (b).**

Illustration of inner leaflet quenching. Note that the inner leaflet 12-DS quencher is within its critical radius, $R_C$, of the surface of the bilayer which is the presumed location of the fluorophore. This is so only if the quencher is located directly below the binding site of melittin, however.

However, based on our observation that quenching in DMPC is less efficient than in DPPC, inner leaflet quenching does not appear to be significant. We treat inner leaflet quenchers as $P_o$ since their distance from the presumed position of the fluorophore is very large.

The quenching efficiency relates to the extent of quenching, whereas the rate of quenching relates to the speed with which the quencher can reach the tryptophan residue. This explains the fact that 12-DS has a higher rate of quenching, $k_2$ or $k_F$ for DMPC and DPPC, respectively, than does 5-DS (see Tables 1 and 2) This piece of data is consistent with the fact that the further down the acyl chain one goes the more the segmental flexibility is enhanced (Marsh, 1990). We can express the movement of the labelled lipid as taking place in a cone (see Figure 25). Marsh (1990) gives an angle of $\Theta=12^{\circ}$ for this movement below the transition temperature of DMPC. The angle would be larger above the transition temperature. It can be seen from this model that 12-DS has a larger range of motion than does 5-DS, which is a direct result of the fact that $AREA_{12} > AREA_5$, where $AREA_5$ stands for the area a 5-DS quencher can subtend in a given interval of time. If AREA is multiplied by the critical radius of the doxyl stearic quencher, $R_c$, then it is possible to determine the volume of the spheroid, Volume, in which quenching can take place in. Obviously, $Volume_{12} > Volume_5$. These volume elements are swept out in the same time period, so 12-DS must be moving faster in solution than 5-DS. Therefore, it is not surprising that 12-DS has a higher $k_2$ or $k_F$ than does 5-DS even though it is the less effective quencher.

The effective overall rate of quenching on the millisecond time scale in DPPC is mainly determined by the fast rate constant, $k_F$ (compare Tables 1 and 2). $k_F$ is generally on the same order of magnitude as the single exponential rate constant, $k_2$, used to model

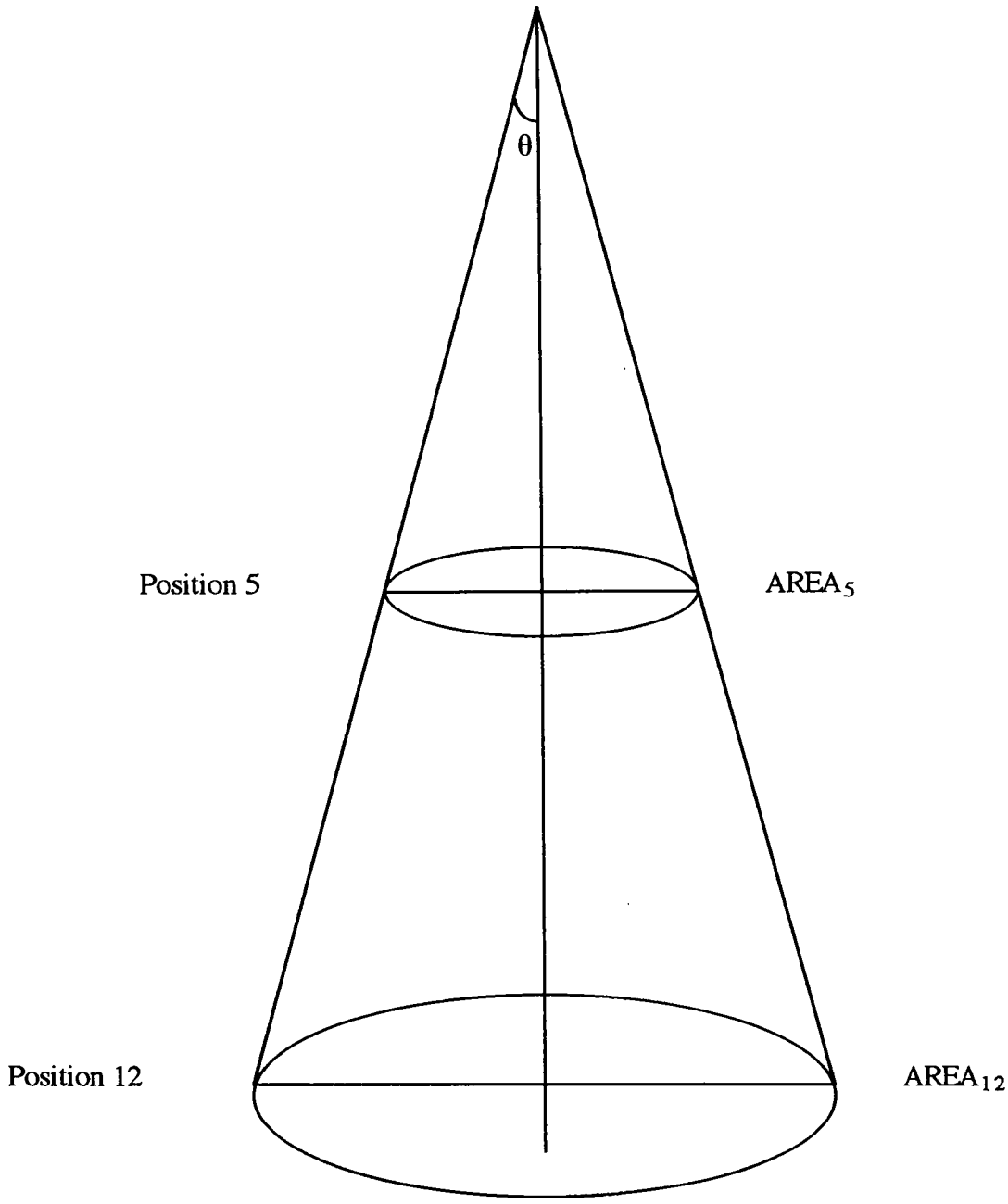


**Figure 25**

Illustration of the cone model for dynamic movement of the acyl chains. $\theta = 12$

DMPC. A qualitative comparison between $k_2$ and $k_F$ shows that the rate of quenching for the n-DS is remarkably faster in DPPC. The rate of melittin binding is much faster for DPPC than it is for DMPC (Bradrick et al., 1995). Therefore, the finding that the quenching process is faster in DPPC is not surprising.

There has been no other study that has sought to identify the position of the tryptophan residue in non-fused vesicles. Two studies were carried out with vesicles that were fused by melittin (Vogel, 1981 and Georghiou et al., 1982). Georghiou et al. showed that bound melittin is accessible to acrylamide, whereas Vogel used spin labels. Both studies reported that the tryptophan residue is located in the vicinity of the glycerol backbone. It should be noted that Vogel did not take into account the mean occupation number of the spin labels he used. There is the possibility that the quenching efficiency is greater for position 1 because the solubility of that spin label in the membrane may be greater than the solubility of the other two spin labels (see the section on the Mean Occupation Number, $\eta$). Of course, in fused vesicles the location of the fluorophore may be different than that in non-fused vesicles. However, the results presented here are in agreement with the aforementioned work (see below).

We find that the n-DS quenchers are more efficient when bound to DPPC (see Tables 1 and 2). This result is independent of whether or not the instantaneous drop in DPPC is taken into account. The instantaneous drop was greater for 5-DS than it was for 12-DS. However, if one uses equations 18, 20b and 21 for the calculation of $\left[(I_o / I) - 1\right]$, as we have used for DMPC, then one obtains a quenching efficiency for DPPC that does not include the instantaneous drop. 5-DS has the most pronounced change in quenching efficiency between the two lipids. The result that n-DS quenchers are more efficient in DPPC is consistent with the work of Bradrick et al. (1995) who report that melittin binds tighter and is better accommodated by DPPC. Also, the chains of DMPC become more

rigid upon protein binding. Thus for any $\eta$, the distance between the average quencher-donor pair would be greater in DMPC than in DPPC.

The position of the fluorophore calculated from the parallax method for DPPC is very unclear. A potential problem is whether or not to incorporate the instantaneous drop into the quenching efficiencies. However, the tryptophan positions calculated in either case do agree with each other: 30 Å taking into account the instantaneous drop and 29 Å when it is neglected. Obviously, the calculated depth of the fluorophore in DPPC does not make sense. The quenching process is very complex in DPPC and it is uncertain as to which parameters are appropriate to use. Nevertheless, regardless of whether we consider the instantaneous quenching or not, a comparison of the quenching efficiencies of both 5-DS and 12-DS for the two lipids suggests that the tryptophan is more external for DPPC. This is shown by taking the ratios of the quenching efficiencies for $\eta \approx 70$ in Tables 1 and 2 (1.42 in the case of DMPC and 1.86 for DPPC.)

The position of the fluorophore indicated by the parallax method for DMPC is more reasonable. These values, 15.5 Å and 8.1 Å obtained from comparing 5-DS and 12-DS and then 7-DS and 12-DS, respectively, can be averaged so that the results are interpreted as the distance from the center of the bilayer to the fluorophore, $Z_{Cf} \approx 12$ Å, or that the fluorophore resides near the glycerol backbone.

In the trans-membranal model (Figure 3A) the location of the fluorophore is very similar to that of the parallel-to-the-surface model (Figure 3B). Either model puts the tryptophan in the vicinity of approximately the fourth position along the acyl chain. Certainly, with the error associated with experiment, either model could produce the results found in the present study. In the trans-membranal model the annulus of the lipids surrounding the protein would not need to fill in the gap under the protein. Therefore, one would expect that in the trans-membranal model the acyl chains of the two lipids would

accommodate the protein in much the same fashion. Thus, one would expect that the presumed depths of the fluorophore in the two bilayers would be similar. The quenching efficiencies of the n-DS quenchers are not the same for DMPC and DPPC, with that for DPPC being greater. Consequently, the presumed depth of the fluorophore does not stay constant, which is contrary to what is expected from the trans-membranal model. This and the consideration that the hydrophilic side chains are forced into the bilayer (see Introduction) seem to cast applicability of the trans-membranal model.

There is no evidence that eliminates the possibility of many different species of bound melittin existing in a single lipid, much less for both lipids. All that is available is information as to which quencher is more efficient. The parallel-to-the-surface model (Figure 3B) and the 'wedge' model (Figure 3C) seem the most likely based on our data. If the α-helix of melittin is parallel to the surface, it will create an empty space underneath it. This is not energetically favored. The lipids will then try to accommodate the protein by filling in the empty space with their acyl chains (Bradrick et al., 1995). Since DPPC has the longer acyl chains, it should be better at filling in the empty space and thus binding the protein more tightly. Therefore, we anticipate that the quenching efficiency would be greater for DPPC in these two models, as we have observed.

The parallel-to-the-surface model (Figure 3b) is the model that is most consistent with all the data. Certainly, the data indicate that the mode of insertion is different for the two lipids. This is consistent with the findings of Bradrick et al. (1995) who reported that there is a compressional wave that extends for at least 50 Å for DMPC. The DPPC bilayer, however, is not disturbed significantly by protein binding. The ability of 12-DS to quench does not eliminate the possibility of bound melittin residing on the surface of the bilayer. The wedge model (Figure 3C) seems somewhat unlikely from the consideration of trying to put the hydrophobic regions of melittin facing the water at the lipid interface. In the wedge

model the N-terminus is electrostatically restricted to the surface of the bilayer. This electrostatic interaction would not be nearly as large as that for the C-terminus that has four charges; however, these interactions would restrict the ability of the N-terminus from entering the bilayer (this is the defining difference between the two models). In the parallel-to-the-surface model the N-terminus is not restricted to reside on the surface (as it is in the wedge model) and so has more degrees of freedom to insert itself deeper into the bilayer. This is the only model in which the N-terminus is not fixed upon the bilayer surface by electrostatic interactions. Thus the parallel-to-the-surface model has the greatest degree of freedom for the tryptophan moeity to change its depth of insertion. Therefore, this model is the most compatible with the notion that melittin is more external in DPPC than in DMPC, as was discussed above.

# REFERENCES

# REFERENCES


Abrams, F. and London, E. (1992) Biochemistry *31*, 5312-5322.

Blatt, E., Chatelier, R. and Sawyer, W.H. (1984) Photochem. Photobiol., *39*, 477-483.

Bradrick, T.D. (1994) Ph.D. Dissertation,University of Tennessee, Knoxville.

Bradrick, T.D., Friere, E. and Georghiou, S. (1989) Biochim. Biophys. Acta *982*, 94-102.

Bradrick, T. D. and Georghiou S. (1987) Biochim. Biophys. Acta *905*, 494-498.

Bradrick, T. D., Philippetis, A. and Georghiou S. (1995) Biophys. J. *69*, 1999-2010.

Brauner, J.W., Mendelsohn, R. and Prendergast , F.G. (1987) Biochemistry *26*, 8151-8158.

Chatelier, R.C. (1984) Biochim. Biophys Acta *776*, 75-82.

Chattopadhyay, A. and London, E. (1987) Biochemistry *26*, 39-45.

Dawson, C.R., Drake A.F. and Helliwell, J. and Hider, R.C. (1978) Biochim. Biophys. Acta *510*, 75-86.

Dayhoff, M.D. and Eck, R.V. (1968) *Atlas of Protein Sequence and Structure*, National Biomedical Research Foundation, Silver Springs, M.D.

Degrado, W.f., Musso, G.F., Lieber, M., Kaiser, E.T. and Kezdy, F.J. (1982) Biophys. J. *37*, 329-338.

Encinas, M. and Lissi, E. A. (1982) Chem. Phys. Lett. *91*, 55-57.

Eytan, G. and Almary, T. (1983) FEBS Lett. *156*, 29-32.

Faucon, J. F., Dufourcq, J. and Lussan, C. (1979) FEBS Lett. *102*, 187-190.

Georghiou, S., Thomson, M. and Mukhopadhyay, A.K. (1982) Biochim. Biophys. Acta *688*, 441-452.

Haberman, E. (1972) Science *177*, 314-322.

Haberman, E. (1980) in *Natural Toxins* (Eaker, D. and Wadstrom, T., eds.), 173-181, Pergamon Press, New York.

Haberman, E. and Jentsch, J. (1967) Hoppe-Seyler's J. Physiol.Chem. *248*, 37-50.

Huang, C., H. (1969) Biochemistry *8*, 344-352.

Lauterwein, J., Brown, L.R. and Wuthrich, K. (1980) Biochim. Biophys. Acta *622*, 219-230.

Lewis, B.A. and Engelman, D.M . (1983) J. Mol. Biol. *166*, 211-217.

London, E. and Feigenson, G. (1981) Biochemistry *20*, 1932-1938.

Marsh, D. (1990) *CRC Handbook of Lipids*, CRC Press, Boca Raton.

Mollay, C. and Kreil, G. (1974) Febs Letters *46*, 141-144.

Morgan, C.G., Williamson, H., Fuller, S. and Hudson (1983) Biochim. Biophys. Acta *732*, 668-674.

Payongayong, A.K. (1995) Ms. Thesis, University of Tennessee, Knoxville.

Schwarz, G. and Beschiaschvili, G. (1989) Biochim. Biophys. Acta *979*, 82-90.

Sessa, G., Freer, J.H., Colacicco, G. and Weissmann, G. (1969), J. Biol. Chem. *244*, 3575-3582.

Sikaris, K. A.,Thulborn, K.R. and Sawyer, W.H. (1981) Chem. Phys. Lipids *29*. 23-36.

Sikaris, K. A. (1982) Biochem. Pharmacol. *31*, 2625-2631.

Terwilliger ,T., Weisman, L. and Eisenburg, D. (1982) Biophys. J. *37*, 353-361.

Terwilliger, T.and Eisenburg (1982) J. Biol. Chem. *257*, 6016-6022.

Tosteson, M.T., Tosteson, J.L. and Rosenblatt, M. (1990) Biophys. J. *58*, 1367-1375.

Vogel, H. (1981) FEBS Lett. *134*, 37-42.

Vogel, H., Jahnig, F., Hoffman, V. and Stumpel, J. (1983) Biochim. Biophys. Acta *733*, 201-209.

Yunes, R., Goldhammer, A.R., Garner, W.K. and Cordes, E.H. (1977) Arch. Biochim. Biophys. *183*, 105-112.

# APPENDIX

## Figures 19

The residuals of the fit to equation (16) are plotted as a function of time for DMPC which is labelled with an n-DS quencher. (The particular n-DS which is being used, the mean occupation number for the quencher in the lipid phase, $\eta$, the concentration of the lipid, the quenching efficiency, $\left[\left(I_0 / I\right) - 1\right]$, and the rate of quenching, $k_2$, are indicated on each figure.) The lipid-protein ratio was 90 and the sample temperature was 21° C. These figures for the residuals correspond to the figures under the Data Analysis in which the actual fit of equation (16) to the data was done.

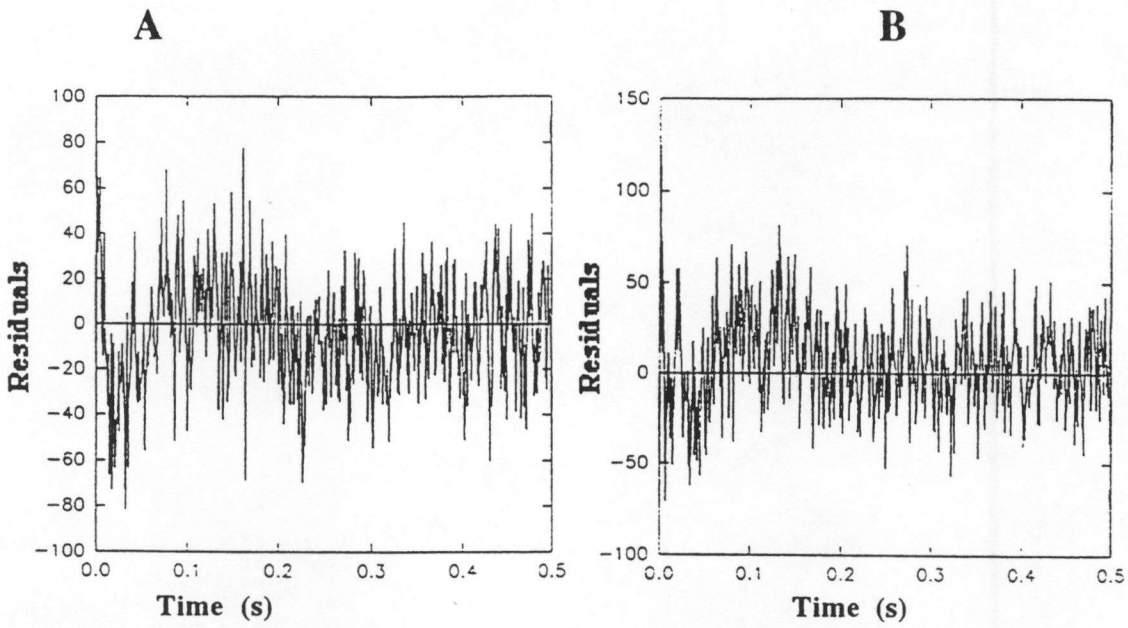


[VES] = 0.55 μmol

[VES] = 0.83 μmol

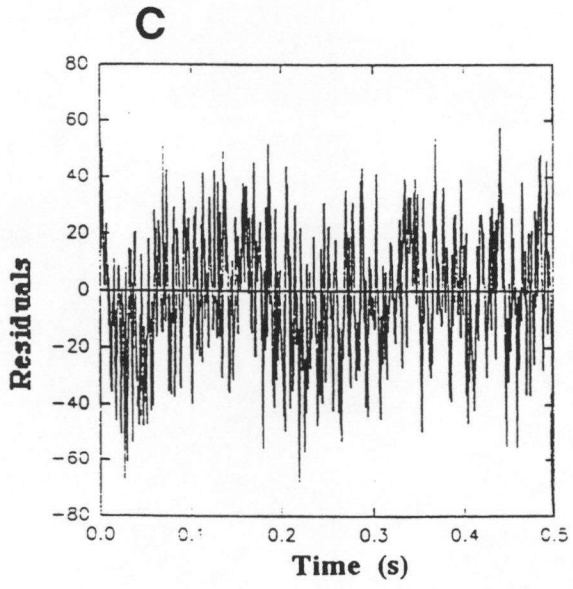


**[Ves] = 1.10 μmol**

**Figure 19.1**
DMPC labelled with 5-DS.

$\eta = 29$

$k_2 = 13 \pm 1\ s^{-1}$

$[(I_o / I) - 1] = 0.34 \pm 0.02$

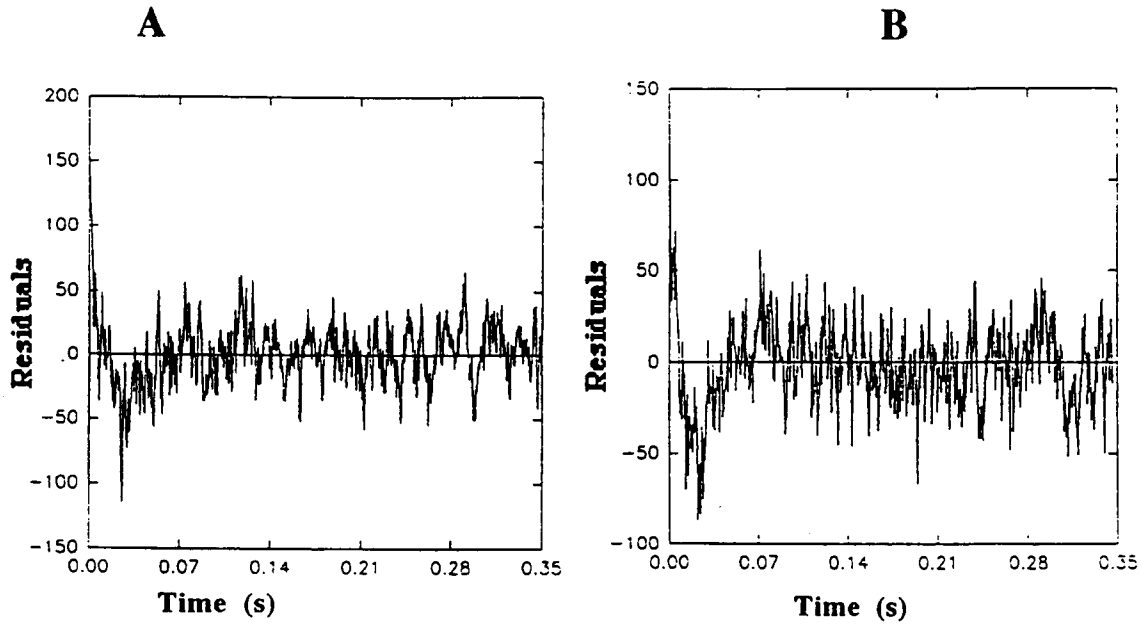


**Figure 19.2**

DMPC labelled with 5-DS.

$\eta = 35$

$k_2 = 23 \pm 2\ s^{-1}$

$[(I_o / I) - 1] = 0.66 \pm 0.03$

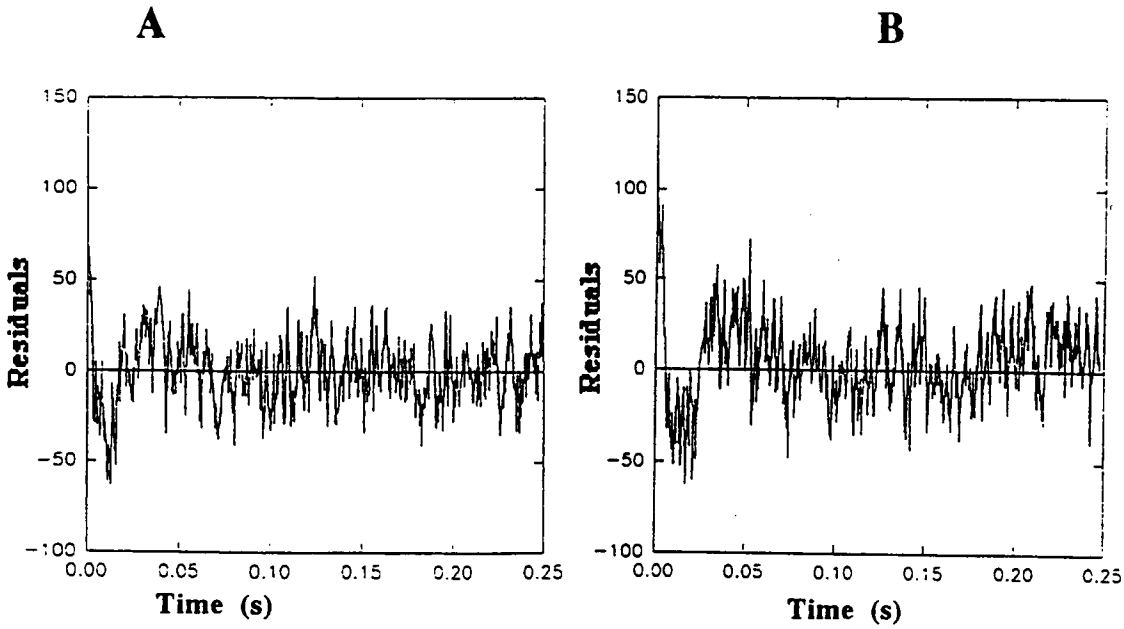


[VES] = 0.55 μmol

[VES] = 0.83 μmol

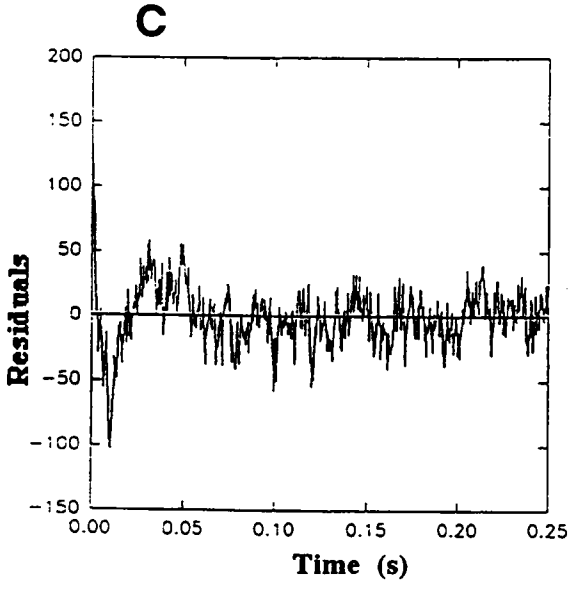


**[Ves] = 1.10 μmol**

**Figure 19.3**
DMPC labelled with 5-DS.
$\eta = 66$
$k_2 = 39 \pm 3\ s^{-1}$
$[(I_o / I) - 1] = 1.04 \pm 0.04$

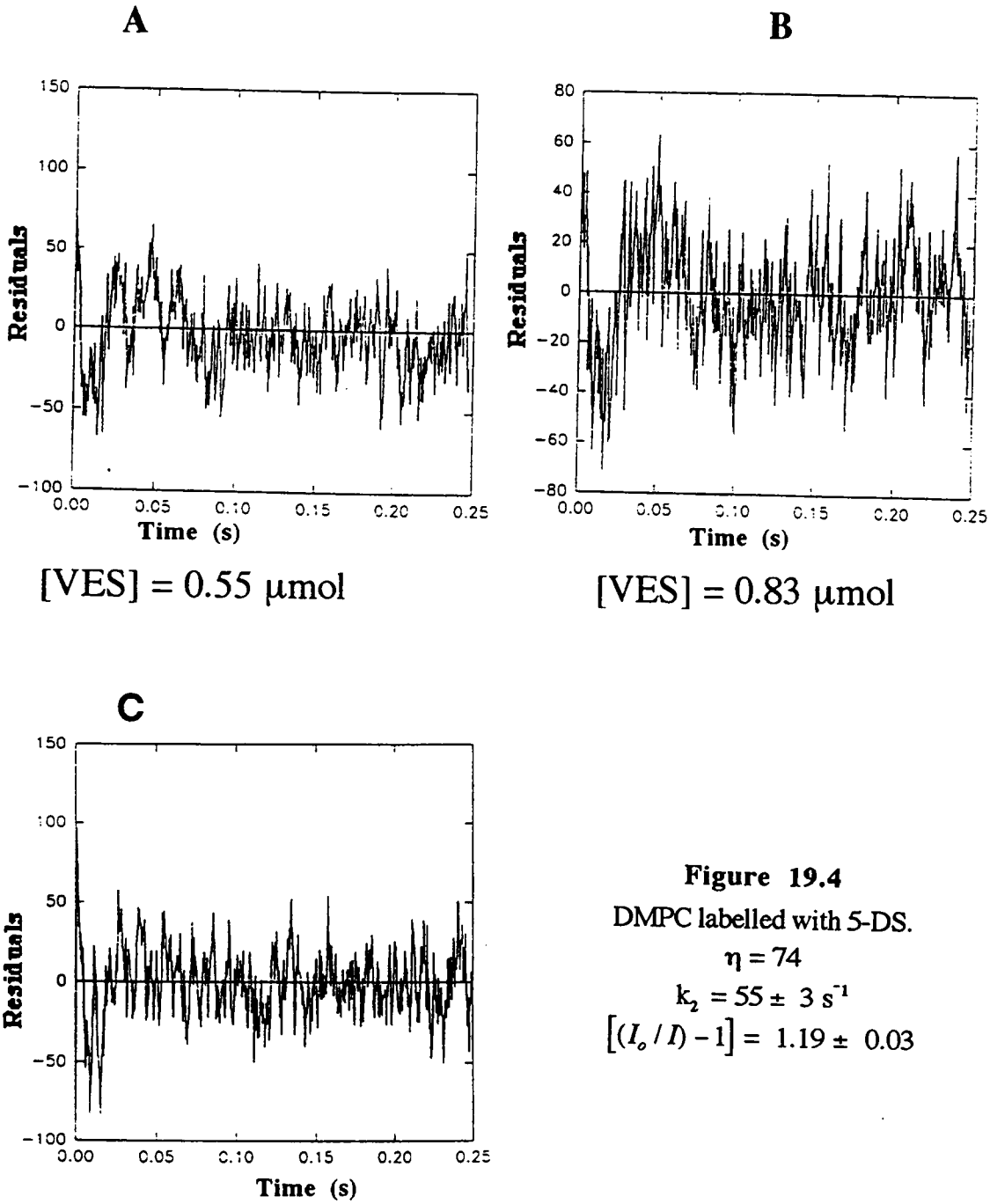


**Figure 19.4**

DMPC labelled with 5-DS.

$\eta = 74$

$k_2 = 55 \pm 3\ s^{-1}$

$\left[(I_o / I) - 1\right] = 1.19 \pm 0.03$

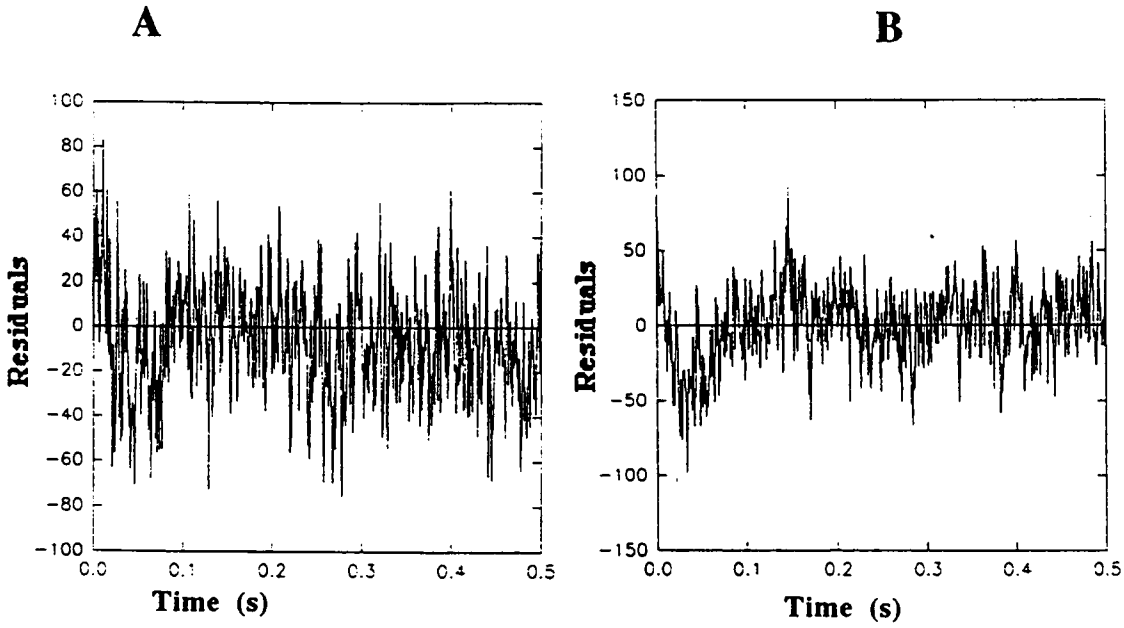


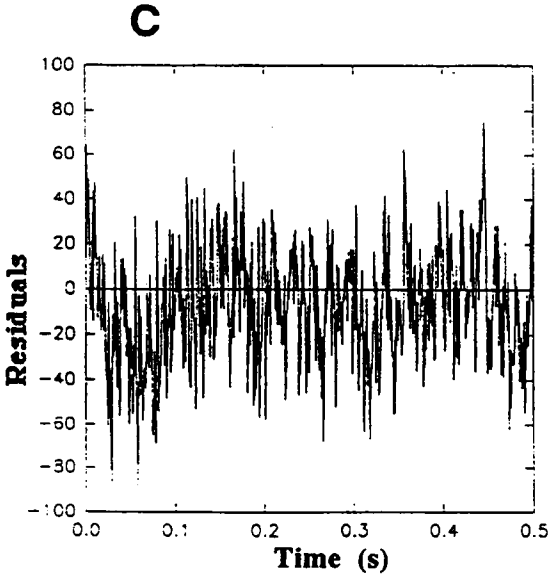


**[Ves] = 1.10 μmol**

**Figure 19.5**

DMPC labelled with 7-DS.

$\eta = 29$

$k_2 = 14 \pm 1\ s^{-1}$

$\left[(I_o / I) - 1\right] = 0.35 \pm 0.02$

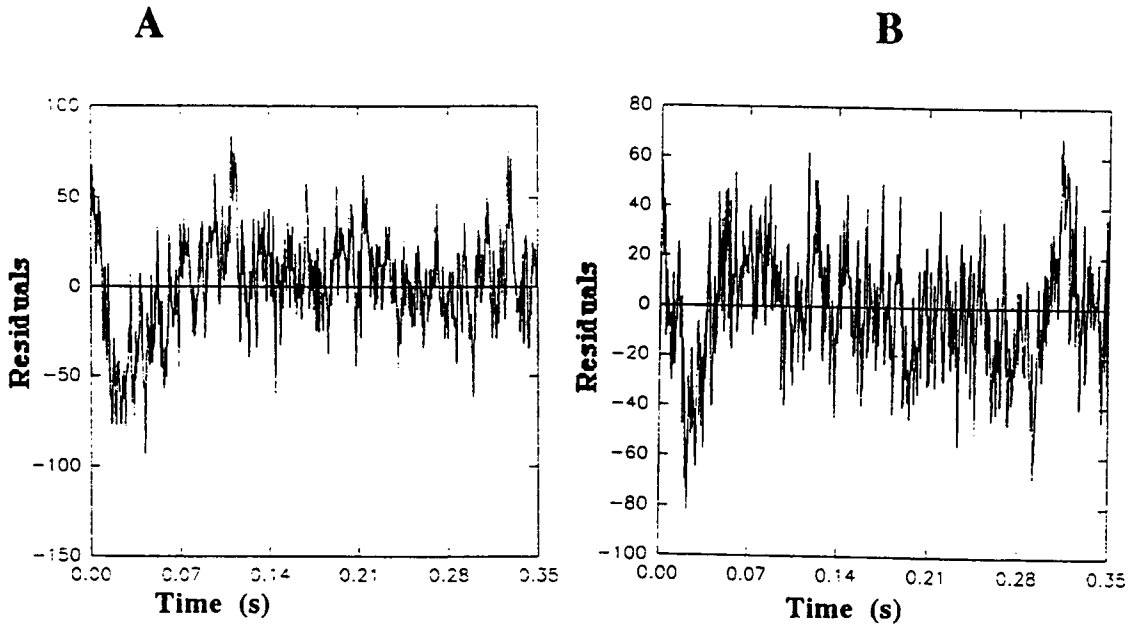


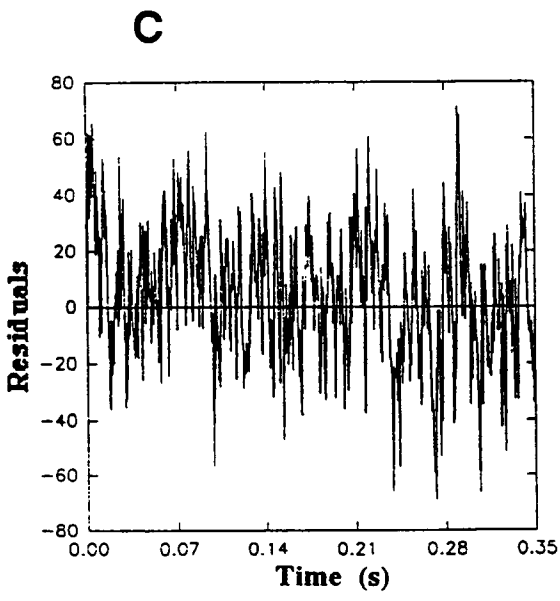


**[Ves] = 1.10 μmol**

**Figure 19.6**

DMPC labelled with 7-DS.

$\eta = 35$

$k_2 = 21 \pm 2\ s^{-1}$

$\left[(I_o / I) - 1\right] = 0.50 \pm 0.03$

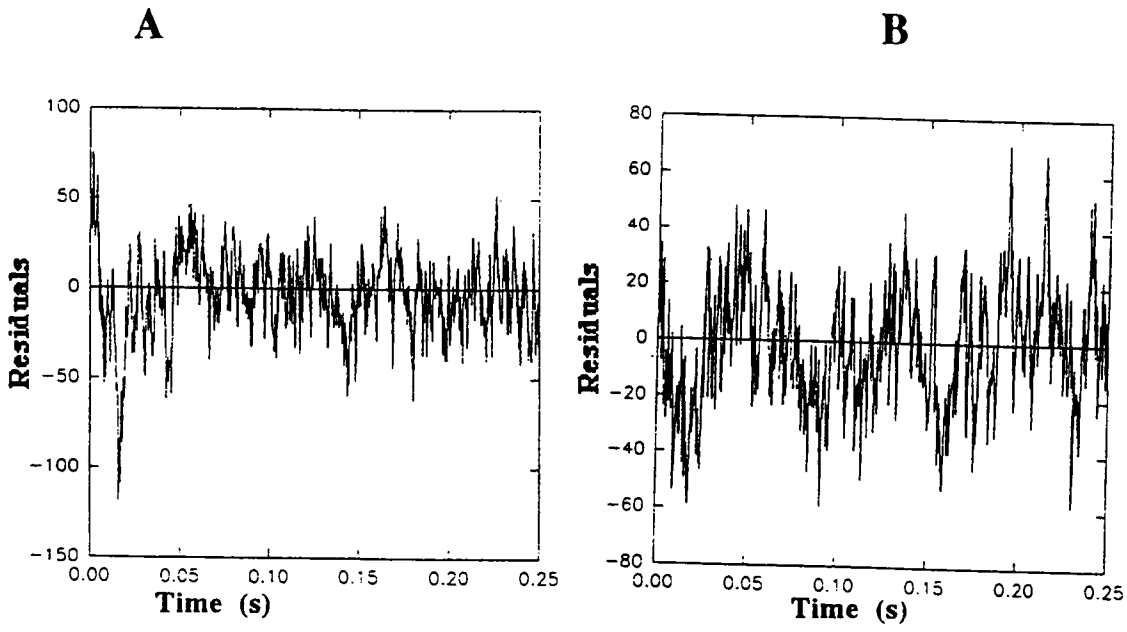


**Figure 19.7**

DMPC labelled with 7-DS.

$\eta = 63$

$k_2 = 40 \pm 4\ s^{-1}$

$[(I_o / I) - 1] = 0.75 \pm 0.04$

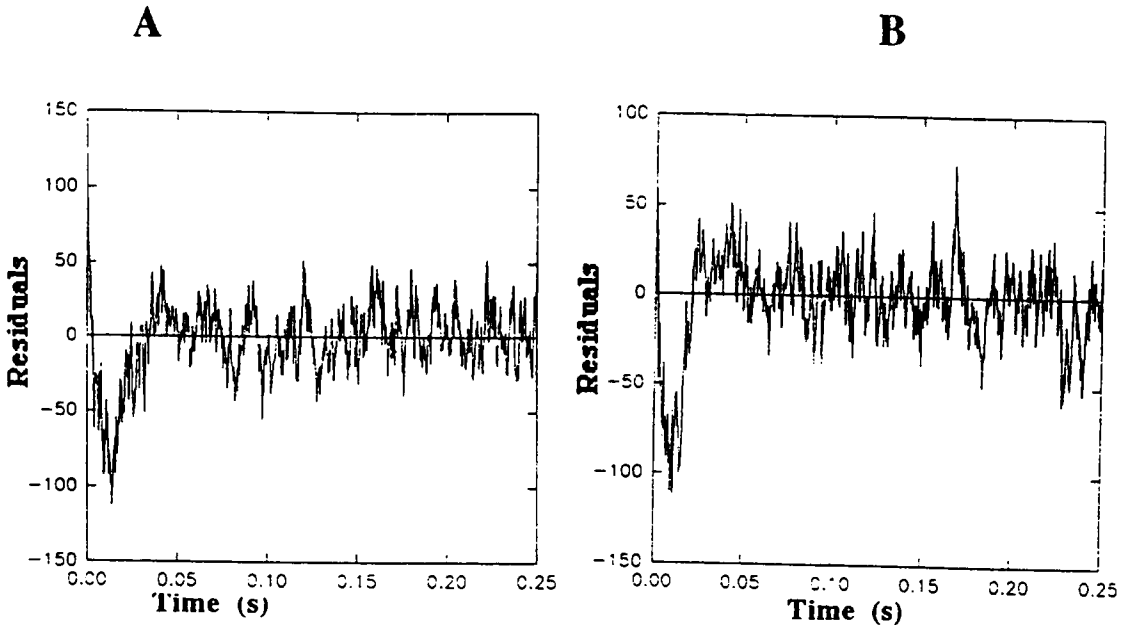


**Figure 19.8**

DMPC labelled with 7-DS.

$\eta = 74$

$k_2 = 56 \pm 6\ s^{-1}$

$[(I_o / I) - 1] = 0.93 \pm 0.03$

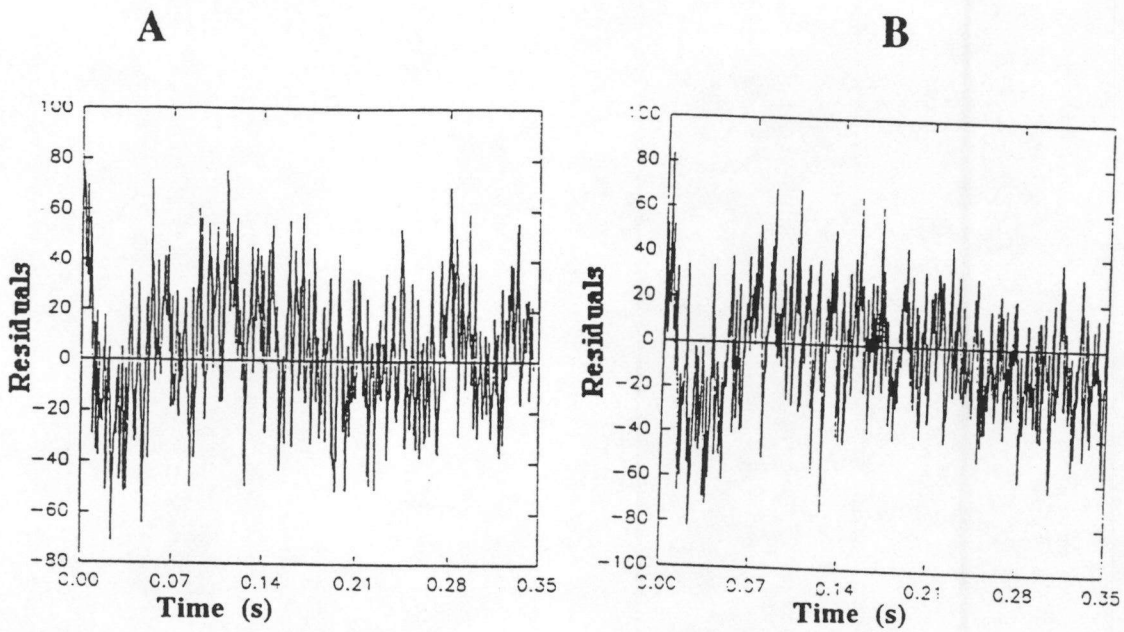


**Figure 19.9**

DMPC labelled with 12-DS.

$\eta = 29$

$k_2 = 22 \pm 1\ s^{-1}$

$\left[(I_o / I) - 1\right] = 0.37 \pm 0.03$

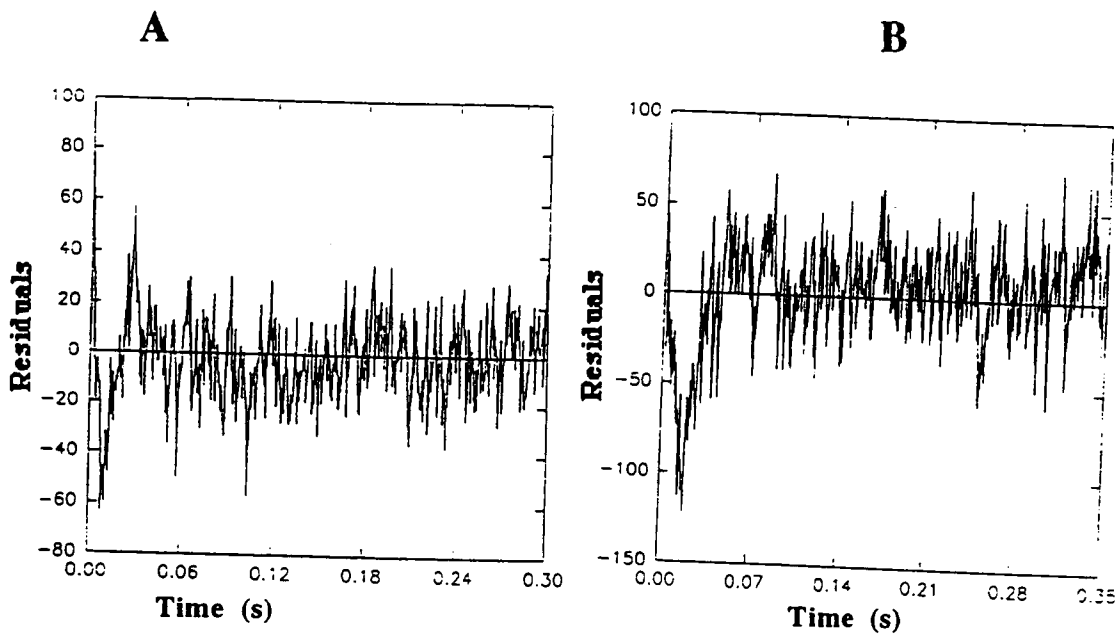


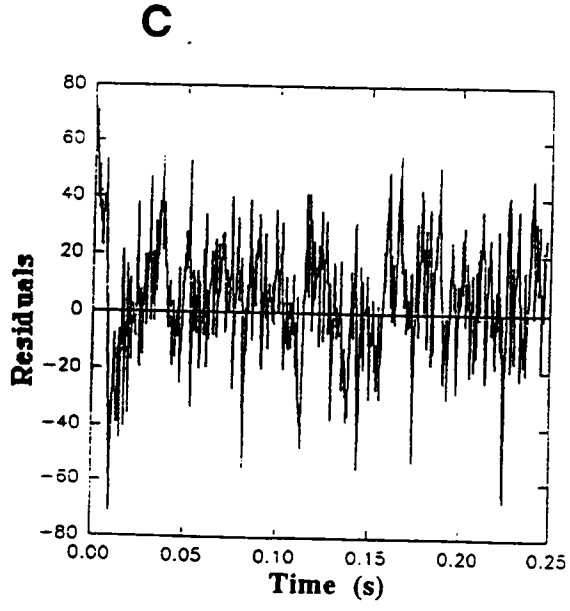


**Figure 19.10**
DMPC labelled with 12-DS.
$\eta = 35$
$k_2 = 35 \pm 3\ s^{-1}$
$[(I_o / I) - 1] = 0.46 \pm 0.03$

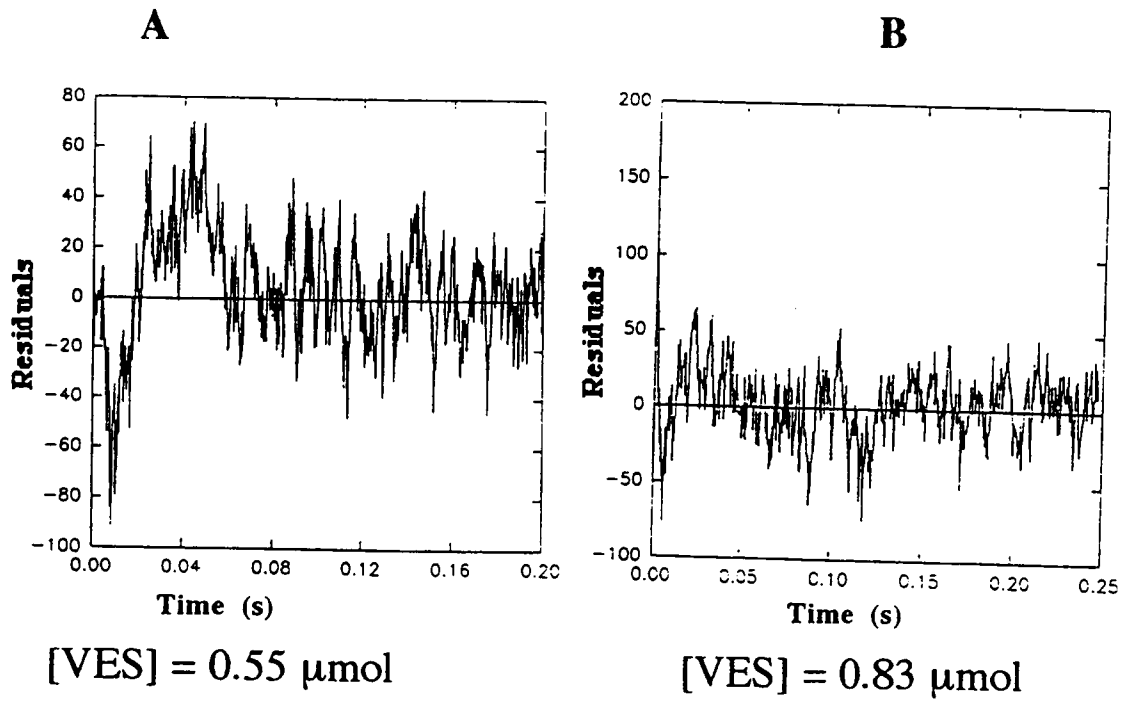


**Figure 19.11**

DMPC labelled with 12-DS.

$\eta = 62$

$k_2 = 47 \pm 4\ s^{-1}$

$[(I_o / I) - 1] = 0.70 \pm 0.03$

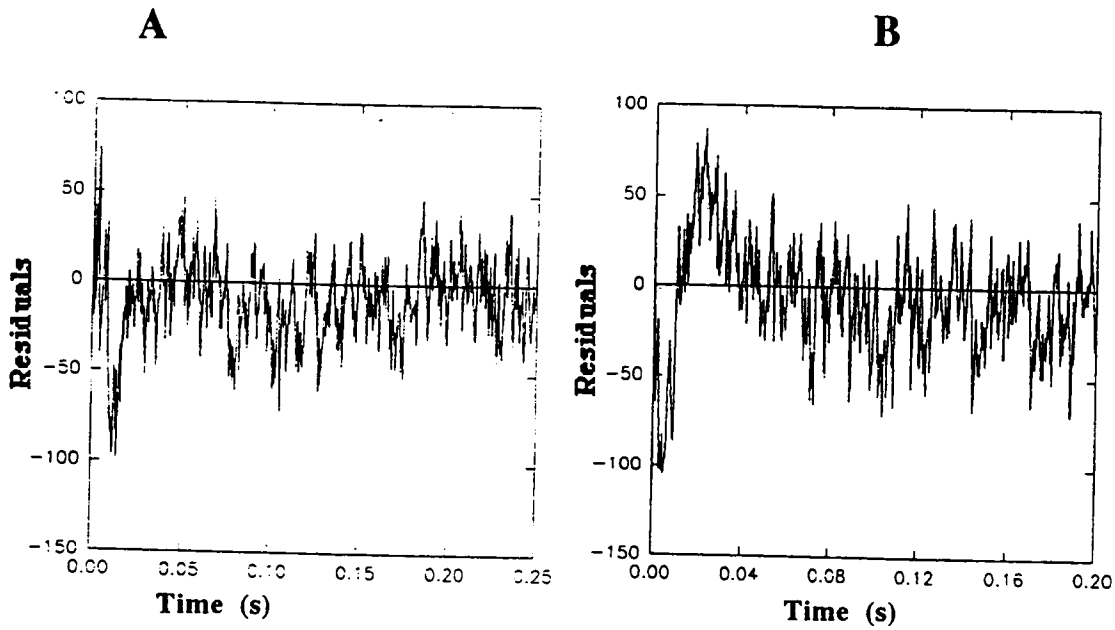


**Figure 19.12**

DMPC labelled with 12-DS.

$\eta = 71$

$k_2 = 69 \pm 7\ s^{-1}$

$[(I_o / I) - 1] = 0.84 \pm 0.04$

## Figures 20

The residuals of the fit to the double exponential equation (18) are plotted as a function of time for DPPC which is labelled with an n-DS quencher. (The particular n-DS which is being used, the mean occupation number for the quencher in the lipid phase, $\eta$, the concentration of the lipid, the quenching efficiency, $\left[\left(I_0 / I\right) - 1\right]$, and the rate of quenching, $k_F$ and $k_S$, are indicated on each figure.) The lipid-protein ratio was 90 and the sample temperature was 37° C. These figures for the residuals correspond to the figures under the Data Analysis in which the actual fit of equation (18) to the data was done.

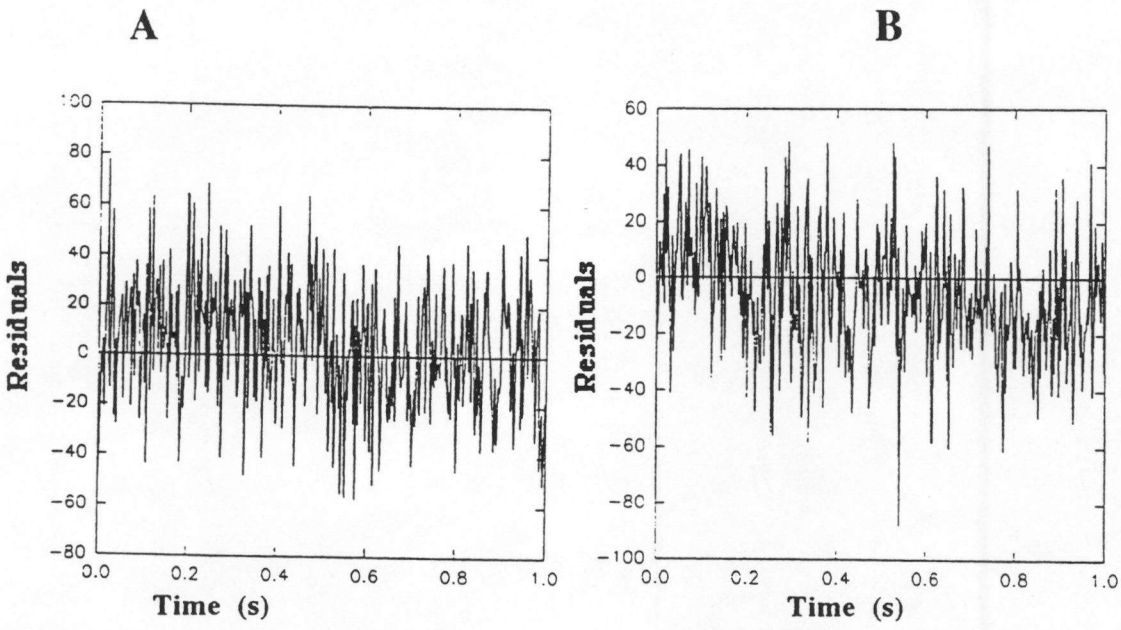


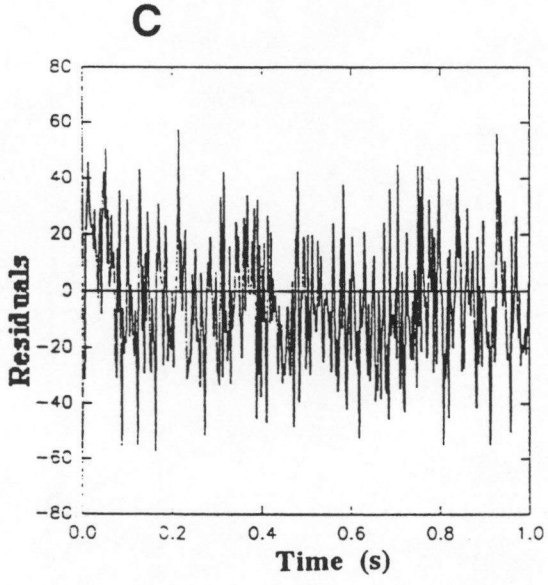


**[Ves] = 1.10 μmol**

**Figure 20.1**

DPPC labelled with 5-DS.

$\eta = 29$

$k_F = 37 \pm 2\ s^{-1}$

$k_S = 2 \pm 0.5\ s^{-1}$

$\left[(I_o / I) - 1\right] = 0.33 \pm 0.04$

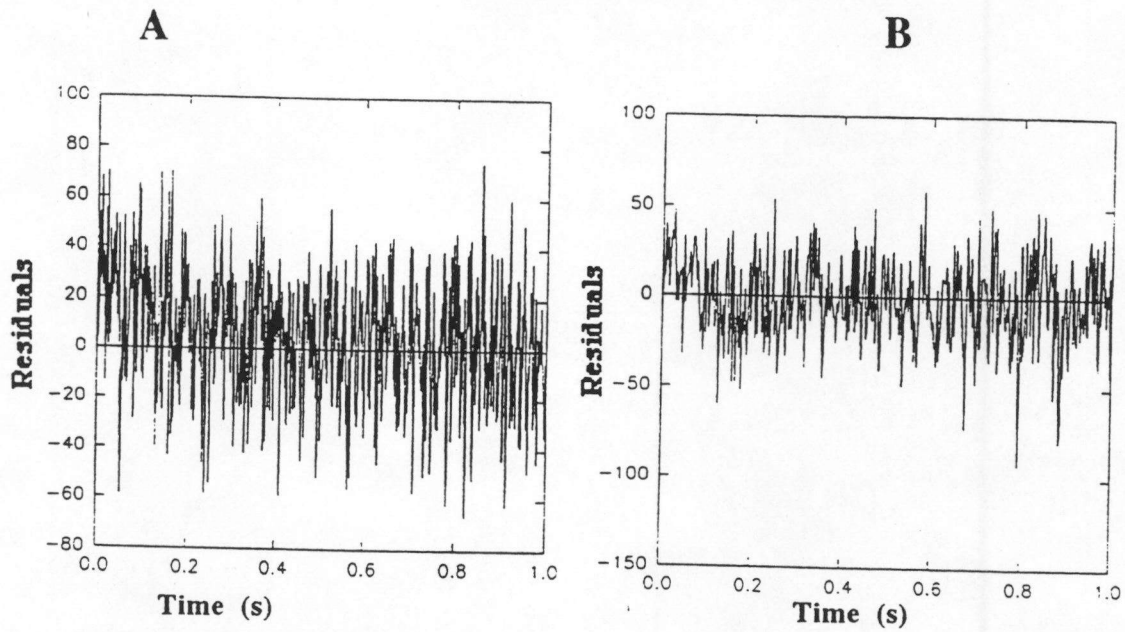


[VES] = 0.55 μmol

[VES] = 0.83 μmol

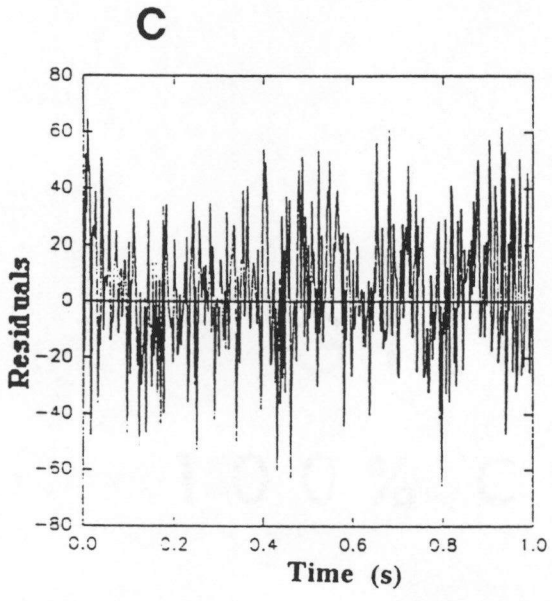


**[Ves] = 1.10 μmol**

**Figure 20.2**

DPPC labelled with 5-DS.

$\eta = 35$

$k_F = 39 \pm 3\ s^{-1}$

$k_S = 2 \pm 0.5\ s^{-1}$

$\left[(I_o / I) - 1\right] = 0.38 \pm 0.04$

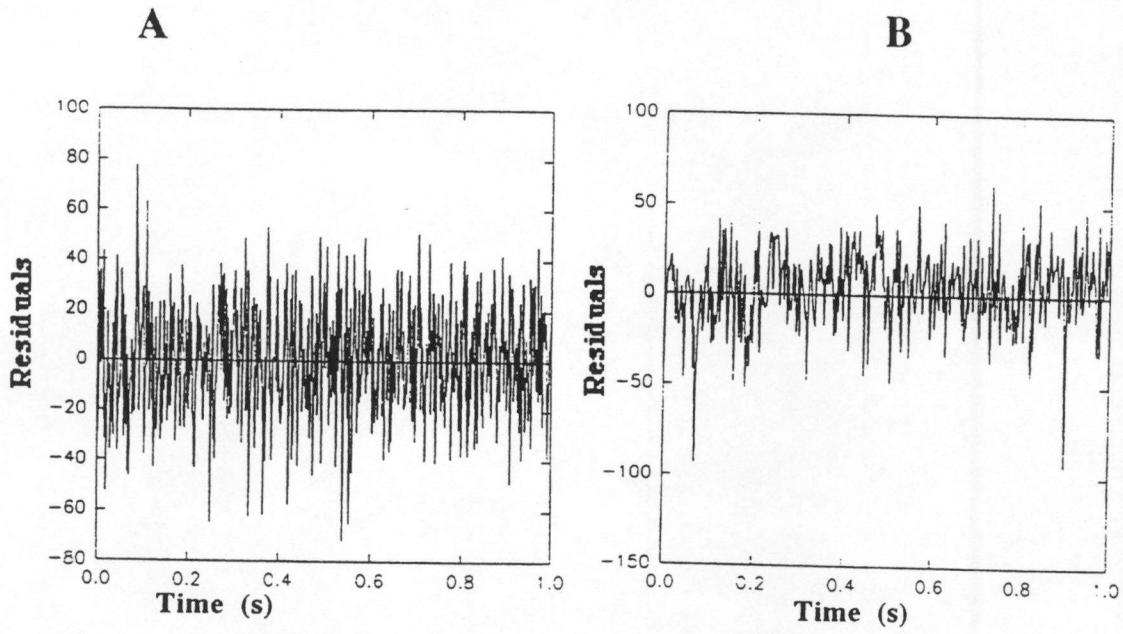


**Figure 20.3**

DPPC labelled with 5-DS.

$\eta = 68$

$k_F = 41 \pm 4\ s^{-1}$

$k_S = 2 \pm 0.5\ s^{-1}$

$\left[(I_o / I) - 1\right] = 1.89 \pm 0.17$

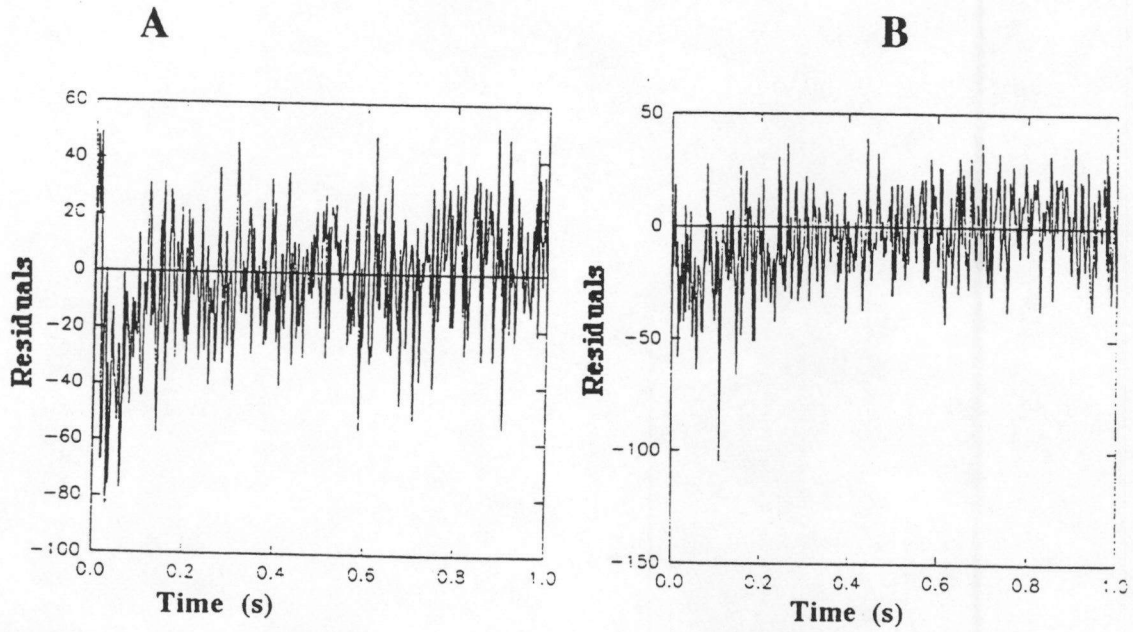


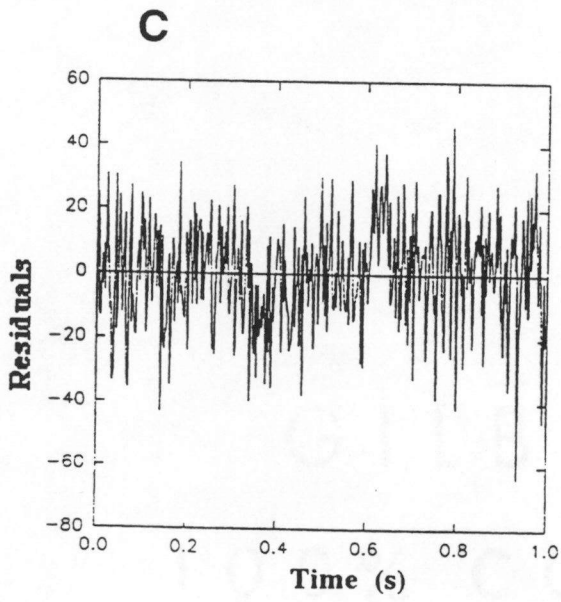


**[Ves] = 1.10 μmol**

**Figure 20.4**

DPPC labelled with 5-DS.

$\eta = 74$

$k_F = 63 \pm 12\ s^{-1}$

$k_S = 7 \pm 1\ s^{-1}$

$\left[(I_o / I) - 1\right] = 2.29 \pm 0.23$

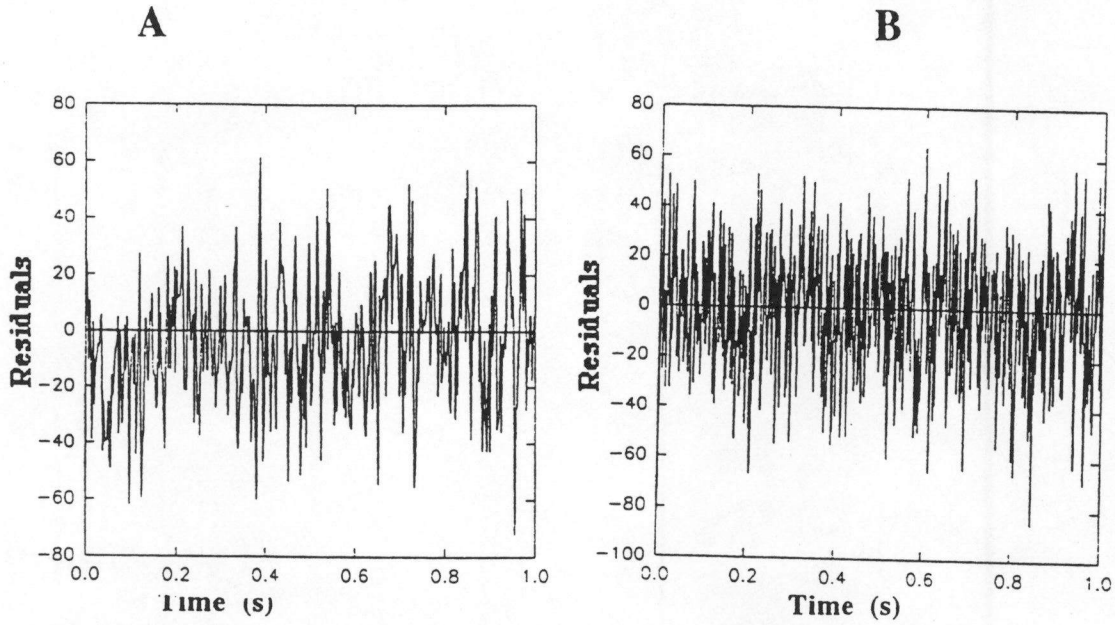


[VES] = 0.55 μmol

[VES] = 0.83 μmol

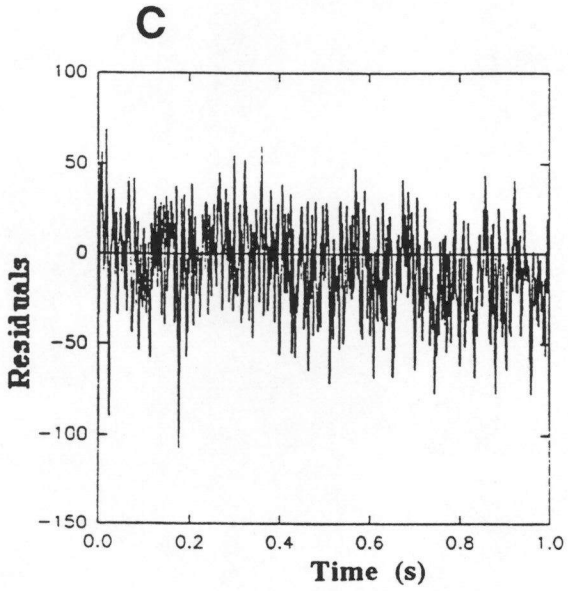


**[Ves] = 1.10 μmol**

**Figure 20.5**

DPPC labelled with 12-DS.

$\eta = 29$

$k_F = 37 \pm 2\ s^{-1}$

$k_S = 2 \pm 0.5\ s^{-1}$

$\left[(I_o / I) - 1\right] = 0.24 \pm 0.05$

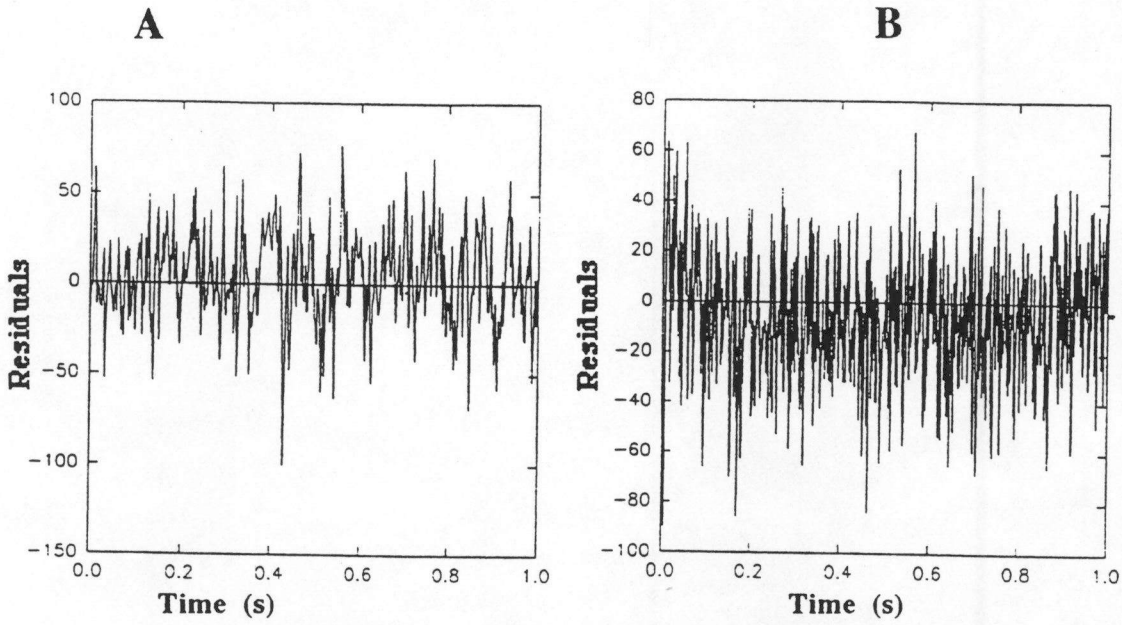


[VES] = 0.55 μmol

[VES] = 0.83 μmol

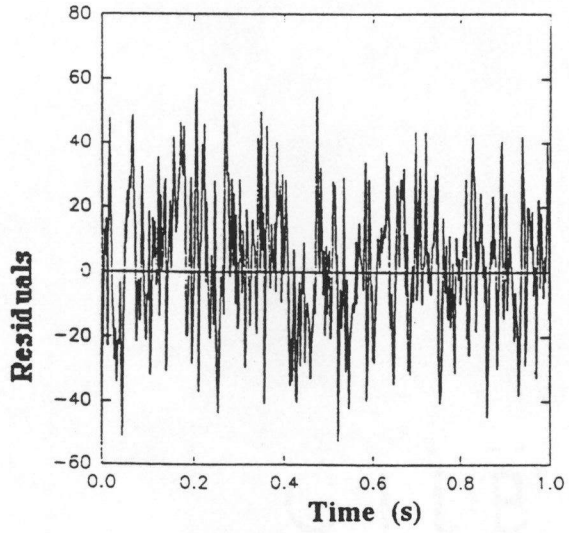


**[Ves] = 1.10 μmol**

**Figure 20.6**

DPPC labelled with 12-DS.

$\eta = 34$

$k_F = 38 \pm 2\ s^{-1}$

$k_S = 2 \pm 0.5\ s^{-1}$

$\left[(I_o / I) - 1\right] = 0.48 \pm 0.07$

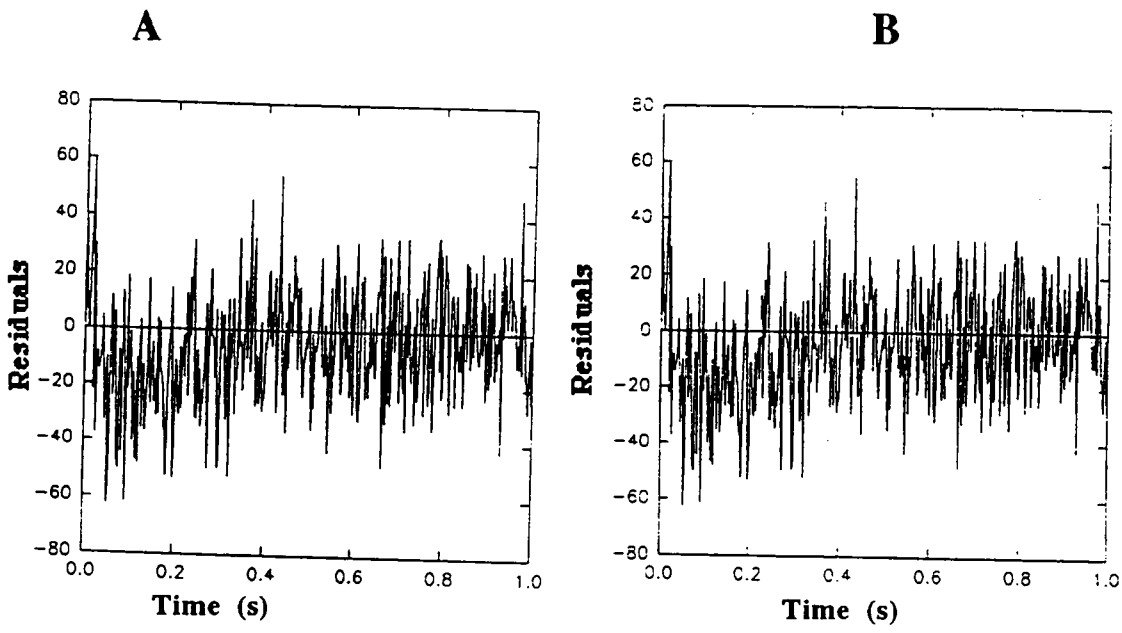


**Figure 20.7**

DPPC labelled with 12-DS.

$\eta = 63$

$k_F = 61 \pm 6\ s^{-1}$

$k_S = 2.5 \pm 0.5\ s^{-1}$

$\left[(I_o / I) - 1\right] = 0.95 \pm 0.11$

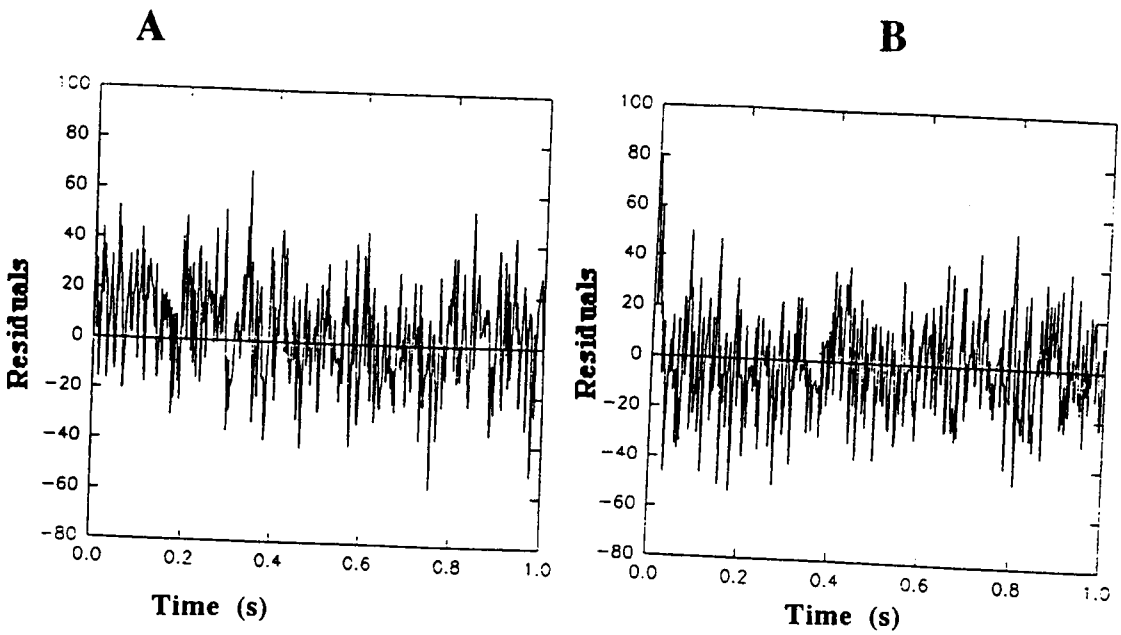


[VES] = 0.55 μmol

[VES] = 0.83 μmol

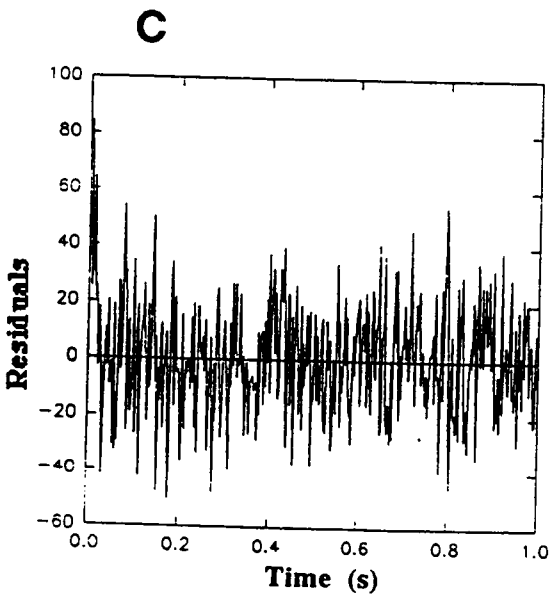


**[Ves] = 1.10 μmol**

**Figure 20.8**

DPPC labelled with 12-DS.

$\eta = 71$

$k_F = 98 \pm 10\ s^{-1}$

$k_S = 3.5 \pm 1\ s^{-1}$

$[(I_o / I) - 1] = 1.23 \pm 0.12$

# Vita

Michael Alan Lipkin was born in Columbia, South Carolina. He graduated from North Forsyth public high school in 1986. He earned a Bachelor of Science degree in biology in 1990 and then a second in physics in 1991 from the University of Tennessee, Knoxville. He obtained a Master of Science degree in physics from the University of Tennessee, Knoxville in May 1997. He is a third Dan black belt in Tae Kwon Do and can be found teaching at the YMCA on Tuesday and Thursday evenings. He has two cats, Kenya and Ludwig. He is also a percussionist/singer/songwriter for the *Boondocks* (available at area record stores).